EFFECT OF PLEISTOCENE CLIMATIC CHANGES ON THE EVOLUTIONARY HISTORY OF SOUTH AFRICAN INTERTIDAL GASTROPODS

BY

TINASHE MUTEVERI

SUPERVISORS:

PROF. CONRAD A. MATTHEE

DR SOPHIE VON DER HEYDEN

PROF. RAURI C.K. BOWIE

Dissertation submitted for the Degree of Doctor of Philosophy in the Faculty of Science at the University of Stellenbosch

March 2013

Declaration

By submitting this thesis/dissertation electronically, I declare that the entirety of the work contained therein is my own, original work, that I am the sole author thereof (save to the extent explicitly otherwise stated), that reproduction and publication thereof by Stellenbosch University will not infringe any third party rights and that I have not previously in its entirety or in part submitted it for obtaining any qualification.

Date: March 2013

ABSTRACT

Historical vicariant processes due to glaciations, resulting from the large-scale environmental changes during the Pleistocene (0.012-2.6 million years ago, Mya), have had significant impacts on the geographic distribution of species, especially also in marine systems. The motivation for this study was to provide novel information that would enhance ongoing efforts to understand the patterns of biodiversity on the South African coast and to infer the abiotic processes that played a role in shaping the evolution of taxa confined to this region. The principal objective of this study was to explore the effect of Pleistocene climate changes on South Africa′s marine biodiversity using five intertidal gastropods (comprising four rocky shore species *Turbo sarmaticus*, *Oxystele sinensis*, *Oxystele tigrina*, *Oxystele variegata*, and one sandy shore species *Bullia rhodostoma*) as indicator species. Sequence data obtained from partial segments of the mitochondrial cytochrome oxidase *c* subunit 1 (COI), and the nuclear ribosomal DNA (encompassing part of 5.8S, second Internal Transcribed Spacer and part of 28S, hereinafter called ITS2; or comprising part of the first Internal Transcribed Spacer, 5.8S, second Internal Transcribed Spacer and part of 28S, hereinafter called ITS), were used as genetic markers to construct phylogeographic patterns and to investigate demographic histories of the taxa. Population structure was investigated using haplotype network analyses, pairwise Φ_{ST} statistics, analysis of molecular variance (AMOVA), isolation by distance analyses, Bayesian analysis of population structure (BAPS) and coalescent analysis of gene flow. Demographic history was analysed through Fu′s F_s tests, mismatch distributions, and Bayesian skyline plots.

Demographic analyses suggest that all five intertidal gastropods studied experienced demographic expansions dating to the late Pleistocene. The sandy shore direct developer *B. rhodostoma* began expansion after the LGM (c. 15 kya) whereas for the four rocky shore broadcast spawners (*T. sarmaticus*, *O. sinensis*, *O. tigrina*, and *O. variegata*) the onset of expansion coincided with or preceded the LGM (c. 25, 60, 50, 40 kya, respectively). Consistent with recent range expansions and gene flow patterns, the population genetic structure in all species was characterised

by shallow or a lack of population differentiation. *Oxystele variegata* was an exception as it showed a deep disjunction, of late Pleistocene origin, between individuals in the west coast Namaqua Bioregion and those in the south coast Agulhas Bioregion. These results provide strong evidence of the vital role that Pleistocene climatic changes and current regimes played in shaping the nature and distribution of biodiversity on the South African coast. In addition, gene flow in all species, except *O. tigrina,* was remarkably asymmetrical with the regions around Cape Infanta and Port Elizabeth acting as source populations. Considering the generally weak population genetic structure and gene flow patterns detected for most gastropod species studied here, it is recommended that *T. sarmaticus*, *O. sinensis*, *O. tigrina* and *B. rhodostoma* be managed as panmictic populations, and that the region encompassing Cape Infanta, and Port Elizabeth should be prioritised for conservation as it appears to harbour source populations. *Oxystele variegata* was the only species showing distinct population structure and in this instance, species specific conservation efforts should recognize this divergence by treating the two genetic assemblages as distinct management units.

OPSOMMING

Historiese vikariante prosesse kan toegeskryf word aan glasiasie, en het tot gevolg gehad dat grootskaalse veranderinge in die omgewing plaasgevind het tydens die Pleistoseen (,012 - 2.6 miljoen jaar gelede, Mjg). Dit het „n beduidende impak gehad op die geografiese verspreiding van spesies, veral ook in die mariene stelsels. Die motivering vir hierdie studie was om nuwe data te voorsien wat sal bydrae tot die voortgesette pogings om die patrone van biodiversiteit langs die Suid-Afrikaanse kus te verstaan. Dit sou ook help om die abiotiese prosesse af te lei wat 'n rol gespeel het in die evolusie van taksa wat in hierdie streek voorkom. Die hoofdoel van hierdie studie was om die effek van die Pleistoseen klimaatsveranderinge op Suid-Afrika se mariene biodiversiteit te bepaal deur gebruik te maak van vyf intergety slak spesies as indikatore (vier wat in rotsagtige gebiede voorkom: *Turbo sarmaticus*, *Oxystele sinensis*, *Oxystele tigrina*, *Oxystele variegata* en 'n sanderige strand spesies: *Bullia rhodostoma*). Volgorde data verkry vanaf gedeeltelike segmente van die mitochondriale sitochroom oksidase c subeenheid 1 (COI), en die kern ribosomale DNA (bestaande uit „n deel van 5.8S, tweede interne getranskribeerde spasieërders en 'n deel van 28S), hierna genoem ITS2 is gebruik as genetiese merkers om filogeografiese patrone te dokumenteer en ook om die demografiese geskiedenis van die spesies te ondersoek. Bevolking struktuur is ondersoek deur gebruik te maak van haplotipe netwerk analise, paarsgewyse ΦST statistiek, analise van molekulêre variansie (AMOVA), isolasie deur afstand analise, Bayesiaanse analise van die bevolking struktuur (BAPS) en analise van gene vloei. Demografiese geskiedenis is ontleed deur Fu se Fs toetse, misparing verdelings, en Bayesiaanse luglyn kurwes.

Demografiese ontleding dui daarop dat al vyf die intergety slakke wat ondersoek is demografiese uitbreidings ervaar het wat terugdateer tot die einde van die Pleistoseen. Die sanderige strand direkte ontwikkelaar, *B. rhodostoma,* het die uitbreiding begin na die LGM (c. 15 Kya), terwyl vir die vier rotsagtige kusbewoners wat eiers oor 'n uitgebreide gebiede versprei (*T. sarmaticus*, *O. sinensis*, *O. tigrina*, en *O. variegata*) het die aanvang van die bevolkings uitbreiding saamgeval met die laaste galsiasie of dit voorafgegaan (c. 25, 60, 50, 40 Kya, onderskeidelik). In ooreenstemming met die onlangse reeks bevolkings uitbreidings, is die bevolking genetiese struktuur in alle spesies gekenmerk deur weinig differensiasie. *Oxystele variegata* was 'n uitsondering en het 'n ontwrigting van laat Pleistoceen oorsprong getoon tussen individue langs die weskus Namaqua Biostreek en dié in die suid kus Agulhas biostreek. Hierdie resultate voorsien sterk bewyse van die belangrike rol wat die Pleistoseen klimaatsveranderinge gespeel het in die vorming en verspreiding van biodiversiteit langs die Suid-Afrikaanse kus. Daarbenewens, geen vloei in alle spesies, behalwe *O. tigrina*, was merkwaardig asimmetries. Kaap Infanta en Port Elizabeth verteenwoordig moontlik die bron bevolkings. Met inagneming van die geringe bevolking genetiese struktuur en geenvloei patrone wat waargeneem is vir die meeste slak spesies wat bestudeer is, word dit aanbeveel dat *T. sarmaticus*, *O. sinensis*, *O. tigrina* en *B. rhodostoma* bestuur word as „n panmiktiese bevolking, en dat die streek wat Kaap Infanta en Port Elizabeth insluit geprioritiseer moet word vir bewaring. *Oxystele variegata* was die enigste spesie wat duidelike bevolking struktuur getoon het en in hierdie geval, moet spesie spesifieke bewaringspogings aangewend word.

ACKNOLEDGEMENTS

First and most importantly I thank my supervisors Professors C.A. Matthee and R.C.K. Bowie, and Dr S. von der Heyden for introducing me to the fascinating field of phylogeography and for their invaluable and insightful guidance throughout my PhD study. I could not have asked for a better supervisory team. I am also indebted to the following people for assisting with sample collection: Dr S. Jackson, Prof S. Daniels, Mr. C. Muller and Miss T. Reynolds. The work was supported by grants from the National Research Foundation (South Africa). I also would like to thank all members of the Evolutionary Genomics Group for being such a wonderful team to work with. I gratefully acknowledge use of facilities on the CBSU computer clusters at the Cornell University Theory Centre for MIGRATE-N analyses.

A warm thank you goes to my wife Morleen for her patience and flexibility and for granting me the time and freedom I needed to carry out this work. Finally, a big thank you to my daughters Laura, Tatenda and Lynn for enduring my long hours in the lab and for believing in me.

CONTENTS

LIST OF TABLES

LIST OF FIGURES

CHAPTER 1

GENERAL INTRODUCTION

1.1 Background to the study

A major goal of phylogeographic studies is to determine historical and contemporary factors contributing to observed genetic structure (Lee and Boulding, 2007). Genetic variation at the population and geographic level bears the footprint of both past demographic events, for instance glaciation, and in the marine context also reflects effects of recurrent processes such as patterns of oceanographic circulation (Pérez-Losada *et al*., 2007; Palero *et al*., 2008). Historical vicariant processes such as the large-scale environmental changes during the Pleistocene glaciations (0.012-2.6 million years ago, Mya, Hewitt, 2011), and especially those dating back to the last glacial maximum (LGM, 19-26.5 thousand years ago, Clark *et al*., 2009), have had significant impacts on the geographic distribution of species in many terrestrial biogeographic regions (Avise, 2000; Hewitt, 2000). In the marine context, alternate recurrent cycles of glacials and interglacials in the Quaternary (last 2.6 Mya, Hewitt, 2011) caused sea level fluctuations (Miller *et al*., 2005), latitudinal shifts in water temperature (Bard and Rickaby, 2009), and physiographic changes to coastal environments (Kenchington *et al*., 2009). The latter generally culminated in the contraction, expansion and fragmentation of species ranges leading to population bottlenecks and significant alteration of the patterns of gene flow (Derycke *et al*., 2008). Evidence now also suggests that earlier Plio-Pleistocene alteration of the patterns of oceanic circulation also affected marine biodiversity (Jolly *et al*., 2006; Derycke *et al*., 2008; Marko *et al*., 2010). However, not all species exhibit demographic or genetic structural response to the Pleistocene sea level changes (e.g. the marine invertebrates *Mytilus carlifornias*, *Semibalanus cariosus*, *Balanus glandula*, Marko *et al*., 2010).

Glacial-interglacial cycles influenced taxa in different ways depending on their life history, physiological tolerances and habitat specificity (Canino *et al*., 2010). Conceivably, sessile and sedentary organisms with specific habitat requirements are more vulnerable to the Pleistocene climatic oscillations owing to their decreased mobility. It is hypothesized that sessile and sedentary organisms with restricted larval dispersal, probably only survived in refugial areas from where they were able to expand once climatic conditions improved (Marko, 2004; Campo *et al*., 2010). The effects of Plio-Pleistocene climatic changes can be investigated using several methods, most frequently through the use of ecological niche models (e.g. Bigg *et al*., 2008), phylogeography (Hewitt, 2004; Bigg *et al*., 2008; Campo *et al*., 2010), or a combination of both (e.g. Graham *et al*. 2006).

The phylogeographic approach that will be used in this study makes use of molecular markers to provide indirect evidence of historical isolation, population expansion or bottlenecks and local extinction-recolonisation dynamics (e.g. Bigg *et al*., 2008; Marko *et al.*, 2010). Traditional genetic methods such as analyses of intraspecific diversity, mismatch distributions and Mantel tests can be used to help understand the putative ages and genetic structure of populations (McGaughran *et al*., 2010). Furthermore, relatively more recent advances in molecular ecology (e.g. coalescent theory in conjunction with Bayesian methods) have provided tools for reconstructing the evolutionary history of particular taxa and to test hypotheses about the influence of past environmental processes on genetic structure (Nicolas *et al*., 2011). The use of molecular data is based on the assumption that effects of historical processes can be detected in the present day patterns of genetic variation (Hewitt, 2000) and rests on the following predictions: (1) spatial population fragmentation coincides with the location of vicariant barriers most likely caused by sea level changes or glaciers, (2) although care must be taken to differentiate between refugial effect and the effect of secondary contact with or without introgression, areas of high genetic diversity generally indicate potential refugia, (3) a signature of demographic expansion is expected in regions

that have recently been colonized through large scale range expansions (4) the timing of genetic divergence events coincides with major environmental changes (Nicolas *et al*., 2011).

Several genetic studies have been conducted to test these predictions, but their focus has centred on the Northern Hemisphere (reviewed in Gómez *et al*., 2007; Maggs *et al*., 2008). The main findings of such studies include detection of Pleistocene glacial refugia located in southern areas of the Northern Hemisphere and inferences were made on the interglacial recolonisation pathways. It is also evident from these studies that many taxa harbour distinct genetic assemblages that began diverging during late Pleistocene glaciations (Avise, 1998; Hewitt, 2001), probably due to vicariant events associated with glaciation formation (Peters *et al*., 2005). Moreover, several recent genetic studies of marine organisms, particularly in temperate habitats, demonstrate that populations have experienced nonequilibrium historical processes such as population range expansion since the LGM. Relevant to the focus of the present study, these include several marine gastropods (e.g. Hellberg *et al*., 2001; Marko *et al*., 2010).

Interestingly, different patterns of genetic diversity have been recovered among co-distributed species, suggesting that climatic change is just one of many factors shaping population genetic patterns (e.g. Hewitt, 2004; Elderkin *et al*., 2008; Marko *et al*., 2010). For example, the metapopulation dynamics of the marine fauna is also directly linked to oceanographic circulation (Perrin *et al*., 2004; Banks *et al*., 2007), habitat specificity (Bilton *et al*., 2001; Elderkin *et al*., 2008), dispersal ability (Bilton *et al*., 2001; Elderkin *et al*., 2008), and the spatial distribution of suitable habitat (Sánchez and Gil, 2000; Marko, 2004; Lourie *et al*., 2005). There is thus still a considerable gap in our understanding of the factors shaping current patterns of biodiversity in the Southern Hemisphere (Teske *et al*., 2011). Against this background, this study aims to use molecular genetic methods to investigate the role of climate change and subsequent changes in coastline (especially those imposed by the Plio-Pleistocene climatic changes) in shaping marine genetic diversity along the South African coast.

The South African coast is situated at the junction of two oceans – the Indian Ocean in the east and the Atlantic in the west. Owing to its location and isolation, the South African coast has attracted considerable interest from a biogeographic point of view (Teske *et al.*, 2011) and has thus been included in studies having a global focus (e.g. Rocha *et al*., 2005). The coast, because of its latitude, did not experience glaciation. Nevertheless, glacial-interglacial induced climate and sea level changes conceivably caused habitat changes and possibly fragmentation, leading to alternate expansions and contractions of species ranges along the coast. Furthermore, unlike other coastal regions (e.g. the Torres Strait land bridge between Northern Australia and New Guinea, Voris, 2000; Bassian Isthmus between main land Australia and Tasmania, Waters *et al*., 2005), there are no obvious geological features, such as land bridges, that could have completely isolated southern African populations of coastal taxa during episodes of low sea level (Teske *et al.*, 2011). Thus, other factors such as changes in oceanographic regime (Pineda, 1999), upwelling zones (Connolly *et al*. 2001), and salinity and sea surface temperatures gradients (Gaylord and Gaines, 2000; Pineda *et al*., 2002) need to be considered in addition to Pleistocene climatic oscillations as modifiers of gene flow that may have led to population structure along the coastline. Moreover, the patchy distribution of rocky coastline and sandy beaches coupled with the palaeoclimatic history of the region offers ample opportunity to study how historical factors could have interacted to influence and shape extant biodiversity.

1.2 Why this study in southern Africa

This study is inspired by the philosophy that the documentation of phylogeographic patterns across different co-distributed taxa in southern Africa will eventually lead to a deeper understanding of the underlying processes shaping biodiversity in the region. In a recent review of the status of phylogeographic studies on the South African coast, Teske *et al*. (2011) indentified several gaps that need to be filled for a better understanding of the processes shaping biodiversity. These gaps

include: (1) focussing on neglected taxa, (2) obtaining samples from regions where little research has been done, (3) generating multispecies and multilocus genetic data sets. This study is an attempt to fill these gaps in a number of ways.

First, new pattern data on previously unstudied taxa will be added and insights will be gained through analyses that have not often been used in previous regional studies (Bayesian reconstruction of demographic history). Thus, analyses will provide background information about historical events to which the ancestors of the present-day gastropods were exposed in the past, which might shed light on patterns of speciation in the future considering the cyclical nature of climatic changes. In meeting its objectives, the study will endeavour to adopt an analytical rather than descriptive approach in line with one of the research directions recommended by Teske *et al*. (2011).

Secondly, despite sandy shores making up about 42% of the South African coastline, most research to date has been focussed on rocky shore or estuarine taxa, and only two studies have been performed on sandy shore organisms (Teske *et al*., 2011). It is therefore instructive to explore how population genetic structuring varies between taxa inhabiting sandy and rocky shores if we are to gain a reliable understanding of the effect of habitat availability on genetic structure of species found around the South African coastline. In line with this observation, a chapter of this study will focus on the phylogeography of a sandy shore plough shell, *Bullia rhodostoma*.

Finally, insight into population genetic structuring is necessary for making informed and effective management decisions in commercially exploited and potentially harvestable marine organisms (Avise, 1998), as well as for the conservation of biodiversity in general. Dispersal potential and realised dispersal are important determinants of the fate of exploited populations, both in terms of re-colonization potential and for predicting the potential for adaptation under shifting selective regimes, like climate change, predation pressure and population collapse (Moritz, 1994; Crandall *et al.*, 2000). The phylogeographic data from this study will be used to infer levels of gene

flow, which will provide further insight into the extent to which present-day populations are connected by dispersal.

1.3 A brief overview of the phylogeography of marine taxa in southern Africa

This brief review summarises a more comprehensive and detailed review of marine phylogeography in southern Africa by Teske *et al*. (2011). Taxa exhibit varying degrees of phylogeographic patterns ranging from those with genetic discontinuities coinciding with boundaries between marine biogeographic provinces (Emmanuel *et al*., 1992; Turpie *et al*., 2000) to those that show genetic homogeneity spanning their entire current distribution. Most of the southern African taxa studied to date that occur in more than one marine biogeographic province are characterised by genetic discontinuities that often coincide with the boundaries between the recognised biogeographic provinces (see **Section 2.1** for description of biogeographic regions). For example, in the South African context phylogeographic discontinuities were reported near Cape Point (e.g. mud shrimp *Upogebia africana*, Teske *et al.*, 2006; bluntnose klipfish *Clinus cottoides*, von der Heyden *et al*., 2008) and Cape Agulhas (e.g. perlemoen abalone *Haliotis midae*, Evans *et al*., 2004; Bester-van der Merwe *et al*., 2010). Disjunctions on the south-east coast in the transition zone between the south-east temperate and subtropical provinces have been reported in the Algoa Bay region around Port Elizabeth and Port Alfred (*Upogebia africana*, Teske *et al*., 2006; *Clinus cottoides*, von der Heyden *et al*., 2008; *Haliotis midae*, Bester-van der Merwe *et al*., 2010). Phylogeographic breaks between the subtropical and tropical provinces occur near St Lucia (sandprawn *Callianassa kraussi*, Teske *et al*., 2007a, 2009), and further north towards Mozambique (spiny lobster *Palinurus delagoae*, Gopal *et al*., 2006; cauliflower corals *Pocillopora verricosa*, Ridgway *et al*., 2008). Several taxa with limited dispersal capacity show phylogeographic breaks that do not coincide with current marine biogeographic breaks (crustacean *Iphinoe truncata,* Teske *et al*., 2006, 2007a). Another important finding is that some species do not show genetic structure

across their entire ranges (e.g. spiny lobster *Palinurus gilchristi*, Tolley *et al*., 2005; goby *Caffrogobius caffer*, Neethling *et al.*, 2008; roman seabream *Chrysoblephus laticeps*, Teske *et al*., 2010).

The southern African coastline is furthermore characterized by asymmetric gene flow along most of the coastline. Four major gene flow patterns have been identified including northward flow with the Benguela Current on the west coast (von der Heyden *et al*., 2008), southward flow on the east coast with the Agulhas Current (Teske *et al*., 2007b), some gene flow in the north-easterly direction inshore of the Agulhas Current on the south-east coast (von der Heyden *et al*., 2008), as well as bidirectional gene flow on the south coast (Teske *et al*., 2007b). There is an occasional transfer of larvae (gene flow) from the Indian Ocean to the Atlantic Ocean via inshore eddies of the Agulhas Current, termed Agulhas eddies (Fig. 2.1), that move around Cape Point and get swept up the west coast. These eddies are probably responsible for transferring larvae between distant areas – something along those lines.

1.4 Choice of methods and of molecular markers

Phylogeography has traditionally been carried out by reconstructing phylogenetic trees or haplotype networks from molecular markers (Posada and Crandall, 2001). Although the traditional methods are still relevant and provide valuable information, the development of coalescent theory in conjunction with Bayesian methods has facilitated the reconstruction of more complex genealogical histories from molecular data (Hey and Nielsen, 2004; Hey, 2006). Coalescent analyses can be used to estimate phylogeographic parameters such as gene flow, and divergence times between genetic assemblages, which have remained relatively difficult to estimate using traditional analyses (Beaumont and Ranala, 2004). This study therefore uses traditional analyses of Φ_{ST} and analyses of molecular variance and mismatch distributions in conjunction with recently developed coalescent

methods to investigate population genetic structure, timing of lineage divergences, demographic history and extent of gene flow.

Mitochondrial DNA is a powerful tool for genealogical and evolutionary studies of animal populations (Zhang and Hewitt, 2003) and has become the work horse of animal phylogeographic studies (Avise, 2000). Apart from exhibiting intraspecific variability and possessing a phylogenetic signal ("… a measure of the statistical dependence among species' trait values due to their phylogenetic relationships.", Revell *et al*. 2008), metazoan mtDNA possesses a suite of unique characteristics that make it suitable for evolutionary and population genetic studies (for review see Avise *et al*., 1987; Moritz *et al*., 1987). However, mtDNA has some unavoidable limitations, which render its exclusive use unadvisable. First, mtDNA reflects only the matrilineal history, which could be different from that of the overall species history (Zhang and Hewitt, 2003). This potential problem is less likely to affect this study since dispersal in the gastropods is only through eggs or larvae and there is no evidence of sex biased dispersal. Secondly, although small effective population size renders mtDNA sensitive to phylogeographic changes owing to a fast rate of lineage sorting and high allele extinction rate, it might result in: (i) underestimation of genetic diversity and, therefore, oversimplification of evolutionary relationships, (ii) increased uncertainty in genealogical analysis, and (iii) failure to detect remote population processes (Zhang and Hewitt, 2003). Furthermore, mtDNA reflects only a small proportion of the total genome content implying that evolutionary inferences might be inflated due to random lineage sorting (Pamilo and Nei, 1988). Additionally, the presence of copies of mtDNA in nuclear DNA (nuclear mitochondrial pseudogenes) and artefacts resulting from introgression, may be problematic in phylogeographic studies, since a mixture of numt DNA and real copies of mtDNA in a data set could infer incorrect relationships when contructing phylogenies (Gaziev and Shaikhaev, 2010). Owing to these limitations it is now common practice to include nuclear genes (nDNA) (e.g. Hare, 2001; Zhang and Hewitt, 2003; Brito and Edwards, 2009) to obtain a fuller picture of the history and evolutionary potential of populations. Since nDNA alleles are biparentally inherited, they complement mtDNA

data by also providing data on paternally derived gene flow (Wirgin *et al*., 2002). The currently recommended approach in phylogeographic studies, which is applied in this study, is to use cytoplasmic DNA (e.g. mtDNA) in conjunction with nuclear DNA (Domínguez-Domínguez and Vázquez-Domínguez, 2009; Gutiérrez-García and Vázquez-Domínguez, 2011). This approach allows higher confidence in reconstructed population history if there is congruence between mtDNA and nDNA (e.g. O′Neill *et al.*, 2009). Also, analysis of multiple loci provides a more in depth picture of the underlying evolutionary process, for example, detecting complex patterns of population divergence, secondary contact and gene flow (e.g. O′Neill *et al.*, 2009).

Avise (2009) identifies three main challenges in using nDNA as a marker in phylogeography: (i) the relatively slow pace of sequence evolution at many nuclear loci; (ii) the difficulty of isolating nuclear haplotypes from diploid organisms, and (iii) intragenic recombination (Avise, 2009). Moreover, because substitution rates for nDNA loci are generally slower than at protein-coding mitochondrial genes, there is usually limited variation within a single coding nuclear gene, i.e. exon (Avise, 2009; O′Neill *et al*., 2009).

The problem of limited sequence evolution can be managed through use of more rapidly evolving DNA regions such as introns. Relatively recent software (e.g. PHASE, Stephens *et al*., 2001; Stephens and Donnelly, 2003) can be used to resolve alleles from heterozygous individuals (Harrigan *et al*. 2008; Avise, 2009; Garrick *et al*., 2010). Although intragenic recombination remains a challenge, as it complicates what would otherwise be clear genealogical signatures from nuclear genome, it is now possible to test if loci have recombination hotspots so as to use suitable analytical approaches. Despite this challenge, single copy nDNA haplotypes have been used in phylogeographic analyses with some of the most informative results from them (for review see Avise, 2009).

1.5 Objectives and scope of study

The principal objective of this study is to use five intertidal gastropods as model species with which to explore the effects of Pleistocene climate changes on South Africa`s marine biodiversity. To achieve this objective, sequence data of segments of the mitochondrial cytochrome oxidase *c* subunit 1 (COI), and a segment of the nuclear ribosomal DNA (comprising part of the first Internal Transcribed Spacer, 5.8S, second Internal Transcribed Spacer and part of 28S, hereinafter called ITS; or in other species, consisting of part of 5.8S, second Internal Transcribed Spacer and part of 28S, hereinafter called ITS2), were used as genetic markers to reconstruct phylogeographic patterns and to determine demographic histories of the model species. The following approaches were used: (i) population genetic structure and gene flow patterns were assessed for each taxon; (ii) the demographic histories of the specific species or any genetic assemblages identified were reconstructed; (iii) the historical processes influencing phylogeographic patterns of the species around the South African coast were inferred, and (iv) the implications of the phylogeographic patterns for management and conservation were discussed.

As previous studies have suggested Pleistocene impacts on southern African marine species (von der Heyden *et al*., 2010; Teske *et al*., 2011), it is hypothesised that species would exhibit phylogeographic patterns and demographic histories bearing signatures of Pleistocene climatic change. However, species specific differences (e.g. habitat preferences, Crandall *et al*., 2008; life history characteristics, Teske *et al*., 2007a) will probably result in different phylogeographic responses. Thus, only by increasing the number of species studied will we be able to draw general conclusions with respect to the processes underpinning phylogeographic structure in southern African marine taxa.

Both traditional (frequentist methods like Analysis of Variance) and coalescent based data analyses are employed in characterising population genetic structure, gene flow, and demographic history. This thesis is divided into six chapters. **Chapter 1** provides background to the study

including: outlining the theoretical base, justifying the approach used, outlining the objectives of the study, and indicating the scope of the thesis. **Chapter 2** describes the study area in terms of the nature of the coast, Pleistocene climatic changes that occurred, oceanographic conditions and, the methods that were used to address the objectives of the study.

For convenience and more focussed treatment, the phylogeographic patterns and demographic histories of the taxa are discussed in three chapters. **Chapter 3** focuses on the genetic signatures of the Pleistocene climatic oscillations on the rocky shore giant periwinkle *Turbo sarmaticus* Linné, 1758. **Chapter 4** presents the comparative phylogeography of three congeneric trochids *Oxystele sinensis (Gmelin, 1791), O. tigrina* (Anton, 1891) and *O. variegata* (Anton, 1839). **Chapter 5** focuses on the population structure and demographic history of the sandy shore plough shell *Bullia rhodostoma* Reeve, L.A., 1847. **Chapter 6** presents the general discussion which puts the thesis into perspective and additionally discusses the implications of the observed phylogeographic patterns for conservation.

CHAPTER 2

MATERIALS AND METHODS

2.1 Study area

The South African shoreline measures about 3650 km in extent, from the mouth of the Orange River on the northern border with Namibia to the Mozambique border (Fig. 2.1) (Kilburn and Rippey, 1982; Griffiths *et al*., 2010). The coast is generally exposed, with a few large bays and lagoons, and no large offshore islands to break the force of oceanic swells (Kilburn and Rippey, 1982). The coastline comprises about 27% rocky shore, 42% sandy beach and 31% mixed shore (Griffiths *et al*., 2010). Using the distribution of marine invertebrates, five coastal biogeographic regions are recognised on the southern African coast based on differences in sea surface temperatures, fauna and flora (Griffiths *et al*., 2010). These are: (1) the cool-temperate Namaqua Bioregion from Lüderizt to Cape Point on the west coast; (2) the south-western Cape Bioregion; (3) the Agulhas Bioregion on the south coast; (4) the subtropical Natal Bioregion on the east coast, and (5) the Delagoa Bay Bioregion further north on the east coast (Fig. 2.1) (Griffith *et al*., 2010).

Life along the South African coast is under the influence of two major current systems. The Benguela Current flows parallel to the west coast from the southern Atlantic northwards as an offshore current before the main flow deflects away to the northwest (Wedepohl *et al.*, 2000) (Fig. 2.1). It is characterised by low temperatures of around 10 ^{o}C (Beckley *et al.*, 2002). In contrast, the east and south coasts are under the influence of the warm (temperatures of about 20 – 28 ^{o}C), southward-flowing Agulhas Current, which originates off East Africa and Madagascar (Kilburn & Rippey, 1982; Zardi *et al*., 2007; Beckley *et al.*, 2002).

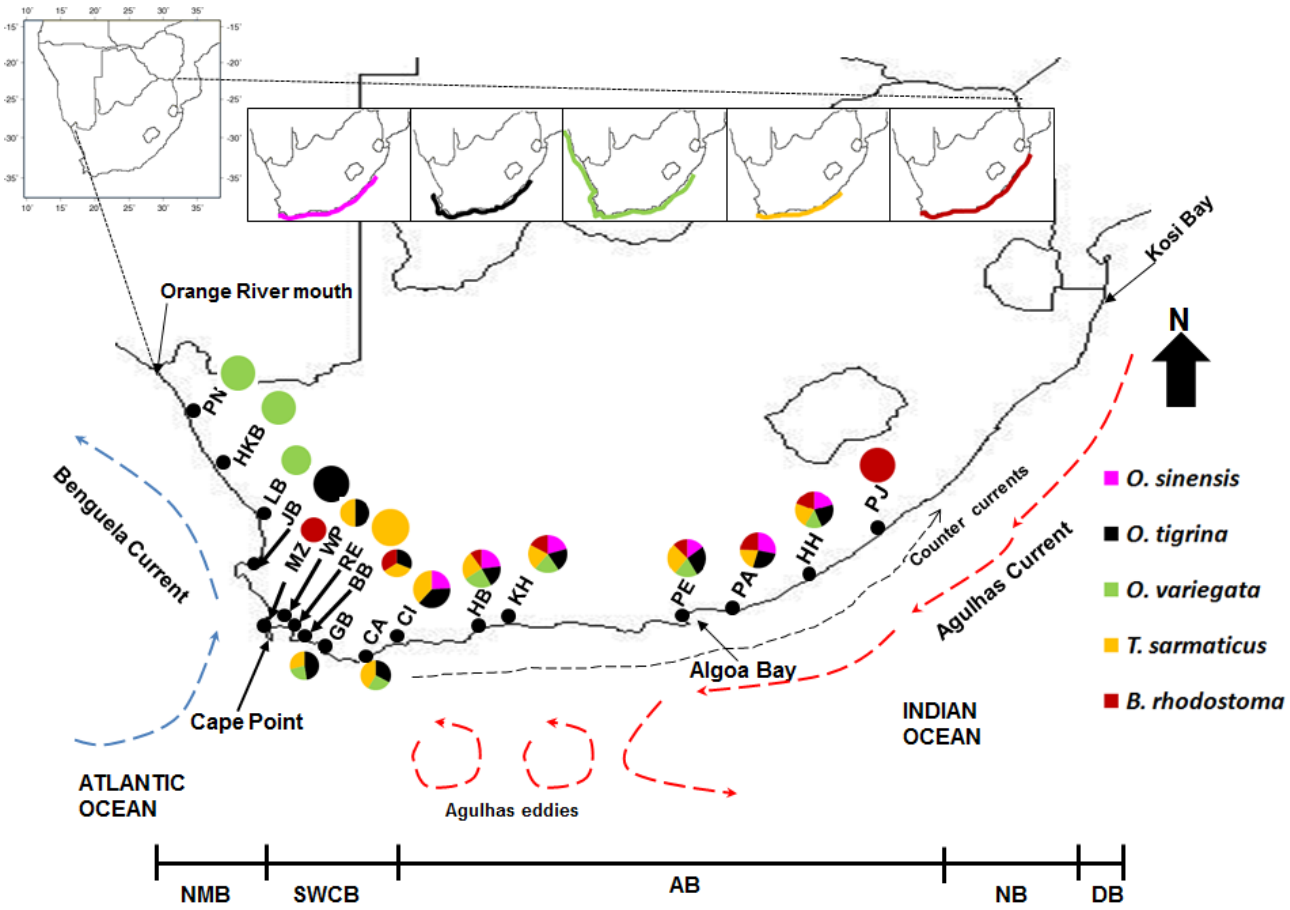

Figure 2.1 Sampling localities of *Turbo sarmaticus*, *Oxystele sinensis*, *O. tigrina*, *O. variegata* and *Bullia rhodostoma*, biogeographic regions and major oceanic currents on the South African coast. Inserts show current distribution of the species studied. Pie charts indicate the relative abundance of specimens of each species collected per locality. Locality abbreviations are as follows: PN, Port Nolloth; HKB, Hondeklip Bay; LB, Lambert′s Bay; JB, Jacob′s Bay; WP, Wooley′s Pool; MZ, Muizenberg; RE, Rooi-Els; BB, Betty′s Bay; GB, Gansbaai; CA, Cape Agulhas, HB, Herold′s Bay; KH, Knysna Heads; PE, Port Elizabeth; PA, Port Alfred; HH, Haga Haga; PJ, Port St Johns. Biogeographic regions abbreviations are as follows: NMB, Namaqua Bioregion; SWCB, South-western Cape Bioregion; AB, Agulhas Bioregion; NB, Natal Bioregion, DB, Delagoa Bioregion.

The course of the Agulhas Current is mainly along the edge of the continental shelf (Kilburn & Rippey, 1982) and it flows to the southwest along the eastern seaboard of South Africa (from 27 ^{o}S to 40 ^{o}S) (Fig. 2.1) at a rate of 10 to 20 km day^{-1} (Zardi *et al*., 2007). The Agulhas Current moves offshore following the edge of the Agulhas Bank along the south coast before it retroflects south of Cape Agulhas to flow back towards the east (Lutjeharms *et al*., 1992; Griffiths *et al*., 2010). The Benguela and Agulhas Currents meet at a transition region between Cape Point and Cape Agulhas (Evans *et al*., 2004) (Fig. 2.1).

It is hypothesised that Plio-Pleistocene sea level changes also affected the South African coastline. From about 50 to 10 thousand years ago (kya), the sea level was much lower than the present level with a minimum of -130 m during the LGM (26.5-19 kya) (Clark *et al*., 2009). During the LGM wide areas of the continental shelf, particularly around the Agulhas Bank were exposed (Dingle and Rogers 1972; Tankard, 1976). The Agulhas Bank is a gently sloping and broad continental shelf thought to cause rapid coastline changes with even small vertical shifts in sea level (Fisher *et al*., 2010). The Bank extends more than 250 km offshore at its widest point and much of it is covered with sandy sediments (Shannon, 1989). Conceivably the oceanic shore line presents features that may influence the occurrence of species and it is likely that sandy patches could form formidable barriers during regressions, especially for rocky shore taxa. Sea level also began to rise around 17 kya during the Flandrian transgression, which was interrupted by brief periods of stability and slight regressions. It is evident that much of the present form of the South African coastline developed during and after the Flandrian transgression (Grindley, 1969).

2.2. Study organisms

This study focuses on five intertidal gastropods, comprising four rocky shore inhabitants: the giant periwinkle, *Turbo sarmaticus*, the congeneric topshells, *Oxystele variegata*, *O. sinensis*, *O. tigrina;* and one sandy shore whelk *Bullia rhodostoma*, as model species (Fig. 2.2). The three *Oxystele* spp. and *T. sarmaticus* belong to the family Trochidae, which is one of the largest families of molluscs with over 60 recognized species in southern Africa (Kilburn and Rippey, 1982).

These five species were chosen as model taxa because they generally meet criteria suggested by Schmitt (2007) and Kenchington *et al*. (2009) for biogeographic studies: (i) they are native (and in this instance to the South African coast), otherwise their genealogies may not reflect the history of the region, (ii) although they have sedentary adult stage, they have potentially high dispersal ability as a consequence of a planktonic larval phase in their life cycle (except *B. rhodostoma*,

which is a direct developer), and this makes them able to spread rapidly into emerging suitable habitat, (iii) their sedentary adult stage ensures that phylogeographic patterns are not blurred by sampling effects due to movement of adults among localities. However, as for many other marine taxa in the region, there is inadequate literature on life history, biology and ecology of these species, which may compromise the depth of interpretation of some of the genetic analyses.

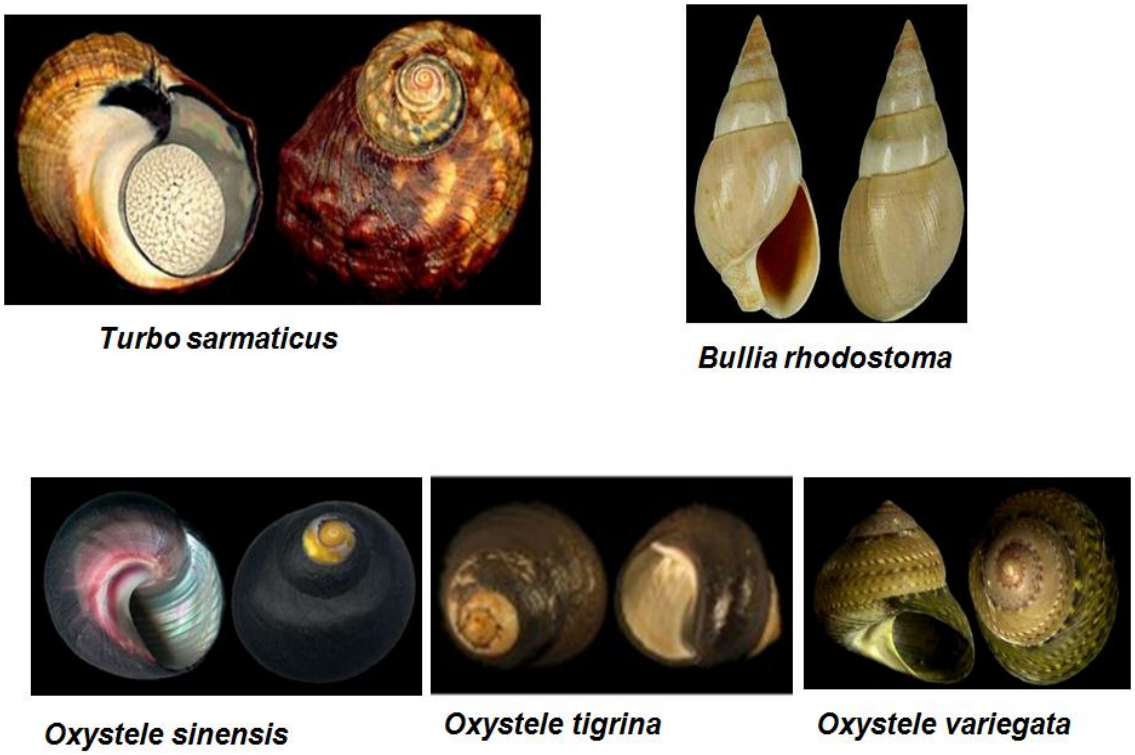

Figure 2.2 Pictures of the fives gastropod species studied (from Google images)

2.3. Sample collection and laboratory work

A total of between 140 to 232 individuals of each species were collected from a maximum of 11 localities spanning each species′ current distribution range (Fig. 2.1). Among all species, 17 localities were sampled collectively (Fig. 2.1): three sampling sites in the Namaqua Bioregion (Port Nolloth, Hondeklip Bay, Lambert′s Bay), six in the South-western Cape Bioregion (Jacob′s Bay, Wooley′s Pool, Muizenberg, Rooi-Els, Betty′s Bay, Gansbaai), five in the Agulhas Bioregion (Cape Agulhas, Cape Infanta, Herold′s Bay, Knysna Heads, Port Elizabeth), and three in the Natal Bioregion (Port Alfred, Haga Haga, Port St. Johns). More information on species specific sampling

is provided in separate chapters dealing with each species/taxonomic group separately. Samples were collected from rocky or sandy shores during low tide and an effort was made to cover most of the current distribution of each of the species along the South African coast (Fig. 2.1). The sampling design was also targeted to span the region (from Port Nolloth to Durban) where continuous range shifts reportedly occurred throughout the Pleistocene during times when the Agulhas Bank was exposed (Dardis and Grindley, 1988; Fisher *et al*., 2010).

Samples were preserved in 90% ethanol. Genomic DNA was extracted from the foot muscle using the Wizard SV Genomic DNA Purification System (Promega). Polymerase chain reactions for COI and ITS2 were conducted in separate 50 µl reactions comprising 50 – 250 ng of DNA template, 1X PCR buffer, 1.5 mM $MgCl_2$, 1mM of dNTPs, 1 pmol of each primer, and 1 U Taq polymerase (Hoffman-La Roche). The PCR thermal cycle profile for COI using the primers LCO1490 and HCO2198 (Folmer *et al.,* 1994) consisted of: an initial denaturation of 3 min at 95 ^{o}C followed by 35 cycles of denaturation for 30 s at 95 ^{o}C, annealing for 30 s at 47 ^{o}C, extension for 45 s at 72 ^{o}C, and a final extension at 72 ^{o}C for 5 min. To obtain more reliable amplification success for *Turbo sarmaticus*, species specific primers TsarmF1: 5′- GGT ATT TGG TCT GGA CTA GTT GG -3′ and TsarmR1: 5′- GGA TCT CCA CCA CCA GCA G -3′ were designed and used in PCR as outlined above except that annealing occurred at 48 ^{o}C. To amplify the nuclear ITS region (see 2.4.1 below for description) the primers PreBF (5′-GTA GGT GAA CCT GCA GAA GGA-3′) and 28Sr1 (5′-CGG TAC TTG TTC GCT ATG GG-3′) were used (Bass *et al*., 2007). The following thermal cycling parameters were used to PCR amplify the nuclear region: an initial denaturing step at 94 ^{o}C for 3 min, followed by 36 cycles of 20 s denaturing at 94 ^{o}C, 20 s of annealing at 55 ^{o}C, and 45 s of extension at 72 ^{o}C, and a final extension of 72 ^{o}C for 7 min. All PCRs were performed on GeneAmp® PCR System 2700 thermocyclers (Applied Biosystems).

PCR products were detected on a 1% agarose gel stained with ethydium bromide before the amplified products were purified using the GFX® DNA or Gel Band purification kits (GE Healthcare). Sequences were generated in one direction with the reverse primers using BigDye

terminator chemistry (Applied Biosystems) and analysed on an ABI-3100 automated sequencer. Sequence data were edited and aligned with ClustalW (Thompson *et al*., 1994) incorporated in BioEdit (Hall, 1999).

2.4. Data analyses

Sequences were collapsed into haplotypes using DnaSP version 5.0 (Librado and Rozas, 2009) and PHASE version 2.0.2 (Stephens *et al*., 2001; Stephens and Donnelly, 2003) was used to predict the allelic phase of the nuclear data. One million iterations were performed and the first 10 000 were discarded as burn-in, and a thinning interval of 1 was used. A probability threshold of 0.60 was used, following the recommendations in Harrigan *et al.* (2008) and Garrick *et al*. (2010). The nucleotide substitution models with best fit to the mitochondrial and nuclear DNA sequences were estimated with jMODELTEST version 0.1.1 (Posada, 2008) and selection of models were done using the Bayesian information criteria (BIC).

2.4.1 Genetic diversity

Genetic diversity within populations was quantified for both COI and the ITS region as haplotype diversity (*h*) and nucleotide diversity (π) (Nei, 1987). For *T. sarmaticus* the amplified ITS region comprised ITS1, 5.8S, ITS2 and part of 28S; (hereinafter called ITS for convenience) whereas for the *Oxystele* species it consisted of 5.8S, ITS2 and part of 28S; (hereinafter called ITS2 for convenience). Haplotype diversity (also known as gene diversity) represents the probability that two randomly sampled alleles are different, whereas nucleotide diversity is defined as the average number of nucleotide differences per site in pairwise comparisons among DNA sequences (Nei, 1987). These indices were estimated for each population, distinct lineages and the entire pooled

population (species) using ARLEQUIN version 3.5.1.2 (Excoffier and Lischer, 2010), which implements the diversity indices algorithms described by Nei (1987).

2.4.2 Intraspecific genealogy

To investigate genealogical relationships of haplotypes for COI and ITS for each species, haplotype networks were constructed using the statistical parsimony procedure in the programme TCS version 1.21 (Clement *et al.*, 2000). This procedure estimates an unrooted network and provides a 95% plausible set of connections for all haplotype linkages.

2.4.3 Population genetic structure and gene flow

2.4.3.1 Analysis of molecular variance

Since the primary genetic barriers on the South African coast have been inferred to occur in the regions around: (1) Cape Point, (2) Cape Agulhas and (3) Algoa Bay (Teske *et al.*, 2011), Analysis of Molecular Variance (AMOVA) as implemented in ARLEQUIN was performed to test hypotheses of population genetic structuring based on these genetic breaks (adapted to the distribution range of each of the study species). The optimal nucleotide substitution model, estimated as explained above, was used for each species.

For both markers, pairwise genetic differentiation between populations was estimated with Φ_{ST} as implemented in ARLEQUIN under the same conditions described for AMOVA. Φ_{ST} incorporates information on haplotype frequencies as well as haplotype sequence differences. Significance of Φ_{ST} values was evaluated using 10 000 permutations at family-wise α (overall α level before adjusting for multiple comparisons) = 0.05. The Benjamini-Yekutieli (B-Y) false

discovery rate corrections (Benjamini and Yekutieli, 2001; Narum, 2006) were applied to minimise inflated Type 1 error caused by simultaneous multiple comparisons.

Since there might be more suitable spatial population groupings than the *a priori* hypotheses tested with AMOVA, the Bayesian analysis of genetic population structure (BAPS version 5.3) (Corander and Tang, 2007; Corander *et al*., 2008) was used to further test for evidence of genetic differentiation. The model investigates whether there is evidence for genetic structuring assuming neutrality of the marker used without making *a priori* assumptions about the location of phylogeographic breaks.

2.4.3.2 Isolation by distance

To test a hypothesis of correlation between pairwise genetic distances and geographic distances between populations, isolation by distance (IBD) analyses were conducted using Mantel tests as implemented in ARLEQUIN with 10 000 simulations for each run. Geographic distances (taken as the shortest along coast distance between localities) were determined in kilometres from a scaled map.

2.4.3.3 Coalescent analysis of gene flow

Coalescent analyses were used to examine historical gene flow using the programme MIGRATE version 3.0.3 (Beerli and Felsenstein, 1999). MIGRATE estimates the Theta parameter ($\theta = N_e\mu$, N_e is effective population size, μ is mutation rate per site per generation) for each population and gene flow ($M = m/\mu$, is a measure of the extent to which immigration exceeds mutation in acting as a source of new variants entering the population; m is migration rate) between multiple populations (Beerli and Felsenstein, 1999). A stepping stone migration model was used considering the linear nature of the South African coastline and therefore gene flow was only estimated between populations occurring adjacent to one another. However, violation of the stepping stone model for rocky shore species could not be ruled out since they have pelagic larvae that could facilitate long-distance dispersal even between distant localities. The MIGRATE analysis

was run for the combined COI and ITS data following the protocol outlined in von der Heyden *et al*. (2008). The MIGRATE analyses were run with the following Markov chain settings. The initial values for theta and *m* were estimated from F_{ST}. Two analytical runs were performed, an initial short run and a subsequent long run. For the long run, 10 short-chains, each with a total of 50 000 generations and a sampling increment of 20 generations, and two long chains with an increment of 50 were run. A total of 2500 and 25000 genealogies were visited by the short and long chains, respectively. The first 5000 genealogies were discarded as burn-in for both short and long chains. An adaptive heating scheme with four chains with the starting values of 5.00, 2.50, 1.50 and 1.00 and a swapping interval of one was used. Default values for the other settings were used. The programme was run 5 times with different random seed numbers using the same conditions for each species. Results from the 10 runs were averaged and used to obtain 95% confidence interval estimates of parameters. Number of migrants per generation (N_em or Nem for mtDNA) between each pair of adjacent populations was then estimated as $N_em_i = \theta_i$ x $M_{j\rightarrow i}$, where i = receiving locality and j = source locality. The 95% confidence intervals incorporated the 2.5% and 97.5% percentiles of both θ_i and $M_{j\rightarrow I}$ were determined following Keeney *et al*. (2009).

2.4.3.4 Time of divergence

Divergence time among distinct genetic assemblages was estimated in BEAST. Details for divergence analysis are given where appropriate in the respective Chapters.

2.4.4 Demographic history

2.4.4.1 Fu's Fs and mismatch distributions

Fu′s F_s (Fu, 1997) test was performed in ARLEQUIN with 10 000 permutations to test for deviations from neutrality consistent with a recent population expansion or a selective sweep in a historically stable population (Fu, 1997). This was conducted for the entire dataset, identified genetic assemblages, as well as for individual sampling localities. This test was chosen because of its statistical power in detecting significant changes in population size when using small sample sizes (Ramos-Onsins and Rozas, 2002). Under the assumption of selective neutrality, a statistically

significant negative value indicates an excess of low-frequency haplotypes, and this could amongst other factors be consistent with a signature of recent demographic expansion (Fu, 1997). Positive values are expected if rare alleles are eliminated from populations following genetic bottlenecks or as a consequence of purifying selection (Tajima, 1989). Following Fu (1997) and Excoffier *et al.* (2006) Fu‟s Fs values were considered as significant at the 5% level, if their p-values were below 0.02, and not below 0.05.

The McDonald and Kreitman (1991) test as implemented in DnaSP was performed to determine whether or not deviations from neutrality were caused by selection acting on the COI gene. This test is based on comparing the ratio of synonymous to nonsynonymous substitutions between the ingroup and the outgroup (a closely related species), and within the ingroup. To further explore the possibility of recent demographic expansion (pure demographic expansion or range expansion), analysis of frequency distributions of the number of pairwise nucleotide differences between haplotypes (= mismatch distribution) (Rogers, 1995; Rogers and Harpending, 1992) was used to specifically test for both pure demographic expansion and range expansion using ARLEQUIN. Both these processes may have influenced gastropods during or after glacial cycles. This was done by comparing the observed distribution with that expected under both a pure demographic expansion model, wherein a stationary population experiences a sudden increase in effective population size (Rogers and Harpending, 1992) and a sudden range expansion model, wherein the range of a population increases (Excoffier, 2004). Under an infinite sites model and in the absence of selection, population expansion would be depicted as a unimodal distribution whereas a ragged and multimodal distribution would indicate population stability (Harpending *et al*., 1998). A bimodal distribution may suggest spatial expansions with low gene flow among populations (Ray *et al*., 2003). The raggedness index (*r*, sum of squared differences between neighbouring peaks) was used to assess the significance of the fit of the mismatch distribution to that of an expanding population, where non-significant and low *r* index values infer population expansion. Additionally, the goodness-of-fit between the observed distributions and those expected

under a pure demographic expansion or a range expansion model was tested by the sum of squared deviations (*SSD*) statistics (Rogers and Harpending, 1992), wherein a significant *SSD* p-value represents a departure from the estimated demographic expansion model. Statistical significance was assessed on the parameters with 10 000 bootstrap replicates under the null hypothesis of recent population expansion. Probability-values were calculated as the proportion of simulations producing a larger SSD than the observed SSD value by chance alone. The mismatch analysis provides estimates of approximate time of population expansion using the formula $t = \tau/2u$ (rearranged from Rogers and Harpending, 1992), where t = time since expansion in generations, τ = the mode of mismatch distribution in mutational units, u = mutation rate per generation for the entire sequence (u = number of nucleotides of the analysed segment * mutation rate per nucleotide * generation time in years). Time since expansion was converted to years by multiplying t by generation time. Two COI mutation rates (0.35% and 2% Myr^{-1} per lineage; see above), corresponding to the lowest and highest divergences for gastropods documented at present in the literature, were used. These substitution rates enable calculation of rough estimates of the timing of the onset of expansion to capture the earliest and last possible times of expansion, respectively, based on the COI gene. It was not possible to convert the peaks of the mismatch distributions for ITS to time since expansion because of the lack of estimates of mutation rate for this DNA marker. Additionally, mismatch analysis provides estimates of θ_0 and θ_1, where $\theta = N_e\mu$, thereby providing estimates of the pre- and post-expansion effective population size, respectively.

2.4.4.2 Bayesian skyline plots

Fu′s F_s and mismatch distributions provide insights into whether or not populations have expanded but they do not indicate the shape of the population growth over time (Nuñez *et al*., 2011). Therefore, population demographic histories were further explored with a Bayesian skyline plot (BSPs) method developed by Drummond *et al.* (2005) as implemented in the programme

BEAST. BEAST uses Markov Chain Monte Carlo sampling procedures to estimate changes in effective population size over time and the approximate time since the beginning of population expansion. Owing to a lack of fossil calibration points or obvious vicariance cases, species specific mutation rates for estimating coalescence times could not be derived for all five taxa. Therefore, for the COI gene, mutation rates from the literature were used to determine priors for estimating substitution rates for each species using the relaxed lognormal option in BEAST. Substitution rates ranging from 0.35 x 10^{-8} site^{-1} yr^{-1} (corresponding to mutation rate of 0.35% Myr^{-1},Marko, 2002) to 4.43 x 10^{-8} site^{-1} yr^{-1} (*Nucella lapillus*, Wares and Cunninghum, 2001) have been recorded for gastropods. To estimate substitution rates in BEAST, with the clock rate set relaxed lognormal and estimate rate, the lowest rate of 0.35 x 10^{-8} site^{-1} yr^{-1} and the highest rate of 4.43 x 10^{-8} site^{-1} yr^{-1} were used as the lower and upper limits, respectively. The mean of the recorded substitution rates (1.17 X 10^{-8} site^{-1} yr^{-1}) was used as the initial value under the uniform priors option. The estimated rates were used to reconstruct BSPs for each species. Data obtained using the lowest rate published for molluscs (0.35 x 10^{-8} site^{-1} yr^{-}1) and the most commonly used rate for gastropods (1.0 x 10^{-8} site^{-1} yr^{-1}) are also included for comparison. For each BSP, between 30 and 90 million steps of the MCMC chains were run under a relaxed uncorrelated molecular clock with uniform distributed priors, sampling every 1000 steps; the first 10% being discarded as burn-in. The length of each run was deemed adequate if the ESS were above 200 and a good mixing of chains was observed. An estimated clock rate, obtained as explained above, was specified to determine timing of expansion for the COI data in years before present. Under these settings, Tracer yields estimates of N_eT over time, where N_e = effective population size and T = generation time. Since the timing of relative changes in N_e rather than absolute values of N_e was of interest, changes in unadjusted values of N_eT over time were reported in BSPs for COI. For ITS, the programme was run with default priors for clock rate (at 1.0) resulting in BSPs showing change in $N_e\mu$ over time in mutational units. The BSPs for each analysis were visualised in Tracer version 1.5 (Rambaut and Drummond, 2007). Because the method used in BEAST assumes that alleles or haplotypes are sampled from the same

population, BSPs for all species exhibiting population structure were performed separately for each genetic assemblage, whereas data were pooled if populations were genetically homogenous.

CHAPTER 3

THE EFFECT OF PLEISTOCENE CLIMATIC CHANGES ON THE PHYLOGEOGRAPHY OF A SOUTH AFRICAN ROCKY SHORE TURBAN SHELL *TURBO SARMATICUS*

3.1. Introduction

The giant periwinkle, *Turbo sarmaticus*, is one of the most heavily exploited molluscan species on the South African coast and is used for food and as bait for angling (Foster and Hodgson, 2000; Proudfoot *et al*., 2006). Given its large size (average shell length = 100 mm) and easy access to its habitat, it is not surprising that *T. sarmaticus* is also ear-marked for commercial exploitation (Griffiths and Branch, 1997; Proudfoot *et al*., 2006).

Turbo sarmaticus inhabits intertidal rocky shores, occurring under submerged rocks, in rocky pools, and enters the shallow subtidal zone down to a depth of about 8 m (Kilburn and Rippey, 1982; Branch *et al.*, 2002). Its distribution is thus closely linked to the changing shoreline and sea level. It grows slowly, reaching its minimum legal collection size (approx 64 mm) in three to four years (Branch *et al*., 2010). The current distribution of *T. sarmaticus* ranges from False Bay (immediately east of Cape Point) to Haga Haga (Kilburn and Rippey, 1982) (Fig. 3.1) and the species is endemic to the South African coast. Despite its economic importance, there are to date no published data on the population genetics or phylogeography of *T. sarmaticus*.

The reproductive biology of the family Turbinidae is characterised by laying eggs in gelatinous masses, external fertilisation with embryos hatching as free-swimming larvae (Kilburn and Rippey, 1982). Although this group is thought to have a short pelagic larval duration, observations of a major reproductive period between September and March, and appearance of recruits in the intertidal in the following winter (June-July) (McQuaid, 1983) suggests a longer pelagic larval duration. This observation suggests a pelagic larval development of four to nine months.

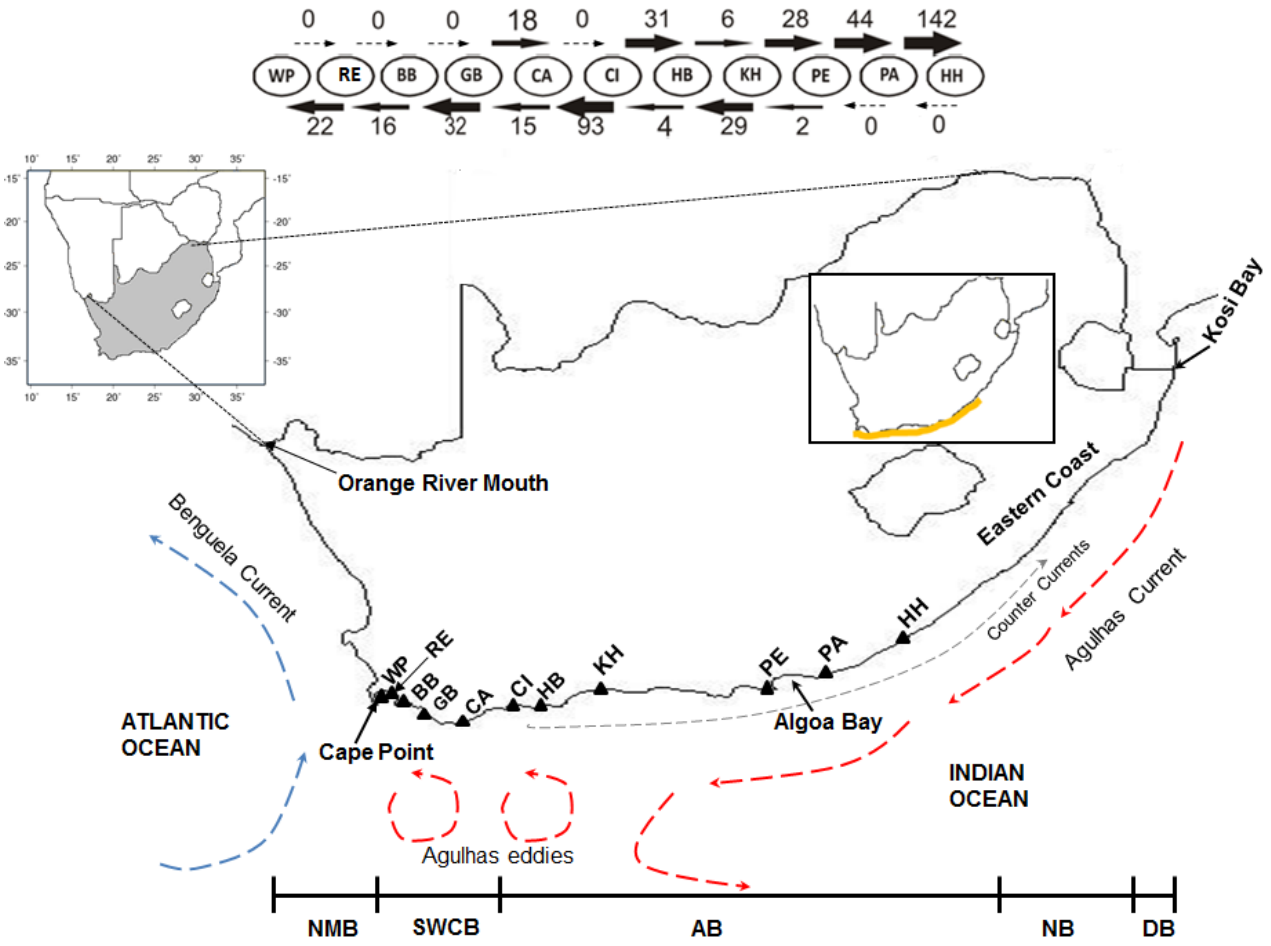

Figure 3.1 Sampling localities for *Turbo sarmaticus*, oceanic currents, bioregions and number of migrants per generation between adjacent localities on the South African coast. Arrows indicate the direction of gene flow and the thickness of an arrow is proportional to the number of migrants per generation. Numbers above and below the arrows indicate the relative migration rates. The insert shows current distribution of *T. sarmaticus*. Locality abbreviations are as follows: WP, Wooley's Pool; RE, Rooi-Els; BB, Betty's Bay; GB, Gansbaai; CA, Cape Agulhas, CI, Cape Infanta; HB, Herold's Bay; KH, Knysna Heads; PE, Port Elizabeth; PA, Port Alfred; HH, Haga Haga. NMB, Namaqua Bioregion; SWCB, South-western Cape Bioregion; AB, Agulhas Bioregion; NB, Natal Bioregion, DB, Delagoa Bioregion.

The adults and juveniles are sedentary, leaving the pelagic larval phase responsible for dispersal and gene flow. Long-range movements by adults, which could blur historical signals, are more than likely absent, making *T. sarmaticus* a suitable species to detect barriers to larval dispersal. This chapter uses sequences of segments of the mitochondrial COI gene and the nuclear Internal Transcribed Spacer region, ITS (encompassing part of ITS1, 5.8S, ITS2 and part of 28S), to explore the range-wide phylogeography and demographic history of *T. sarmaticus*. Specifically, the

chapter focuses on unravelling the footprints of Pleistocene climatic changes on: (1) genetic diversity, (2) population subdivision, and (3) the demographic history of the species.

Given the paleogeographic history of the South African coast, and the life history of *T. sarmaticus*, a number of predictions about its phylogeographic history can be tested in the present study. First, if there is structure in the population as a result of Pleistocene sea level fluctuations, it is expected that divergences among populations should date to the Pleistocene. Secondly, it is expected that species will bear a signature of demographic expansion subsequent to the Pleistocene climatic changes. Thirdly, shallow or no phylogeographic genetic structuring is expected since *T. sarmaticus* is a broadcast spawner with a planktonic larval stage.

3.2 Materials and Methods

Materials and methods used in this chapter were as given in **Chapter 2** with the following additional information. Two hundred and thirty two specimens of *T. sarmaticus* were collected from 11 localities as indicated on Fig. 3.1 and Table 3.1. All of the genetic structure calculations were performed in ARLEQUIN using the Tamura-Nei nucleotide substitution model (Tamura and Nei, 1993) for COI and Kimura 2 parameter (K80, Kimura, 1980) model was used for ITS. The same substitution models were used in BEAST to construct BSPs. A substitution rate of 2.4% Myr^{-1} or 2.4×10^{-8} substitutions $site^{-1}$ yr^{-1} was estimated for this species in BEAST using published substitution rates for other gastropods (see 2.4.4.2 for details) as informative priors. The McDonald and Kreitman (1991) test was performed with *Turbo jonathani* as an outgroup using sequences from GenBank (accession numbers AM403884 and AM403883).

Table 3.1 Geographical location and sample size of the 11 localities sampled for *Turbo sarmaticus*

Bioregion	Locality (Abbreviation)	Latitude	Longitude	Sample size
Agulhas	Woolley‟s Pool (WP)	S34^{0}04	E18^{0}16	21
Agulhas	Rooi-Els (RE)	S34^{0}10	E18^{0}29	21
Agulhas	Betty‟s Bay (BB)	S34^{0}12	E18^{0}33	24
Agulhas	Gansbaai (GB)	S34^{0}21	E19^{0}11	11
Agulhas	Cape Agulhas (CA)	S34^{0}29	E20^{0}00	24
Agulhas	Cape Infanta (CI)	S34^{0}15	E20^{0}30	22
Agulhas	Harold‟s Bay (HB)	S34^{0}01	E22^{0}13	22
Agulhas	Knysna Heads (KH)	S34^{0}03	E23^{0}01	24
Agulhas	Port Elizabeth (PE)	S33^{0}34	E25^{0}23	23
Agulhas	Port Alfred (PA)	S33^{0}21	E26^{0}31	17
Agulhas	Haga Haga (HH)	S32^{0}27	E28^{0}08	23
	Total			232

3.3 Results

3.3.1 Genetic diversity

A total of 232 COI sequences (each 549 bp long) containing 45 polymorphic nucleotide positions that defined 35 haplotypes, were sampled (Table 3.2). These haplotypes are available in GenBank under accession numbers JX303523-JX303557. The most common haplotype occurred in 168 individuals (72% of the individuals sampled) and was sampled at all localities across the species range. The second most common haplotype occurred in 33 individuals (16% of the total sample) of which most individuals (27) were sampled from geographically central localities of Cape Infanta and Herold's Bay. Twenty three (66 %) haplotypes were private (unique to a single population), most of them being singletons (Fig. 3.2; Table 3.2).

Haplotype diversity (h) within sampling sites ranged from 0.35±0.17 to 0.68±0.11 (Table 3.3). Nucleotide diversity (π) was consistently low, ranging from 0.001±0.001 to 0.003±0.002 (Table 3.3). The overall values of the haplotype diversity and nucleotide diversity for the entire data set were 0.63±0.03 and 0.002±0.002, respectively.

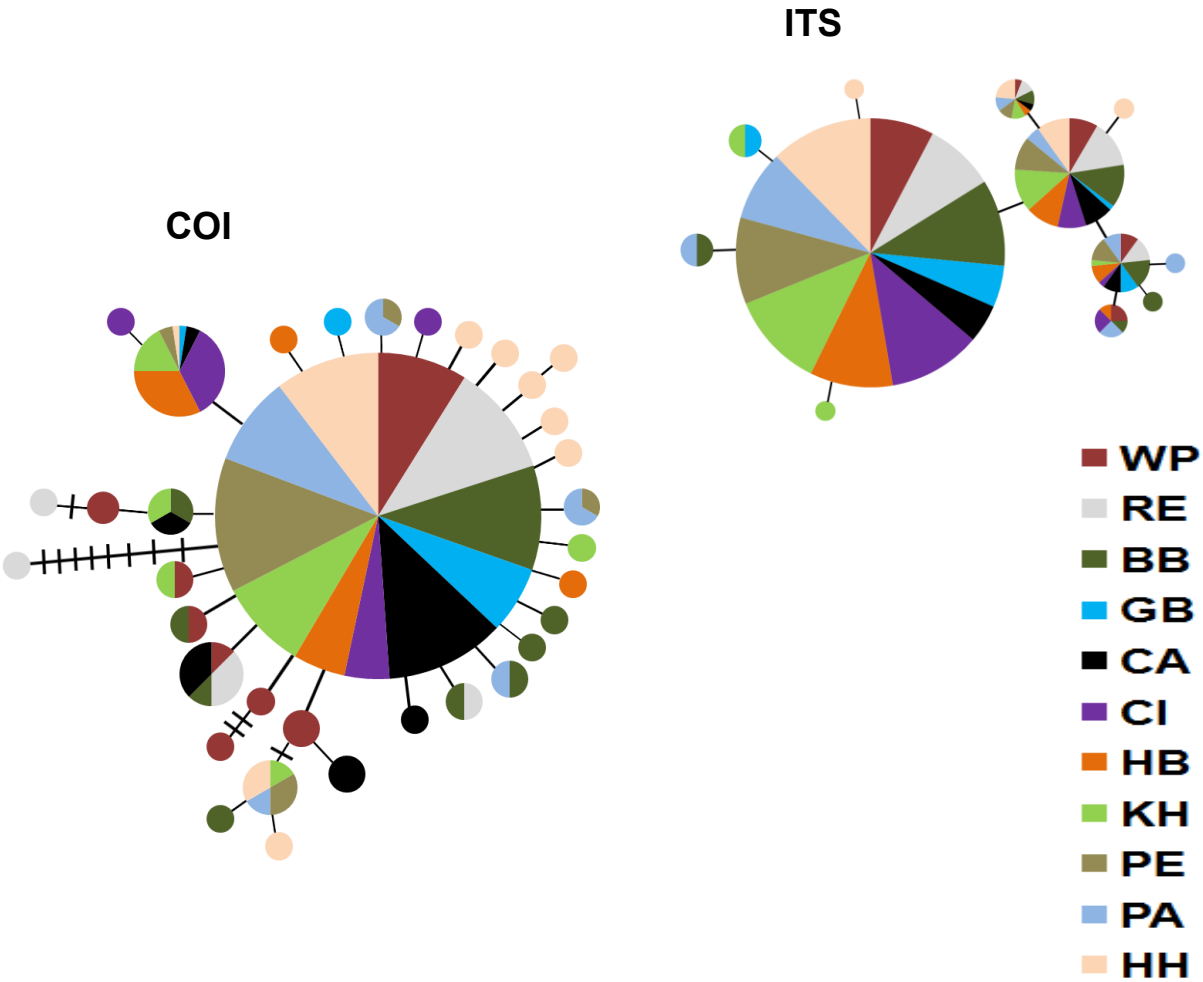

Figure 3.2 Parsimony network of 36 COI haplotypes of *T. sarmaticus* based on 232 sequences. A circle represents a haplotype and its size is proportional to the frequency of the haplotype. The smallest solid circle represents a frequency of one. Cross hatching indicate inferred intermediate haplotypes (mutational steps) not observed in the data. Locality abbreviations are as follows: WP, Wooley′s Pool; RE, Rooi-Els; BB, Betty′s Bay; GB, Gansbaai; CA, Cape Agulhas, CI, Cape Infanta; HB, Herold′s Bay; KH, Knysna Heads; PE, Port Elizabeth; PA, Port Alfred; HH, Haga Haga.

For ITS, 777 bp (encompassing part of ITS1, 5.8S, ITS2 and part of 28S) were obtained from 198 individuals. Eleven variable sites were recovered, which yielded a total of 12 haplotypes (Table 3.2). Haplotypes have been deposited with GenBank under the following accession numbers JX303649-JX303660. Unlike COI, only four (33%) of the ITS haplotypes were private, three being singletons. The most common haplotype, A1, (with an overall frequency of 66%) was observed at all sampled locations across the distribution range (Table 3.2). The second most common haplotype, A3, also occurred in all populations, but with a much lower overall frequency (18%). Haplotype

diversity ranged from 0.40±0.09 to 0.64±0.08 and nucleotide diversity (π) ranged from 0.063±0.054 to 0.121±0.088 (Table 3.3).

3.3.2. Population structure and gene flow

3.3.2.1 Analysis of spatial structure and pairwise population differentiation

Pairwise Φ_{ST} values for COI indicated that two localities (CI and HB) close to the centre of the distribution were genetically homogenous and were both differentiated from most populations to their east and west (Table 3.4). In contrast, all pairwise Φ_{ST} values for ITS were low; most of them zero, and all were not significant ($p > 0.011$) after the B-W false discovery rate correction (Table 3.4). When AMOVA was run without defining population groups, low but significant global Φ_{ST} values were obtained for both loci ($\Phi_{ST} = 0.12$, $p < 0.05$ for COI and $\Phi_{ST} = 0.01$, $p < 0.05$ for ITS; Table 3.5) with variation within populations accounting for about 90% and 98% of total variation for COI and ITS, respectively.

When the localities were partitioned into three bioregional groups: South-western Cape Bioregion (WP, RE, BB, GB, CA), Agulhas Bioregion (CI, HB, KH, PE), and Natal Bioregion (PA, HH) to test for possible genetic barriers around Cape Agulhas and Algoa Bay, AMOVA showed shallow but significant variation among the bioregional groups ($\Phi_{CT} = 0.09$, $p < 0.05$, for COI) with variation among regions accounting for about 9% of total variation (Table 3.5). There was no significant variation among localities within regions ($\Phi_{SC} = 0.127$, $p > 0.05$; Table 3.4). Additionally, most molecular variation (85%) was explained by within locality variability (Table 3.5), which agrees with the high levels of haplotype diversity found in most populations. Similarly, a weaker but significant genetic structure was observed for ITS ($\Phi_{CT} = 0.02$, $p < 0.05$, Table 3.5) for the same bioregional grouping configuration. As for COI, variability within populations explained most of the variation (98%) but variation among localities within groups was non-significant (Table 3.5).

BAPS recovered no spatial genetic structure for either marker, casting doubt on the significance of the genetic structuring suggested by the other analyses. The Mantel test did not recover a significant relationship ($p > 0.05$, $r = 0.09$) between geographic distance and genetic distance across all localities.

Table 3.2 Haplotype frequencies for the 11 localities for *Turbo sarmaticus* sampled along the South African coast. N is the number of individuals sequenced for COI or ITS for each locality.

Locality	N	haplotypes																																
		COI																																
		1	**2**	**3**	**4**	**5**	**6**	**7**	**8**	**9**	**10**	**11**	**12**	**13**	**14**	**15**	**16**	**17**	**18**	**19**	**20**	**21**	**22**	**23**	**24**	**25**	**26**	**27**	**28**	**29**	**30**	**31**	**32**	**33**	**34**	**35**	**36**
WP	**21**	12	1	1	1	1	2	1	1	1																										
RE	**21**	15		0		3					10	1	1																							
BB	**24**	14				1		1			1			1	1	1	1	2	1																	
GB	**11**	9																2		1																
CA	**21**	16				3									1			2			2															
CI	**22**	6																14				1	1													
HB	**22**	7																13						1	1											
KH	**24**	12								1					1			7								1	1	1								
PE	**23**	18																2									2		1							
PA	**17**	12												1													1		2	1						
HH	**23**	14																1									2				1	1	1	1	1	1
		ITS																																		
WP	**16**	20	3	6	2	11																														
RE	**19**	22	4	10		2																														
BB	**23**	27	5	9	1	2	1	1																												
GB	**10**	13	3	1	2				1																											
CA	**11**	12	3	6		1																														
CI	**19**	29	1	6	2																															
HB	**19**	26	3	7	1	1																														
KH	**22**	30	1	9		2			1	1																										
PE	**20**	27	4	7		2																														
PA	**16**	22	3	3		2		1			1																									
HH	**23**	32		7		4						1	2																							

Table 3.3 Molecular diversity indices for COI and ITS sequences for *Turbo sarmaticus* from 11 localities. Localities, number of individuals sequenced (N), number of haplotypes (N_h), haplotype diversity (h), nucleotide diversity (π) are listed.

Population/lineage	COI				ITS			
	N	N_h	h±SD	π±SD	N	N_h	h±SD	π±SD
Wooley′s Pool	21	9	0.68±0.11	0.002±0.002	8	5	0.58±0.09	0.098±0.074
Rooi-Els	21	6	0.55±0.12	0.003±0.002	19	4	0.60±0.06	0.080±0.064
Betty′s Bay	24	10	0.67±0.11	0.002±0.002	23	7	0.62±0.07	0.100±0.074
Gansbaai	11	3	0.35±0.17	0.001±0.001	10	5	0.57±0.12	0.121±0.088
Cape Agulhas	24	5	0.55±0.11	0.001±0.001	11	4	0.64±0.08	0.086±0.068
Cape Infanta	22	4	0.54±0.09	0.001±0.001	19	4	0.40±0.09	0.065±0.056
Herold′s Bay	22	4	0.57±0.08	0.001±0.001	19	5	0.50±0.08	0.076±0.062
Knysna Heads	24	7	0.68±0.07	0.002±0.001	22	6	0.50±0.08	0.063±0.054
Port Elizabeth	23	4	0.39±0.12	0.001±0.001	19	4	0.51±0.08	0.074±0.060
Port Alfred	17	5	0.51±0.14	0.001±0.001	16	6	0.52±0.10	0.093±0.071
Haga Haga	23	9	0.64±0.11	0.003±0.002	23	5	0.49±0.08	0.069±0.058
Whole data set	232	36	0.63±0.03	0.002±0.002	198	12	0.53±0.03	0.072±0.058

Table 3.4 Pairwise Φ_{ST} values of mitochondrial COI (above diagonal) and nuclear ITS (below diagonal) among the 11 *Turbo sarmaticus* sampling localities included in the present study. Φ_{ST} Values in bold represent those that were significant after B-Y false discovery rate correction ($p < 0.011$).

	WP	RE	BB	GB	CA	CI	HB	KH	PE	PA	HH
WP		0.004	0	0	0	**0.325**	**0.269**	**0.063**	0.01	0	0.017
RE	0		0	0.010	0	**0.299**	**0.246**	**0.069**	**0.028**	0.015	**0.036**
BB	0	0		0	0	**0.275**	**0.214**	0.016	0	0	0.003
GB	0	0	0		0	**0.346**	**0.276**	0.007	0	0	0
CA	0	0.013	0	0		**0.323**	**0.260**	0.045	0.011	0.018	0.029
CI	0.006	0.027	0.015	0.037	0.006		0	0.131	**0.323**	**0.378**	**0.289**
HB	0	0	0	0	0	0		0.074	**0.258**	**0.319**	**0.236**
KH	0.023	0.021	0.023	0.036	0.048	0	0		0.021	**0.067**	0.046
PE	0	0	0	0	0	0	0	0		0	0
PA	0	0	0	0	0	0	0	0	0		0.003
HH	0.039	0.032	0.037	0.049	0.071	0.008	0.008	0	0	0.002	

WP, Wooley′s Pool; RE, Rooi-Els, BB; Betty′s Bay; GB, Gansbaai; CA, Cape Agulhas; CI, Cape Infanta; HB, Herold′s Bay; KH, Knysna Heads; PE, Port Elizabeth; PA, Port Alfred; HH, Haga Haga

Table 3.5 Hierarchical analysis of molecular variance for the mitochondrial COI and nuclear ITS in *Turbo sarmaticus* from 11 localities grouped as follows: (a) whole population; (b) among putative groups defined by known genetic barriers: south-western (WP, RE, BB, GB, CA) vs south (CI, HB, KH, PE) vs south-east (PA, HH).

Source of Variation	df	Variation (%)	Φ statistics	P	df	Variation (%)	Φ statistics	P
	COI				ITS			
(a) Global								
Among localities	9	12.14	0.12	0.00	9	1.18	0.01	0.11
Within localities	211	87.86			324	98.82		
(b) Among putative groups								
Among groups	2	9.12	0.09	0.02	2	2.00	0.02	0.01
Among localities within groups	8	5.40	0.05	0.00	7	0.00	0.00	0.62
Within localities	211	85.48	0.15	0.00	324	98.00	0.02	0.11

WP, Wooley′s Pool; RE, Rooi-Els, BB; Betty′s Bay; GB, Gansbaai; CA, Cape Agulhas; CI, Cape Infanta; HB, Herold′s Bay; KH, Knysna Heads; PE, Port Elizabeth; PA, Port Alfred; HH, Haga Haga

3.3.2.2 Coalescent analysis of gene flow

The pairwise estimates of the number of migrants per generation (N_em) obtained for the combined COI and ITS data, together with their 95% confidence intervals are presented in Table 3.6. Gene flow is clearly asymmetrical being westwards on the south-west coast from CI to WP (Fig. 3.1) with no evidence of gene flow in the reverse direction with the exception of between GB and CA (Fig. 3.1) where gene flow seems symmetrical.

Table 3.6 Directionality of gene flow for *T. sarmaticus* between each locality pair for the stepping stone migration model along the South African coast based on the combined COI and ITS data set. Numbers indicate relative migration rates (N_em) and in brackets are the 95% confidence intervals.

From population	To population	N_em	95% Confidence Interval
Wooley′s Pool (WP)	Rooi-Els	0.00	0.00-0.00
Rooi-Els (RE)	Wooley′s Pool	21.91	3.97-87.92
Rooi-Els	Betty′s Bay	0.00	0.00-1.56
Betty′s Bay (BB)	Rooi-Els	15.93	8.21-31.14
Betty′s Bay	Gansbaai	0.00	0.00-0.00
Gansbaai (GB)	Betty′s Bay	31.68	8.69-62.01
Gansbaai	Cape Agulhas	18.30	0.85-98.83
Cape Agulhas (CA)	Gansbaai	14.52	9.00-53.58
Cape Agulhas	Cape Infanta	0.00	0.00-171.90
Cape Infanta (CI)	Cape Agulhas	93.02	30.82-381.22
Cape Infanta	Herold′s Bay	30.89	13.94-73.62
Herold′s Bay (HB)	Cape Infanta	3.80	2.20-6.38
Herold′s Bay	Knysna Heads	5.96	3.52-79.04
Knysna Heads (KH)	Herold′s Bay	28.96	12.94-69.62
Knysna Heads	Port Elizabeth	27.57	15.85-48.95
Port Elizabeth (PE)	Knysna Heads	2.15	0.99-38.32
Port Elizabeth	Port Alfred	44.23	20.53-102.93
Port Alfred (PA)	Port Elizabeth	0.00	0.00-1.01
Port Alfred	Haga Haga	141.74	39.43-763.42
Haga Haga (HH)	Port Alfred	0.00	0.00-0.00

In contrast, gene flow is predominantly north-eastwards on the east coast (from PE to HH) against the Agulhas Current, but in the direction of the in-shore wind-induced counter currents (Fig. 3.1). However, bidirectional gene flow is recorded between localities in the region stretching from CI to PE. The CI and the KH regions, in the middle of the range, appear to provide a high number

of migrants to their east and to the south-west (Fig.3.1), but receive little or no migrants in return from either direction.

3.3.3 Demographic history

3.3.3.1 Intraspecific genealogy

A star-shaped haplotype network was recovered for COI; with most of the haplotypes occurring at low frequencies being separated from the central, most common haplotype by one mutational step (Fig. 3.2). The most divergent haplotype was eight mutational steps from the central haplotype. This star-shaped haplotype network is typical of populations that have experienced a recent expansion following a severe bottleneck. A similar haplotype network was obtained for ITS (Fig. 3.2).

3.3.3.2 Fu's F_s and mismatch distribution

As only shallow genetic structure was observed for *T. sarmaticus* demographic history analyses were performed separately for both COI and ITS2 using pooled data set for each marker. Fu′s F_s statistics were negative for all populations, indicating an excess of rare haplotypes over what would be expected under neutrality, but only values for populations at or close to bioregional boundaries (WP, BB , HH) and for the data set as a whole were significant ($p < 0.02$, Table 3.7). The McDonald and Kreitman test showed a significant deviation from selective neutrality (Neutrality index = 16.20, Fisher test $p < 0.05$), meaning that deviations from neutrality shown by Fu′s F_s could not be unambiguously ascribed to demographic expansion.

Mismatch distributions for COI for the whole data set conformed to both the pure demographic expansion and the range expansion models (Fig. 3.3). The close fit of the observed distributions to these models was supported by non-significant *r* and SSD statistics (Table 3.7). A substitution rate of 0.35% Myr^{-1} provides estimates of the timing of expansion for the whole

population at c. 240 kya (180-360 kya) whereas the higher substitution rate of 2% Myr^{-1} recovers an estimate of c. 40 kya (30-60 kya). In each case, the timing of demographic expansion predates the LGM (19-26.5 kya).

At the ITS locus, mismatch distributions were unimodal and the *r* and SSD values were generally small and non-significant (except SSDs for GB and PA), supporting a recent demographic expansion at these two localities (Table 3.8). However, Fu′s F_s values were negative but non-significant (Table 3.8), suggesting neutrality or modest demographic changes.

Table 3.7 Demographic parameters for COI sequences of *Turbo sarmaticus* from 11 localities. Localities, number of individuals sequenced (N), Fu′s F_s values (* means significant at $p < 0.02$), Harpending′s raggedness indices (*r*), sum of squared deviations (SSD) and mismatch distribution parameters τ (5% confidence intervals) are listed.

Locality	N	Fu′s F_s	Pure demographic expansion			Range expansion		
			r	SSD	**τ**	*r*	SSD	**τ**
Wooley′s Pool	21	-5.47*	0.08	0.01	1.05(0.11;1.93)	0.08	0.01	1.05(0.35;1.97)
Rooi-Els	21	-1.00	0.08	0.00	0.78(0.00;1.78)	0.10	0.00	0.62(0.10;1.88)
Betty′s Bay	24	-7.32*	0.14	0.02	0.98(0.38;1.92)	0.14	0.02	0.98(0.42;1.79)
Gansbaai	11	-1.25	0.20	0.00	0.44(0.00;1.25)	0.21	0.00	0.45(0.05;1.30)
Cape Agulhas	24	-1.50	0.06	0.00	0.91(0.00;2.37)	0.06	0.00	0.56(0.22;2.23)
Cape Infanta	22	-0.64	0.14	0.01	0.75(0.01;1.55)	0.14	0.01	0.74(0.23;1.74)
Herold′s Bay	22	-0.76	0.13	0.01	0.84(0.00;1.84)	0.13	0.01	0.83(0.31;1.79)
Knysna Heads	24	-1.90	0.14	0.02	1.00(0.41;1.90)	0.16	0.02	1.03(0.36;1.84)
Port Elizabeth	23	-0.52	0.23	0.02	0.67(0.37;46.25)	0.23	0.01	2.96(0.00;8.53)
Port Alfred	17	-1.89	0.13	0.01	0.14(0.00;1.41)	0.13	0.01	0.46(0.09;2.24)
Haga Haga	23	-4.47*	0.05	0.32	0.98(0.00; 0.66)	0.05	0.00	0.13(0.18;8.34)
All samples combined	232	-29.40*	0.09	0.01	0.94(0.69; 1.38)	0.09	0.01	0.93(0.53;1.17)

Table 3.8 Demographic parameters for ITS sequences of *Turbo sarmaticus* from 11 localities. Localities, number of individuals sequenced (N), number of haplotypes, Fu′s F_s values (* means significant at $p < 0.02$), Harpending′s raggedness indices (r), sum of squared deviations (SSD) and mismatch distribution parameters τ (95% confidence intervals), (** means $p < 0.05$).

Locality	N	Fu′s F_s	Demographic expansion			Range expansion		
			r	SSD	**τ**	*r*	SSD	**τ**
Wooley′s Pool	21	-0.72	0.05	0.00	1.48(0.00;3.52)	0.05	0.00	1.14(0.12;3.16)
Rooi-Els	21	-0.06	0.08	0.00	0.95(0.45;1.67)	0.08	0.00	0.94(0.34;1.57)
Betty′s Bay	24	-2.21	0.04	0.00	1.20(0.00;2.88)	0.04	0.00	1.14(0.25;2.66)
Gansbaai	11	-0.81	0.09	0.43**	0.00(0.00;0.59)	0.09	0.00	1.89(0.08;4.58)
Cape Agulhas	24	-0.26	0.09	0.00	1.04(0.29;2.01)	0.09	0.00	1.04(0.32;1.86)
Cape Infanta	22	-0.52	0.16	0.00	3.68(0.06;46.68)	0.16	0.00	0.08(0.00;3.57)
Herold′s Bay	22	-1.17	0.07	0.00	1.13(0.00;2.88)	0.07	0.00	0.97(0.00;2.97)
Knysna Heads	24	-2.62	0.09	0.00	0.70(0.24;1.26)	0.09	0.00	0.70(0.22;1.28)
Port Elizabeth	23	-0.10	0.09	0.00	1.43(0.00;3.20)	0.09	0.00	1.17(0.08;6.04)
Port Alfred	17	-1.92	0.11	0.38**	0.00(0.00;0.50)	0.11	0.01	1.49(0.07;4.00)
Haga Haga	23	-1.21	0.08	0.00	0.91(0.00;2.85)	0.08	0.00	0.85(0.08;2.51)
All samples combined	232	-5.40*	0.06	0.00	1.16(0.00;3.08)	0.06	0.00	1.03(0.15;2.75)

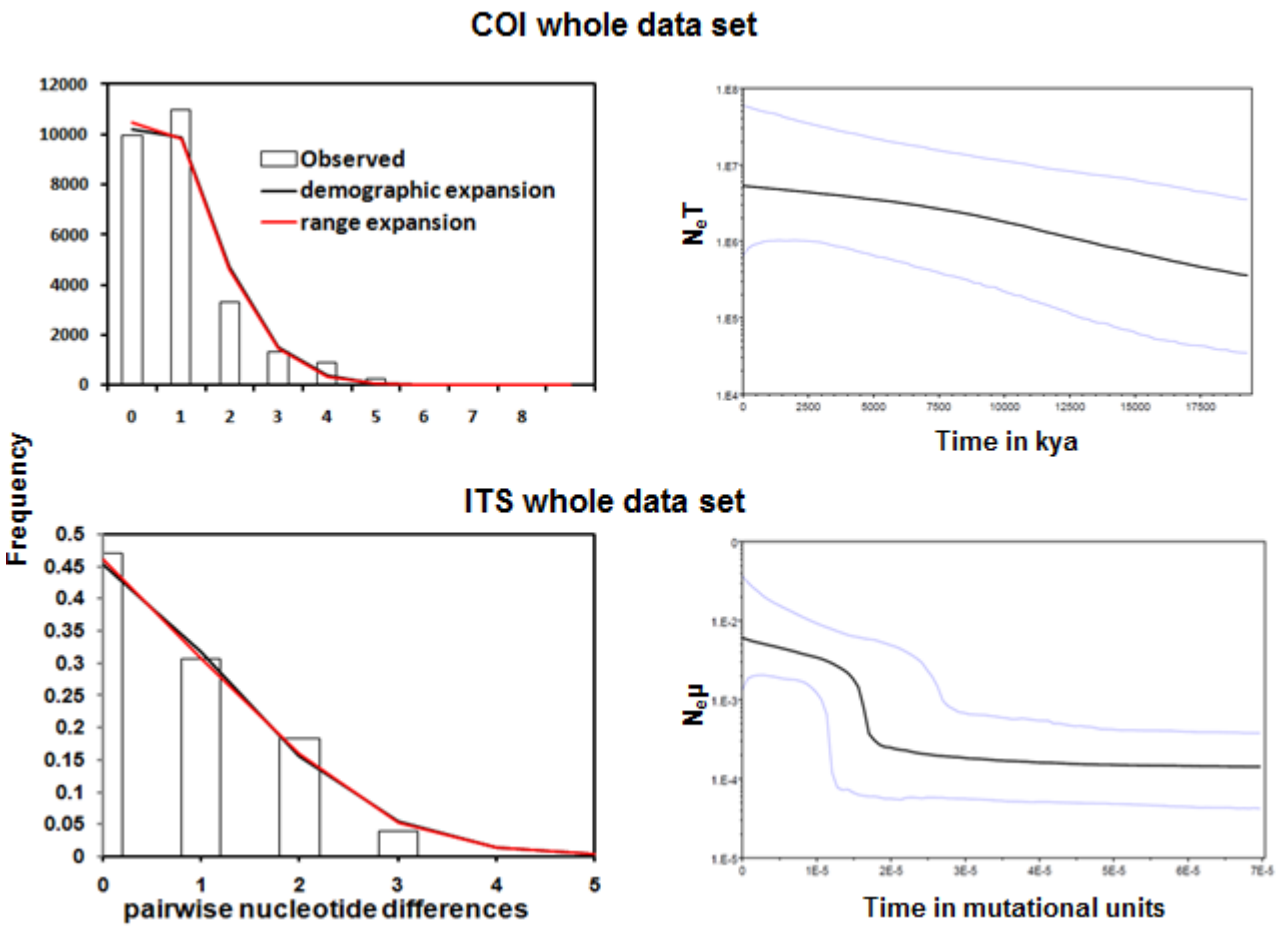

Figure 3.3 Demographic history of *Turbo sarmaticus* inferred from COI and ITS2 sequences for the whole data set. **(left)** Frequency distribution of pairwise differences among COI haplotypes: histograms show the observed distribution; lines show the expected distribution under a model of pure demographic expansion (solid line) and spatial expansion (dashed line). **(right)** Bayesian skyline plot for: COI (based on a mutation rate of 2.4 x 10^{-8}substitutions $site^{-1}$ yr^{-1}) and ITS2 (no specified mutation rate). Time (x-axis) is in thousands of years ago (kya) for COI and mutational units for ITS2. The central bold line represent the median value of N_eT for COI or $N_e\mu$ for ITS2, where N_e = effective population size, T = generation time, μ = mutation rate. The narrow lines denote the upper and lower confidence limits of the 95% Highest Posterior Density (HPD) interval.

3.3.3.3 Bayesian skyline plots

BSPs for both COI and ITS further support the hypothesis of population expansion. The COI BSP of the whole population indicates that there was a significant population expansion beginning c. 17 kya (at 2.6% Myr^{-1}) or 140 kya (at 0.35% Myr^{-1}) and lead to a 40-fold increase in effective population size (Fig. 3.3). The population expansion phase continued until c. 5 kya before the effective population size began to stabilize. The ITS data show an exponential growth preceded by a period of demographic stability (Fig. 3.3), but the timing of expansion could not be estimated in years owing to lack of substitution rate for this marker.

3.4 Discussion

3.4.1 Population genetic structure and gene flow patterns

Although previous studies have reported restriction of gene flow around the Cape Agulhas region (e.g. Evans *et al*., 2004; Teske *et al*., 2004; Teske *et al*., 2007b; von der Heyden *et al*., 2008), there is no strong evidence to support gene flow restrictions in *T. sarmaticus*. Instead, evidence from pairwise population comparisons (Table 3.4) for the mitochondrial COI suggests that two genetic assemblages comprising CI and HB in one central group and the rest of the localities forming another. A similar scenario was recorded for the co-distributed rocky pool goby *Caffrogobius caffer*, in which individuals in the Jongesfontein region, which lies between CI and HB, grouped separately from the rest of the localities (Neethling *et al*., 2008). Although this finding was dismissed by Neethling *et al*. (2008) as biologically insignificant, it is here proposed that it might be a sign that the region encompassing CI and HB might be somehow separated from the regions to the west and to the east.

A brief review of the relationship between the Agulhas Current and the Agulhas Bank might help to understand the gene flow patterns and genetic structure observed for *T. sarmaticus* (for detail see Jackson *et al*. 2012). Between Durban and PE the continental shelf is narrow and the Agulhas Current

closely follows the continental margin (Lutjeharms, 2006). Around PJ as the continental shelf begins to widen gradually towards the Agulhas Bank the current is deflected from the coast and its impact on the coastal waters diminishes (Lutjeharms, 2006; Roberts, 2010; Jackson *et al*. 2012). Instabilies of the Agulhas Current develop along the its inshore boundary resulting in laterally moving waves that reach the coast. In addition, a large solitary meander known as the Natal Pulse is generated around KwaZulu Natal and moves downstream. The Natal Pulse is important in that it associated with cyclonic circulation which results in northward currents on the shelf (Lutjeharms *et al*. 2003). Evidence is accumulating that the coastal region of the Agulhas Bank, stretching from the coastline up to 15 km offshore is dominated by wind-driven coastal upwelling (Schumann *et al.* 1982) and alongshore coastal currents (Roberts , 2010). Although the whole of the Agulhas Bank is highly productive, the region between Cape Agulhas and Port Elizabeth is exceptionally productive probably due to wind-driven upwelling that brings up nutrients for primary production (Schumann *et al.* 1984; Demarcq *et al.* 2003). Most (76%) of particles entrapped by the Agulhas Current especially from the south-east coast is lost offshore to the deep sea (Jackson *et al*. 2012).

The genetic structure and gene flow pattern for *T. sarmaticus* could be a result of the interplay between the topology of the coastline and oceanography. Possibly, the region including CI, HB and KH is difficult to reach and is thus likely to be the least exploited area by migrants from other regions. There is evidence that the Agulhas Current entrap larvae from the south-east coast around Port Elizabeth and release them just south of the Cape Agulhas through annual rings that are shed off and sometimes advect onto the Agulhas Bank around this region. This scenario might explain the genetic connectivity between the regions east and west of the central region (CI-HB-KH). Moreover, the waters around the central region are highly productive is (facilitating growth) than when compared to the East Coast (Shannon *et al*., 1984), and in gastropods, larger animals tend to have higher reproductive output. The reproductive output could mean more larvae are available for dispersal to other regions probably through a series of coastal wind-induced local eddies. Purely speculative, the CI-HB group could have had a smaller effective population size and, thus, differentiated from others due to genetic drift. In contrast, the other

regions have large effective population sizes and are, therefore, not prone to genetic drift resulting in their high genetic connectivity.

Considering the directionality of gene flow and the occurrence of fewer haplotypes in the central CI-HB region than in the rest of localities, it appears that current oceanographic conditions facilitate gene flow from the CI-HB region to the other regions but little in reverse. The central region donates a huge number of migrants to adjacent localities but receives none or little in return. Similarly, von der Heyden *et al.* (2008) show that the De Hoop region, which borders with CI, have the same pattern. Possibly, whereas mutations that arise in the CI region are shared with other regions, haplotypes derived from new mutations elsewhere do not reach the CI region again. The gene flow pattern could also explain why CI has a fewer number of private haplotypes than the other regions. New private haplotypes were established in the east and west regions as there was no reciprocal gene flow. Shared haplotypes and a lack of unique haplotypes in the east and west regions suggests that they have not been isolated from each other or that they have been colonized from the same source and random settling causes differences between some populations. The hypothesis of a recent demographic expansion could also explain the observed lack of an isolation by distance pattern, which was expected given that this species has a pelagic larval phase and thus a high dispersal ability (Porreta *et al*. 2007; Porreta *et al*., 2011).

The north-eastward gene flow on the south-east coast indicates that *T. sarmaticus* larvae utilise the inshore wind-driven counter currents, which flow opposite to the stronger offshore Agulhas Current. The influence of these counter currents has also been suggested for the rock-pool fish *Clinus cottoides* (von der Heyden *et al*., 2008). The currents are thought to originate around De Hoop on the south coast and their influence is evident along most of the South African east coast, especially where the Agulhas Current is further offshore. The bidirectional gene flow between KH and PE, PE and PA on the south-east coast and the predominantly westward gene flow on the south –west coast from CA to WP would be difficult to explain without the knowledge of coastal wind-induced currents. The Agulhas Current would be too distant from the coast to cause any meaningful influence on dispersal of coastal organisms so the westward flow cannot be attributed to it. It is now evident that dispersal on the coast along the Agulhas

Bank is influenced by an array of cyclonic eddies, wind-induced currents and temporary northward counter currents associated with the Natal Pulse (Roberts *et al*. 2010;).

Another plausible explanation of the population genetic structure observed in *T. sarmaticus* is that a recent spatial expansion occurred from a single refugium and, therefore, owing to incomplete lineage sorting or ancestral polymorphism, the assemblages show only weak or no differentiation. This scenario has been shown to result in weak signals of differentiation because of insufficient time for population differentiation (e.g. Zane *et al*., 2006).

The failure to detect pairwise population differentiation and the weaker structure recovered by AMOVA for ITS in comparison with COI data might be a result of lack of variation in the nuclear DNA. A possible cause of this is a lower evolutionary rate and a higher effective population size of nuclear DNA compared to the mitochondrial DNA, leading to incomplete lineage sorting in nuclear DNA (Hudson and Turelli, 2003; Zink and Barrowclough, 2008; Toews and Brelsford, 2012), which results in an apparent lack of genetic isolation signatures. By virtue of a sedentary adult stage in *T. sarmaticus*, male biased dispersal cannot be an explanation for the differences between ITS2 and COI.

3.4.2 Demographic history

The demographic history of *T. sarmaticus* bears a signature of late Pleistocene influence in that both the BSP and mismatch distributions analysis suggest demographic expansion which began in the late Pleistocene Concordance between the mitochondrial COI and the nuclear ITS, and the substantial agreement between traditional and coalescent analyses enhances confidence in these results.

At the COI locus, fairly high haplotype diversity (h = 0.35-0.68) was associated with low nucleotide diversity values (π = 0.001-0.003) indicating that small differences occur among most haplotypes (see Palero *et al*., 2008 for a similar description of genetic variation). A pattern of high haplotype diversity and low nucleotide diversity has been found in several studies of marine invertebrates with high dispersal potential (e.g. Uthicke and Benzie, 2003; Cassone and Boulding, 2006; Lee and

Boulding, 2007) and has been attributed to sudden population expansions following severe bottlenecks (Grant and Bowen, 1998).

Consistent with low nucleotide diversity, the COI haplotype network showed mostly single nucleotide differences between the central haplotype and the other low-frequency haplotypes, resulting in a star-like topology (Figs 3.2 and 3.3). A combination of a star-like haplotype network and negative neutrality tests, as observed in *T. sarmaticus*, is thought to be produced after a range expansion especially if there is high gene flow in a species with a high dispersal ability (Ray *et al*., 2003). Additionally, *T. sarmaticus* had (1) significantly negative Fu′s F_s values for the COI gene, (2) and a unimodal mismatch distribution associated with low non-significant raggedness indices and SSDs.

For ITS, similar levels of haplotype diversity (0.40 to 0.64) were observed, but nucleotide diversity was higher (0.07-0.12). Although Fu′s F_s values for ITS were all negative, they were not significant. This could suggest demographic stability, a modest population size or contraction. Alternatively, this could be interpreted as a sign of too little genetic variation at the ITS locus as only 12 haplotypes were recovered but the high nucleotide diversity implies that there was high nucleotide divergence among haplotypes within populations. The combination of a star-like haplotype network and an L-shaped mismatch distribution could be interpreted in two different ways. (1) First, this pattern could be evidence of a sudden population expansion following a bottleneck event or founder effect (Slatkin and Hudson, 1991; Ibáñez *et al*., 2011). Secondly, a similar pattern of genetic variation could result from a selective sweep (Skibinski, 2000; Ibáñez *et al*., 2011). A selective sweep is defined as the process by which a phenotypically beneficial mutation increases in frequency relative to other alleles in a population and ultimately becomes fixed (Ibáñez *et al*., 2011; Karl *et al*., 2012). Although the McDonald Kreitman test suggests that deviations from neutrality due to selection could not be ruled out, the latter explanation seems more unlikely for the following reasons. (1) A selective sweep affecting only the mtDNA would have resulted in demographic equilibrium at the nDNA locus but departure from equilibrium at the mtDNA locus (Babbucci *et al*., 2010). (2) Empirical evidence suggests that selective sweeps of the mitochondrial genome are rare (Karl *et al*., 2012).

Further evidence of recent demographic expansion in *T. sarmaticus* is provided by the Bayesian skyline plots depicting population growth. The subsequent demographic expansion in the proximity of the LGM suggests that the climatic changes since the LGM might have played a major role in the recent demographic history of *T. sarmaticus*. Factors proposed for other taxa in the region -namely changes in sea level accompanied by changes in water temperature and nutrient concentrations, and the availability of more suitable habitat (Tolley *et al*., 2005; von der Heyden *et al*., 2007) might have led to both spatial and pure demographic expansion.

Mismatch distribution analyses recovered substantial variance in the estimates of the onset of population expansions. At the higher mutation rate of 2.4% Myr^{-1} it would appear that the *T. sarmaticus* began expansion recently (between c. 30-60 kya, Table 3.8), indicating that demographic expansion coincided with the last glacial period that culminated into the LGM (19-26.9 kya, Clark *et al*., 2009). Estimates based on the BSP, at the same mutation rate, also suggest a post-LGM expansion (c. 18 kya) for the whole population. These results of demographic expansion dating in the proximity of the LGM corroborate those obtained for other coastal taxa on the South African coast (e.g. *Palinurus gilchristi*, Tolley *et al*., 2005; *Palinurus delagoae*, Gopal *et al*., 2006; *Jasus tristani*, von der Heyden *et al*., 2007; *Caffrogobius caffer*, Neethling *et al*., 2008)**.** Since the coastal habitat moves with the sea level it is unlikely that climatic changes in the late Pleistocene affected availability of shallow suitable habitat for *T. samarticus*. Perhaps, the drop in temperature associated with the last glacial restricted the distribution range of this species to the south-east coast. Under the influence of the warm Agulhas Current, which probably was closer to the coast than it is currently, the south-east coast could have provided suitable temperatures for *T. sarmaticus*. After the LGM the temperatures began to rise again and this allowed range expansion as the species recolonized areas to the west and east of its refugium. This would result in population expansion. However, surprisingly, the population expansion did not drop-off when habitat became reduced as the sea level rose on entering the current interglacial. A most likely explanation is that the continued high genetic diversity, a consequence of high gene flow induced by the rearrangement of currents following the LGM, results in the maintenance of a very large nearly panmictic population. A

less likely explanation would be that this scenario could be an indication that not enough time has passed since the expansion and given that population sizes are still fairly large, the effects of fixation from genetic drift are not showing yet.

At the lower mutation rate of 0.35% Myr^{-1}, mismatch distributions estimated that demographic expansions began between 180 and 360 kya (Table 3.8). The corresponding BSP recovered estimates of c.140 kya, thus suggesting that population expansions began in the late Pleistocene. The expansion times span a much wider range which makes it difficult to associate them with any particular Pleistocene event and hence difficult to explain. However it is interesting that whether the higher rate or lower rate is used, the hypothesis of late Pleistocene expansion cannot be rejected.

3.4.3 Conclusions

The phylogeographic structure of *T. sarmaticus* characterised by shallow population differentiation and lack of isolation by distance is most likely a signature of recent (Late Pleistocene) demographic expansion. The genetic structure observed for *T. sarmaticus* was expected given that it is a broadcast spawner with a relatively long pelagic phase. The central region around CI, HB and KH is likely to have been isolated from other regions during the Pleistocene glacial-interglacial cycles resulting in genetic drift. This study corroborates phylogeographic patterns found in other marine species showing the important role played by climatic changes in the late Pleistocene in shaping the distribution of biodiversity on the South African coast.

CHAPTER 4
RESPONSES OF THREE SOUTH AFRICAN ROCKY SHORE CONGENERIC TOPSHELLS (TROCHIDAE: GASTROPODA) TO PLEISTOCENE CLIMATIC OSCILLATIONS

4.1 Introduction

The congeneric topshells *Oxystele sinensis, Oxystele tigrina* and *Oxystele variegata* inhabit rocky shores and are endemic to the South African coast. *Oxystele variegata* has the widest range, extending from Namibia on the west coast to the Natal south coast in eastern South Africa (Kilburn & Rippey, 1982) (Fig. 4.1). It is common on rocks between high and low-water neaps, both under sheltered conditions and between wave-battered boulders. *Oxystele variegata* is highly tolerant of temperature and salinity stress as befits its wide distribution (Kilburn and Rippey, 1982). The distribution of *O. sinensis* ranges from False Bay on the south coast to Haga Haga in the Natal Bioregion (Fig. 4.1). It occurs near the low spring-tide level down to a depth of about seven metres (Kilburn and Rippey, 1982). The distribution of *O. tigrina* ranges from Jacob`s Bay in the Namaqua Bioregion to Haga Haga in the Natal Bioregion (Fig. 4.1). It is common on and under rocks in the mid-tidal region and when compared to *O. sinensis,* it occurs higher on the rocky shore.

The trochids have separate sexes and fertilisation is external. There are at present no published data on the developmental modes of southern African trochid species. However, in several trochid species from other regions, eggs are shed singly into the plankton, enclosed in a gelatinous layer, which swells in the water before hatching occurs at either the trochophore or veliger stage (Kilburn and Rippey, 1982). No data are available on the length of the veliger or trochophore stages. Other species in the family deposit eggs bound into a lump, sheet or ribbon of jelly, and eggs hatch at the crawling, post-veliger stage (Kilburn and Rippey, 1982). Although the life history of other trochids suggests a short pelagic phase, it is predicted that the *Oxystele* species

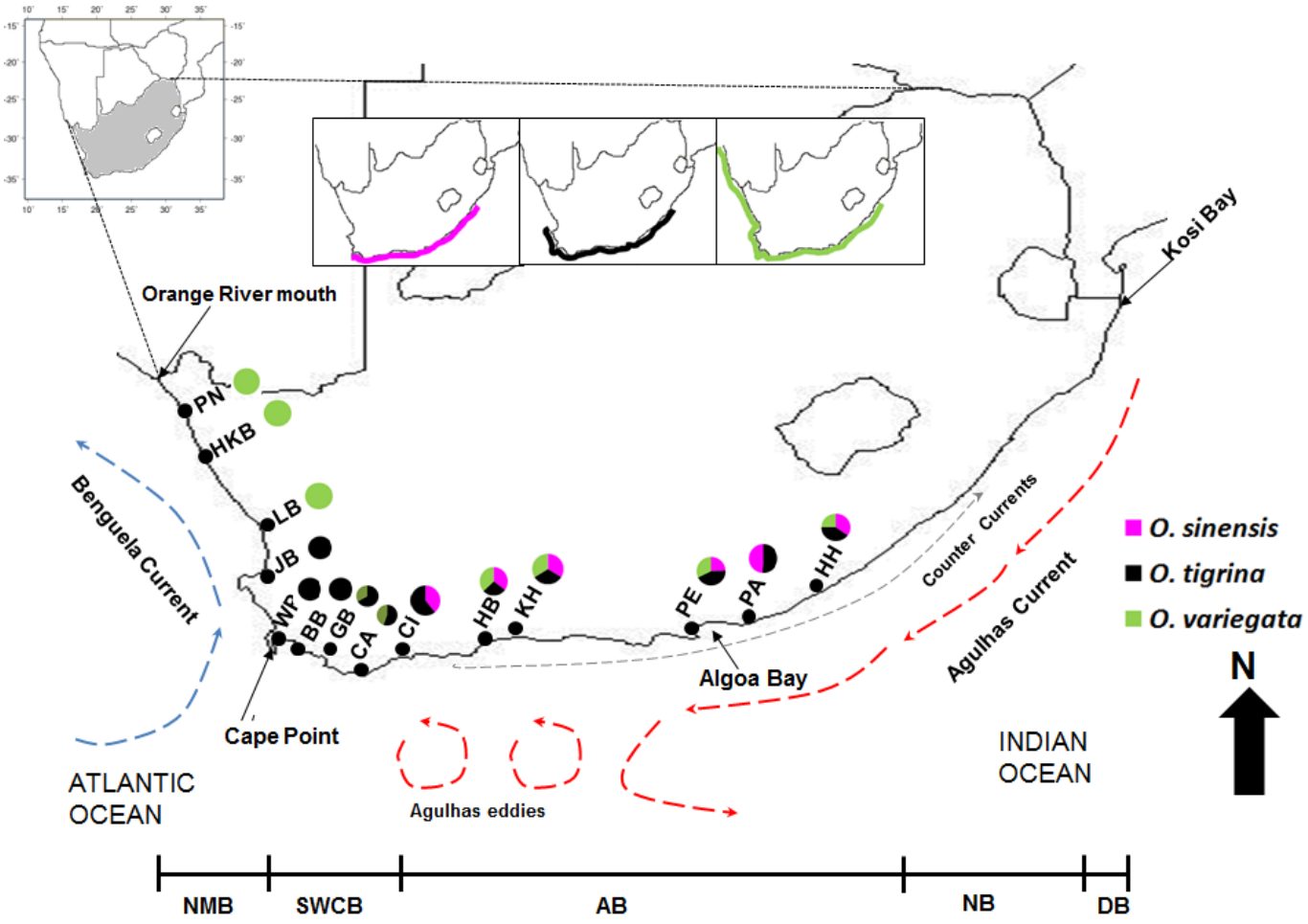

Figure 4.1 Sampling localities of *Oxystele sinensis*, *O. tigrina*, *O. variegata*, geographic areas, coastal bioregions and major oceanic currents on the South African coast are depicted. Inserts show current distribution of the three species. Pie charts show relative abundance of specimens of each species collected per site. Locality abbreviations are as follows: PN, Port Nolloth; HKB, Hondeklip Bay; LB, Lambert′s Bay; JB, Jacob′s Bay; WP, Wooley′s Pool; BB, Betty′s Bay; GB, Gansbaai; CA, Cape Agulhas, HB, Herold′s Bay; KH, Knysna Heads; PE, Port Elizabeth; PA, Port Alfred; HH, Haga Haga; Bioregion abbreviations are as follows: NMB, Namaqua Bioregion; SWCB, South-western Cape Bioregion; AB, Agulhas Bioregion; NB, Natal Bioregion, DB, Delagoa Bioregion.

will show high dispersal ability and therefore low population genetic structuring since Teske *et al*. (2007a) concluded that it was not the pelagic larval duration but the presence or absence of a pelagic phase that determined dispersal ability. But Neethling *et al*. (2008) concluded that larval duration plays an important role in the dispersal ability of a rocky pool goby *Caffrogobius caffer*.

As for *Turbo sarmaticus*, there are no published data on the phylogeography or population genetics of the southern African *Oxystele* species. Thus, the primary aim of this chapter is to explore the phylogeographic structure and demographic histories of *O. sinensis*, *O. tigrina* and *O. variegata*, for signatures of impact from Pleistocene climatic change. The following questions are addressed. (1) Do the three species exhibit spatially concordant phylogeographic patterns? (2) Do the species display temporally concordant demographic histories? Positive answers to both of these questions would indicate that shared historical environmental processes (for example the effect of Pleistocene climate change and sea level fluctuation on the distribution of lineages) have shaped genetic structure in these taxa. However, different locations of disjunctions or different demographic histories would strongly suggest that these species responded differently to share environmental histories perhaps due to differences in their reproductive systems, dispersal ability or habitat specificity (McGovern *et al*., 2010). Additionally, the hypothesis of genetic assemblages corresponding to bioregions was tested.

4.2 Materials and Methods

Materials and methods were as described in **Chapter 2** with the following particular information. The geographic locations of localities and number of individuals of each *Oxystele* species sampled are shown in Fig, 1 and Table 4.1.The best-fit models of COI substitution estimated with jMODELTEST were (*O. tigrina*: TrN+G, Tamura and Nei, 1993; and for both *O. sinensis* and *O. variegata*: HKY + G, Hasegawa *et al*., 1985). The best-fit models for ITS2 were as follows: HKY +I (*O. sinensis*), HKY+G (*O. tigrina*), and TrN +G (*O. variegata*). However, molecular diversity, population pairwise Φ_{ST} and AMOVA were conducted following the TrN +G model for all species for both markers since the HKY model is not available in ARLEQUIN and the TrN +G was the second best available one. BEAST was run to construct BSPs and estimate divergence time (for *O. variegata* only) using the respective estimated substitution rates as follows (in substitutions site^{-1} yr^{-1}): *O. sinensis* (2.3 x 10^{-8}), *O. tigrina* (2.4 x 10^{-8}) and

O. variegata (2.4×10^{-8}).The McDonald Kreitman test was performed in DnaSP using *O. sinensis* as an outgroup for *O. tigrina* and *O. variegata*, and *O. tigrina* as an outgroup for *O. sinensis*.

Since distinct genetic assemblages were recovered in *O. variegata*, a Bayesian MCMC approach was used to estimate divergence times (i.e. time to most recent common ancestor, TMRCA) between the Namaqua Bioregion assemblage and the Agulhas Bioregion assemblage, as implemented in BEAST version 1.6.1 (Drummond and Rambaut, 2007). TMRCA estimates when genes last shared a common ancestor, can be used as a proxy for ancestral population age (Nicolas *et al*., 2008). For each analysis, the model of nucleotide substitution estimated by jMODELTEST was used and a Yule (speciation) model was specified. MCMC was run for 30 million generations with a sampling interval of 3000 genrations aiming to achieve Effective Sample Sizes (ESS) above 200. A substitution rate was estimated as explained under 2.4.4.2. Results were visualised in TRACER version 1.5 (Rambaut and Drummond, 2007).

Table 4.1 Geographical location and sample size of the localities sampled for *Oxystele sinensis*, *O. tigrina* and *O. variegata*

Bioregion	Locality (Abbreviation)	Latitude Longitude		Sample size		
				O. sinensis	*O. tigrina*	*O. variegata*
Namaqua	Port Nolloth (PN)	S29^{0}08	E16^{0}31			20
Namaqua	Hondeklip Bay (HKB)	S30^{0}11	E17^{0}09			21
Namaqua	Lambert‟s Bay (LB)	S34^{0}12	E18^{0}33			21
Namaqua	Jacob‟s Bay (JB)	S32^{0}58	E17^{0}52		22	0
Agulhas	Woolley‟s Pool (WP)	S34^{0}04	E18^{0}16	0	21	0
Agulhas	Betty‟s Bay (BB)	S34^{0}12	E18^{0}33	0	22	0
Agulhas	Gansbaai (GB)	S34^{0}21	E19^{0}11	0	18	9
Agulhas	Cape Agulhas (CA)	S34^{0}29	E20^{0}00	0	19	15
Agulhas	Cape Infanta (CI)	S34^{0}15	E20^{0}30	14	22	0
Agulhas	Herold′s Bay (HB)	S34^{0}01	E22^{0}13	21	17	22
Agulhas	Knysna Heads (KH)	S34^{0}03	E23^{0}01	23	22	23
Agulhas	Port Elizabeth (PE)	S33^{0}34	E25^{0}23	13	23	17
Agulhas	Port Alfred (PA)	S33^{0}21	E26^{0}31	23	22	0
Agulhas	Haga Haga (HH)	S32^{0}27	E28^{0}08	21	24	15
	Total			115	234	163

4.3 Results

4.3.1 Identification of Oxystele variegata

Oxystele variegata and *O. impervia* were once regarded as one species owing to their morphological similarities, which made it difficult to tell them apart in the field. However, Heller and Dempster (1991) used radular morphology and allozymes to confirm that *O. variegata* and *O. impervia* were separate species. Two lineages in the *O. variegata*/*impervia* complex were sampled in this study whose sequences consistently differed at two nucleotide sites. Based on morphology alone, these lineages still could not be clearly distinguished as either *O. variegata* or *O. impervia.* Therefore to verify identifications, ten specimens (five from each lineage) were sent to experts (L. M. Griffiths[a] and G.M. Branch[a]). The experts identified five from one lineage as *O. variegata*, two from the second lineage as *O. impervia* but were unsure about the identity of three specimens. Only individuals from the lineage identified as *O. variegata* were included in this study but the species identification should be taken with caution, since these two taxa are morphologically variable and it is difficult to assign some variations to either species. All of the below is based on the assumption that the clade included in this study was correctly identified as *O. variegata.*

4.3.2 Genetic variation

A 607-bp fragment of COI was obtained for all three species after aligning and trimming the sequences. A total of 42 unique COI haplotypes was recovered in 115 *O. sinensis* individuals, 32 (76%) of which were private (Fig. 4.2, Table 4.2), 31 being singletons. Forty three substitutions were observed comprising 40 transitions and 3 transversions. For *O. tigrina*, 73 unique haplotypes were recovered, consisting of 53 (72%) singletons (Fig. 4.2, Table 4.2) from 234 specimens examined. A total of 73 substitutions were observed, transitions outnumbering transversions 55:18. For *O. variegata*, the 163

[a]Marine Biology Research Centre, Zoology Department, University of Cape Town, Rondebosch, 7701, South Africa

individuals examined yielded 45 haplotypes of which 37 (82%) were private (Fig. 4.2, Table 4.2), 35 of them being singletons. Substitution comprised 44 transitions and eight transversions.

Haplotype diversity (*h*) for *O. sinensis* was consistently high (0.79-0.94) across all localities, as was nucleotide diversity (0.04-0.07) (Table 4.2). A similar trend was recorded for *O. tigrina* (h = 0.83-0.96; π = 0.05-0.07) (Table 4.2). For *O. variegata*, haplotype diversity was high on the south-east coast (roughly corresponding to the Agulhas Bioregion) (h = 0.78-0.92), but much lower on the west coast (corresponding to the Namaqua Bioregion) (h = 0.19-0.35) (Table 4.2). Nucleotide diversity exhibited a similar pattern being high on the south-east coast (π = 0.03-0.07) but an order of magnitude lower on the west coast (π = 0.00-0.02) (Table 4.2). In addition, of the 45 COI haplotypes recovered for *O. variegata*, only three were shared between the two assemblages, six being unique to the west coast and 36 to the south-east coast. All haplotypes for COI have been deposited with GenBank under the following accession numbers: JX303336-JX303377 (*O. sinensis*), JX303378-JX303450 (*O. tigrina*) and JX303451-JX303495 (*O. variegata*).

For ITS2, allelic reconstruction for *O. sinensis* estimated 41 haplotypes from a 665 bp fragment, of which 22 (54%) were private (Table 4.2) and nearly half (51%) were singletons. For *O. tigrina*, 32 haplotypes were estimated including 28 (82%) which were private (Table 4.2). A total of 57 haplotypes were recovered in *O. variegata* comprising 9 shared between the Namaqua and the Agulhas Bioregions, 18 unique to the former and 30 unique to the latter (Table 4.1) and 58% singletons. As for COI, the haplotype diversity and nucleotide diversity were high across all populations in *O. sinensis* (Table 4.1), but were relatively lower in *O. tigrina* and *O. variegata* (Tables 4.1). Unlike COI, there were no differences in haplotype diversity and nucleotide diversity between the south-east and west coasts in *O. variegata* (Table 4.1). Haplotypes for ITS2 were deposited in GenBank under accession numbers: JX145347-JX145387 (*O. sinensis*), JX303558-JX303591 (*O. tigrina*) and JX303592-JX303648 (*O. variegata*).

Table 4.2 Sampling localities, sample size (N), number of haplotypes (N_h with private haplotypes shown in brackets), haplotype diversity (h±SD, standard deviation), nucleotide diversity (π±SD, standard diversity) for COI and ITS2 sequences in *Oxystele sinensis*, *O. tigrina* and *O. variegata*

Locality	COI				ITS2			
	N	N_h(private)	h±SD	π±SD	N	N_h(private)	h±SD	π±SD
O. sinensis								
Cape Infanta	14	10(5)	0.92±0.06	0.07±0.05	11	8(1)	0.81±0.04	0.04±0.03
Herold′s Bay	21	11(3)	0.90±0.05	0.07±0.04	21	18(5)	0.90±0.03	0.05±0.03
Knysna Heads	23	15(11)	0.92±0.04	0.07±0.04	19	13(2)	0.85±0.04	0.05±0.03
Port Elizabeth	13	8(2)	0.90±0.07	0.07±0.05	14	14(4)	0.92±0.03	0.05±0.03
Port Alfred	23	8(5)	0.79±0.06	0.04±0.03	19	15(4)	0.86±0.04	0.04±0.03
Haga Haga	21	13(6)	0.94±0.03	0.07±0.04	23	18(6)	0.92±0.02	0.05±0.03
All localities	115	42	0.90±0.01	0.07±0.04	107	41	0.89±0.01	0.07±0.04
O. tigrina								
Jacob′s Bay	22	12(3)	0.93±0.03	0.06±0.04	18	7(2)	0.60±0.08	0.03±0.02
Wooley′s Pool	21	13(7)	0.91±0.05	0.05±0.04	13	5(1)	0.68±0.07	0.03±0.03
Betty′s Bay	22	14	0.94±0.04	0.07±0.04	21	5	0.71±0.05	0.04±0.03
Gansbaai	18	13(2)	0.95±0.03	0.05±0.03	21	8(4)	0.65±0.07	0.03±0.02
Cape Agulhas	19	13(5)	0.96±0.03	0.05±0.03	24	9(5)	0.63±0.06	0.03±0.03
Cape Infanta	22	15(9)	0.93±0.04	0.06±0.04	22	5(2)	0.60±0.07	0.03±0.02
Herold′s Bay	17	13(3)	0.96±0.03	0.05±0.03	15	12(8)	0.82±0.06	0.05±033
Knysna Heads	22	13(7)	0.93±0.04	0.05±0.03	17	5(2)	0.59±0.07	0.02±0.02
Port Elizabeth	23	11(3)	0.83±0.06	0.05±0.03	19	6(2)	0.59±0.07	0.02±0.02
Port Alfred	22	11(2)	0.90±0.04	0.06±0.04	16	5(1)	0.65±0.07	0.03±0.02
Haga Haga	24	13(3)	0.90±0.05	0.05±0.03	21	4(1)	0.56±0.06	0.02±0.02
All localities	234	73	0.92±0.01	0.05±0.03	173	32	0.63±0.02	0.03±0.02

Table 4.2 continued

Locality	COI				ITS2			
	N	N_h(private)	h±SD	π±SD	N	N_h(private)	h±SD	π±SD
O. variegata								
Namaqua Bioregion								
Port Nolloth	20	3(1)	0.19±0.11	0.00±0.01	18	11(2)	0.66±0.09	0.016±0.012
Hondeklip Bay	21	5(3)	0.35±0.13	0.01±0.01	20	12(6)	0.64±0.09	0.022±0.015
Lambert′s Bay	21	5(1)	0.35±0.13	0.02±0.01	20	12(7)	0.61±0.09	0.014±0.011
Agulhas Bioregion								
Gansbaai	9	7(4)	0.92±0.09	0.04±0.03	7	6(1)	0.60±0.15	0.019±0.014
Cape Agulhas	15	9(6)	0.85±0.09	0.05±0.03	11	7(5)	0.72±0.07	0.024±0.017
Herold′s Bay	22	13(10)	0.91±0.04	0.07±0.04	15	10(5)	0.64±0.10	0.024±0.016
Knysna Heads	23	8(3)	0.78±0.07	0.04±0.03	22	19(9)	0.77±0.07	0.028±0.018
Port Elizabeth	17	10(5)	0.84±0.09	0.03±0.02	14	1(3)	0.71±0.09	0.017±0.013
Haga Haga	15	9(4)	0.89±0.07	0.03±0.02	12	7(1)	0.61±0.11	0.016±0.012
Namaqua Bioregion	62	9(6)	0.30±0.08	0.01±0.01	58	27(18)		
Agulhas Bioregion	101	39(36)	0.86±0.03	0.05±0.03	81	39(30)		
All localities	163	45	0.82±0.02	0.05±0.03	139	57	0.68±0.03	0.021±0.014

4.3.3 Population structure and gene flow

4.3.3.1 Analysis of spatial structure and pairwise population differentiation

Haplotype networks for COI for *O. sinensis* and *O. tigrina* did not show any evidence of geographic association of haplotypes whereas that of *O. variegata* showed clear frequency differences of haplotypes between the west coast and the south-east coast lineages (Fig. 4.2).

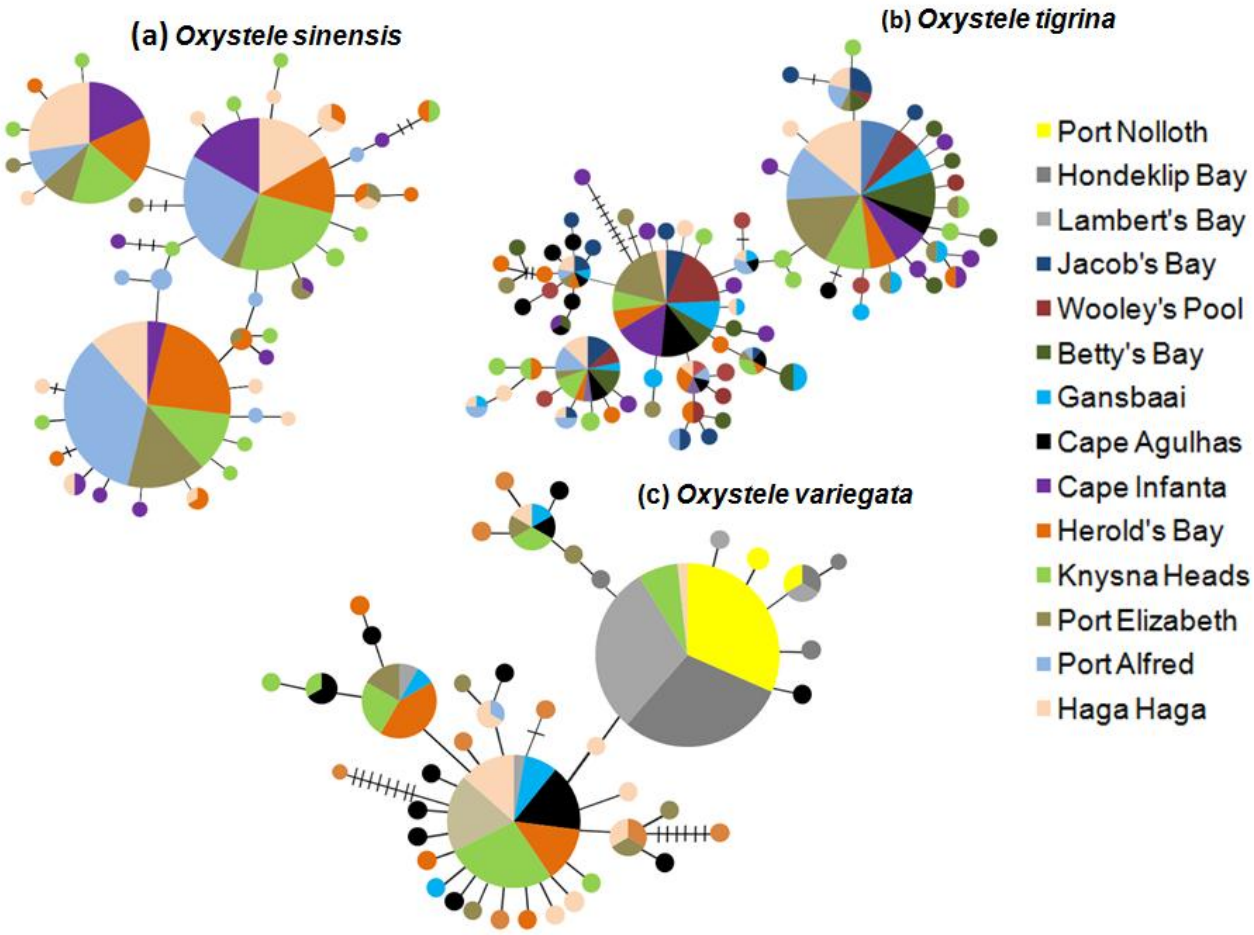

Figure 4.2 Statistical-parsimony networks of COI haplotypes of (a) *Oxystele sinensis*, (b) *O. tigrina* and (c) *O. variegata*. Each circle represents a haplotype and its size is proportional to the frequency of the haplotype over the whole data set. Colours indicate the location of the haplotype. The smallest solid circle represents a frequency of one. Cross hatching indicates inferred intermediate haplotypes (mutational steps) not observed in the data.

All COI pairwise Φ_{ST} values were low and non-significant ($p > 0.015$, after the B-Y false discovery rate correction) for *O. sinensis* (Table 4.3) and for *O. tigrina* (Table 4.4). In contrast, *O. variegata* exhibited relatively high and significant ($p < 0.012$) pairwise Φ_{ST} values between all localities on the west coast Namaqua Bioregion and those on the south coast Agulhas Region, but there was no differentiation between populations within each region (Table 4.5).

Table 4.3 Pairwise Φ_{ST} values of mitochondrial COI (above diagonal) and nuclear ITS2 (below diagonal) among the 11 *Oxystele sinensis* sampling sites included in the present study. Φ_{ST} Values in bold represent those that were significant after B-Y false discovery rate correction ($p < 0.015$).

	CI	HB	KH	PE	PA	HH
CI		0.00	0.00	0.00	0.03	0.00
HB	0.01		0.00	0.01	0.00	0.00
KH	0.03	0.02		0.00	0.07	0.00
PE	0.01	0.02	0.03		0.00	0.00
PA	0.00	0.01	0.03	0.01		0.03
HH	0.13	0.00	0.04	0.00	0.00	

CI, Cape Infanta; HB, Herold′s Bay; KH, Knysna Heads; PE, Port Elizabeth; PA, Port Alfred; HH, Haga Haga

Table 4.4 Pairwise Φ_{ST} values of mitochondrial COI (above diagonal) and nuclear ITS2 (below diagonal) among the 11 *Oxystele tigrina* sampling sites included in the present study. Φ_{ST} Values in bold represent those that were significant after B-Y false discovery rate correction ($p < 0.011$).

	JB	WP	BB	GB	CA	CI	HB	KH	PE	PA	HH
JB		0.00	0.33	0.47	0.00	0.00	0.17	0.00	0.00	0.26	0.34
WP	0.20		0.00	0.17	0.00	0.00	0.00	0.00	0.00	0.00	0.00
BB	0.02	0.10		0.15	0.00	0.00	0.00	0.00	0.00	0.00	0.00
GB	0.03	0.40	0.11		0.13	0.19	0.06	0.13	0.23	0.08	0.07
CA	0.01	0.09	0.00	0.10		0.00	0.04	0.00	0.04	0.00	0.00
CI	0.00	0.06	0.00	0.10	0.00		0.03	0.00	0.00	0.00	0.00
HB	0.00	0.38	0.01	0.00	0.02	0.00		0.01	0.07	0.00	0.00
KH	0.00	0.10	0.00	0.00	0.00	0.00	0.00		0.00	0.00	0.00
PE	0.00	0.18	0.01	0.00	0.00	0.00	0.00	0.00		0.00	0.00
PA	0.00	0.24	0.02	0.02	0.00	0.00	0.00	0.00	0.00		0.00
HH	0.06	0.03	0.02	0.23	0.00	0.00	0.18	0.00	0.00	0.09	

JB, Jacob′s Bay; WP, Wooley′s Pool; BB, Betty′s Bay; GB, Gansbaai; CA, Cape Agulhas; CI, Cape Infanta; HB, Herold′s Bay; KH, Knysna Heads; PE, Port Elizabeth; PA, Port Alfred; HH, Haga Haga

Table 4.5 Pairwise Φ_{ST} values of mitochondrial COI (above diagonal) and nuclear ITS2 (below diagonal) among the nine *Oxystele variegata* sampling sites included in the present study. Φ_{ST} Values in bold represent those that were significant were significant after B-Y false discovery rate correction ($p < 0.012$).

	PN	HKB	LB	GB	CA	HB	KH	PE	HH
PN		0	0.01	**0.71**	**0.57**	**0.50**	**0.51**	**0.67**	**0.68**
HK	0		0.01	**0.67**	**0.54**	**0.49**	**0.49**	**0.64**	**0.64**
LB	0	0.03		**0.56**	**0.45**	**0.42**	**0.39**	**0.55**	**0.54**
GB	0	0	0		0	0	0	0	0.04
CA	**0.14**	**0.14**	**0.15**	0.12		0.01	0	0	0.01
HB	0.02	0.06	0.02	0.02	0.08		0.02	0.01	0.06
KH	0.01	0.02	0.02	0	**0.12**	0.04		0.02	0.05
PE	0	0	0	0	**0.14**	0.04	0.01		0
HH	0	0.01	0	0	**0.13**	0	0.01	0	

PN, Port Nolloth; HKB, Hondeklip Bay, LB, Lambert′s Bay; GB, Gansbaai; CA, Cape Agulhas; HB, Herold′s Bay; KH, Knysna Heads; PE, Port Elizabeth; HH, Haga Haga

AMOVA did not recover any significant structure in *O. sinensis* (Table 4.6). However, AMOVA returned weak though significant genetic structuring for *O. tigrina* when localities were pooled into four groups defined by the known genetic barriers around Cape Point, Algoa Bay and the Cape Agulhas ($\Phi_{CT} = 0.11$, $p < 0.05$, Table 4.7). Genetic structuring was most pronounced in O. *variegata,* in which 48% of the variation was explained when localities were split into the Namaqua Bioregion and the Agulhas Bioregion ($\Phi_{CT} = 0.48$, $p < 0.05$,Table 4.8). Although AMOVA also recovered significant structure for *O. variegata* when localities were grouped into four bioregions with genetic breaks around Cape Point, Cape Agulhas and Algoa Bay (Table 4.8), no structure was recovered when the west coast localities were removed from the analysis ($\Phi_{CT} = 0$, $p > 0.05$, AMOVA table not shown), indicating that the significant result was caused by the disjunction between the Namaqua Bioregion and the Agulhas Bioregion.

Accordingly, BAPS returned no significant spatial structure in *O. sinensis* and *O. tigrina*, but confirmed the Namaqua Bioregion versus Agulhas Bioregion disjunction recovered by AMOVA in *O. variegata* by recovering two spatial population groups, one corresponding to the Namaqua Bioregion and the other corresponding to the Agulhas Bioregion (Fig. 4.3).

Table 4.6 Hierarchical analysis of molecular variance for COI and ITS2 in *Oxystele sinensis*. (a) whole population; (b) among putative groups define by known genetic barriers: south-east (CI, HB, KH, PE) vs east (PA, HH).

Source of Variation	df	Variation (%)	Φ statistics	P	df	Variation (%)	Φ statistics	P
	COI				ITS2			
(a) Global								
Among localities	5	0.00	0.00	0.49	5	1.63	0.02	0.02
Within localities	109	100.00			208	98.37		
(b) Among biogeographic provinces (south-east vs east)								
Among groups	1	0.93	0.01	0.26	1	0.53	0.01	0.20
Among localities within groups	4	0.00	0.00	0.49	4	1.32	0.01	0.07
Within localities	109	99.07	0.00	0.61	208	98.14	0.02	0.03

CI, Cape Infanta; HB, Herold′s Bay; KH, Knysna Heads; PE, Port Elizabeth; PA, Port Alfred; HH, Haga Haga

Table 4.7 Hierarchical analysis of molecular variance for COI and ITS2 in *Oxystele tigrina*. (a) whole population; (b) among putative groups define by known genetic barriers: west (JB) vs south coast (GB, CA) vs south-east (HB, KH, PE) vs east (HH).

Source of Variation	df	Variation (%)	Φ statistics	P	df	Variation (%)	Φ statistics	P
	COI				ITS2			
(a) Global								
Among localities	10	5.10	0.05	0.50	10	4.69	0.05	0.10
Within localities	221	94.90			403	95.31		
(b) Among putative groups (west vs south vs south-east vs east)								
Among groups	3	8.00	0.08	0.00	3	0.00	0.00	0.61
Among localities within groups	7	0.00	0.00	0.26	7	11.00	0.11	0.05
Within localities	221	92.00	0.08	0.00	403	89.01	0.11	0.06

JB, Jacob′s Bay; GB, Gansbaai; CA, Cape Agulhas; HB, Herold′s Bay; KH, Knysna Heads; PE, Port Elizabeth; HH, Haga Haga

Table 4.8 Hierarchical analysis of molecular variance for COI and ITS in *Oxystele variegata*. (a) Namaqua Bioregion (PN, HKB, LB) vs south coast Agulhas Bioregion (GB, CA, HB, KH, PE, HH); (b) among putative groups defined by known genetic barriers: west (PN, HKB, LB) vs south coast (GB, CA) vs south-east (HB, KH, PE) vs east (Haga Haga).

Source of Variation	df	Variation (%)	Φ statistics	P	df	Variation (%)	Φ statistics	P
	COI				ITS2			
(a) west coast Namaqua Bioregion vs south coast Agulhas Bioregion								
Between bioregions	1	47.77	0.48	0.01	1	0.00	0.00	0.67
Among localities within bioregions	7	0.83	0.02	0.18	7	3.71	0.04	0.00
Within localities	154	51.40	0.49	0.00	269	96.29	0.03	0.00
(b) Among putative groups (west vs south vs south-east vs east)								
Among groups	3	39.21	0.39	0.00	3	0.11	0.00	0.31
Among localities within groups	5	0.53	0.01	0.26	5	3.41	0.03	0.03
Within localities	154	60.26	0.40	0.00	269	96.48	0.04	0.00

PN, Port Nolloth; HKB, Hondeklip Bay; LB, Lambart′s Bay; GB, Gansbaai; CA, Cape Agulhas; CI, Cape Infanta; HB, Herold′s Bay; KH, Knysna Heads; PE, Port Elizabeth; PA, Port Alfred; HH, Haga Haga

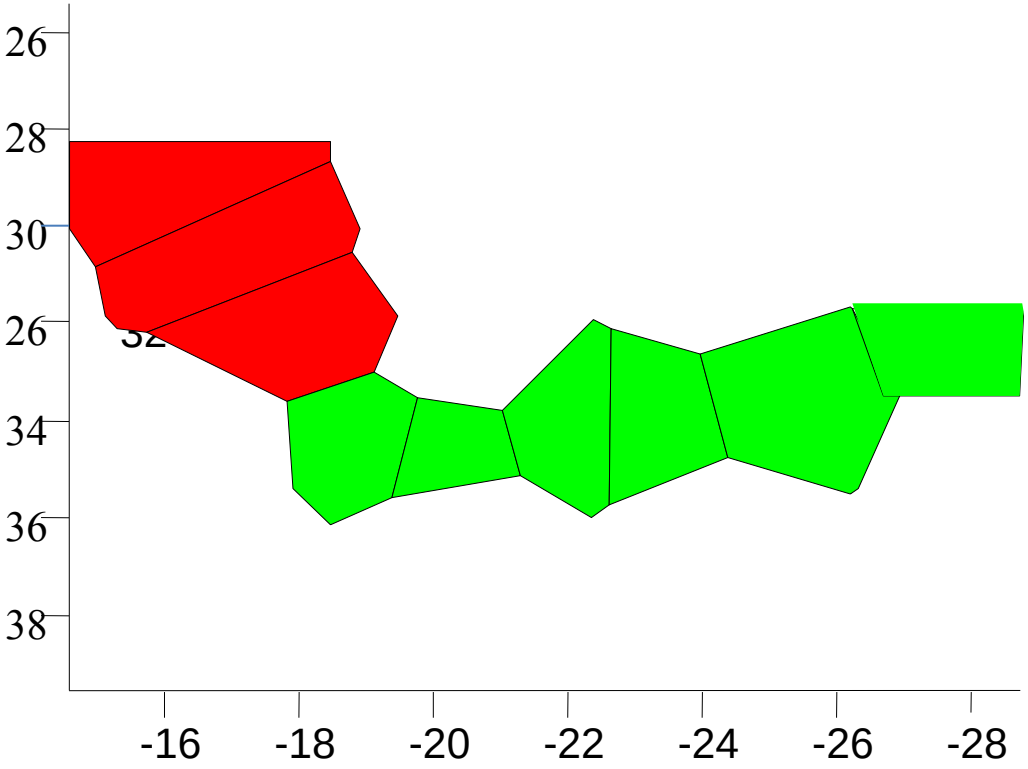

Figure 4.3 Two spatial population groups returned by BAPS for COI data in *Oxystele variegata*. Y-axis = latitude, x-axis = longitude; Red = Namaqua Bioregion (Port Nolloth, Hondeklip Bay, Lambert′s Bay; Green = Agulhas Bioregion (Gansbaai, Cape Agulhas, Herold′s Bay, Knysna Heads, Port Elizabeth, Haga Haga).

Mantel tests based on COI were performed on the whole data for *O. sinensis* and *O. tigrina* since they did not exhibit strong population genetic structure, but for *O. variegata*, the Mantel test was carried out for the south-east (GB-HH) populations and the west coast populations (PN-LB) separately because of a significant disjunction around the Cape Point region. The tests did not detect significant correlations between genetic and geographic distance for all three species/groups within species, *O. sinensis* ($r = -0.32$, $p > 0.05$), *O. tigrina* ($r = 0.16$, $p > 0.05$) and *O. variegata* ($r = 0.21$, $p > 0.05$; $r = 0.31$, $p > 0.05$, for the south-east and west coast lineages, respectively); suggesting a lack of genetic isolation by geographic distance in all of three species.

For ITS2, there was no evidence of spatial genetic structuring neither from pairwise Φ_{ST} values nor AMOVA for *O. sinensis* and *O. tigrina*. All pairwise Φ_{ST} values were close to zero and non-significant (after the B-W false discovery rate correction, Tables 4.3 and 4.4). *A priori*

grouping configurations of populations according to known genetic breaks did not yield any significant structuring from AMOVA for these two species either (Tables 4.6 and 4.7).

In *O. variegata*, the *a priori* grouping that split populations into west coast and south-east coast did not yield any significant structure from AMOVA at the ITS2 locus (Table 4.8). But the pairwise Φ_{ST} values between CA and all other populations except HB, were significant (Table 4.5). BAPS did not recover any significant population spatial structure at the ITS2 locus for any of the three species.

4.3.3.2 Coalescent analysis of gene flow

The COI and ITS2 data were combined for coalescent analyses of gene flow. In *O. sinensis*, gene flow is generally asymmetrical. Gene flow is predominantly south-westward in the direction of the Agulhas Current from PE to CI, except between HB and KH where gene flow is bi-directional (Fig 4.4; Table 4.9). From PE to HH, gene flow is predominantly north-eastwards against the Agulhas Current (Fig. 4.4; Table 4.9), indicative of the flow of the inshore counter currents. Compared to other species, gene flow looks high and predominantly bi-directional between many localities in *O. tigrina* (Fig. 4.4; Table 4.10). However, it appears that between BB and HB gene flow is predominantly north-eastwards with the inshore counter current but from PA to HB it is south-westwards with the Agulhas Current. In *O. variegata*, gene flow is clearly asymmetrical on the west coast Namaqua Bioregion, being north-westwards in the direction of the Benguela Current from (LB to PN) with no gene flow in the opposite direction (Fig. 4.4; Table 4.11). Notably there is no gene flow from the west coast (LB) to the east (GB) whereas there is substantial gene flow in the reverse direction.

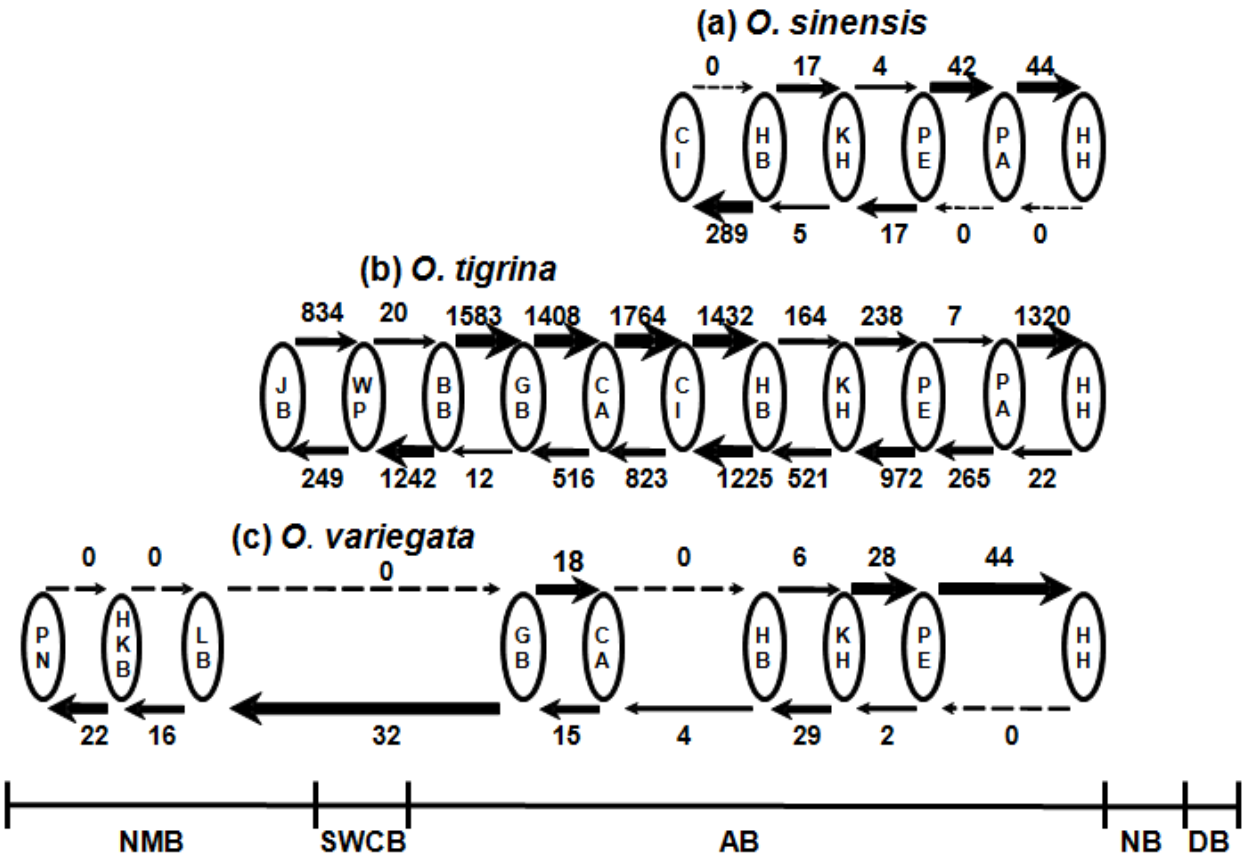

Figure 4.4 Directionality of gene flow between adjacent localities on the South African coast for *Oxystele sinensis*, *O. tigrina* and *O. variegata* based on a stepping stone migration model. Shown at the bottom are bioregions on the South African coast. Arrows indicate the direction of gene flow and the thickness of an arrow is proportional to relative migration rate. Numbers above and below the arrows indicate the relative migration rates. Locality abbreviations are as follows: PN, Port Nolloth; HKB, Hondeklip Bay; LB, Lambert′s Bay; BB, Betty′s Bay; GB, Gansbaai; CA, Cape Agulhas, HB, Herold′s Bay; KH, Knysna Heads; PE, Port Elizabeth; HH, Haga Haga. Bioregion abbreviations are as follows: NMB, Namaqua Bioregion; SWCB, South-western Cape Bioregion; AB, Agulhas Bioregion; NB, Natal Bioregion, DB, Delagoa Bioregion

On the south coast Agulhas Bioregion, gene flow is predominantly south-westwards in the direction of the Agulhas Current from KH to GB. This pattern is interrupted in the False Bay region where symmetrical gene flow is recorded between GB and CA. Except for the bidirectional gene flow between KH and HB, gene flow is mainly north-eastwards from KH to HH (Fig. 4.4; Table 4.11) opposite to the Agulhas Current.

Table 4.9 Directionality of gene flow for *Oxystele sinensis* between each locality pair for the stepping stone migration model along the South African coast based on the combined COI and ITS data set. Numbers indicate relative migration rates (N_em) and the 95% confidence intervals.

From population	To population	N_em	95% Confidence Interval
(Cape Infanta) (CI)	(Herold′s Bay)	0.2	0.0-0.9
(Herold′s Bay) (HB)	(Cape Infanta)	288.6	45.9-6953.5
(Herold′s Bay)	(Knysna Heads)	16.7	8.8-31.9
(Knysna Heads)	(Herold′s Bay)	4.6	2.5-8.1
(Knysna Heads)	(Port Elizabeth)	3.6	2.1-5.9
(Port Elizabeth) (PE)	(Knysna Heads)	17.6	9.3-33.4
(Port Elizabeth)	(Port Alfred)	42.5	20.3-94.7
(Port Alfred) (PA)	(Port Elizabeth)	0.0	0.0-0.2
(Port Alfred)	(Haga Haga)	44.3	16.6-133.2
(Haga Haga) (HH)	(Port Alfred)	0.0	0.0-2.5

Table 4.10 Directionality of gene flow for *Oxystele tigrina* between each locality pair for the stepping stone migration model along the South African coast based on the combined COI and ITS data set. Numbers indicate relative migration rates (N_em) and the 95% confidence intervals.

From population	To population	N_em	95% Confidence Interval
(Jacob′s Bay) (JB)	(Wooley′s Pool)	834.4	53.3-1947.1
(Wooley′s Pool)	(Jacob′s Bay)	48.5	44.3-188.4
(Wooley′s Pool)	(Betty′s Bay)	20.1	0.1-135.2
(Betty′s Bay) (BB)	(Wooley′s Pool)	1242.3	82.8-1981.4
(Betty′s Bay)	(Gansbaai)	1582.7	130.0-1993.4
(Gansbaai) (GB)	(Betty′s Bay)	12.1	0.1-67.8
(Gansbaai)	(Cape Agulhas)	1407.7	118.5- 1997.4
(Cape Agulhas) (CA)	(Gansbaai)	516.4	6.5-1423.3
(Cape Agulhas)	(Cape Infanta)	1764.0	143.3-1993.4
(Cape Infanta) (CI)	(Cape Agulhas)	823.2	61.5-1982.8
(Cape Infanta)	(Herold′s Bay)	1432.4	114.2-1996.0
(Herold′s Bay) (HB)	(Cape Infanta)	1225.4	67.2-1993.4
(Herold′s Bay)	(Knysna Heads)	163.5	15.6-1624.6
(Knysna Heads) (KH)	(Herold′s Bay)	520.9	75.3-1969.4
(Knysna Heads)	(Port Elizabeth)	38.3	34.4-1839.9
(Port Elizabeth) (PE)	(Knysna Heads)	972.0	124.3-1997.4
(Port Elizabeth)	(Port Alfred)	6.6	0.1-34.9
(Port Alfred) (PA)	(Port Elizabeth)	264.6	72.7-1982.6
(Port Alfred)	(Haga Haga)	1314.9	128.9-1992.0
(Haga Haga) (HH)	(Port Alfred)	21.9	0.3-100.4

4.3.3.3 Divergence times

Considering the shallow genetic structuring observed for the other two species, divergence time was estimated only between the west coast Namaqua Bioregion and the south-east Agulhas Bioregion genetic assemblages for *O. variegata*. At 2.4% Myr^{-1}, the two genetic assemblages appear to have diverged between c. 110 and 230 kya and sequences within each genetic assemblage coalesced between c. 100 and 210 kya, and 85 and 190 kya, respectively. At the lower mutation rate of 0.35% Myr^{-1}, the genetic assemblages would have diverged much earlier between c. 630 and 1 350 kya. Coalescences within genetic assemblage would date to between c. 550 and 1 200 kya, and 450 and 1 100 kya, for the south-east and west coast genetic assemblages, respectively.

Table 4.11 Directionality of gene flow for *Oxystele variegata* between each locality pair for the stepping stone migration model along the South African coast based on the combined COI and ITS data set. Numbers indicate relative migration rates (N_em) and the 95% confidence intervals.

From population	To population	N_em	95% Confidence Interval
(Port Nolloth) (PN)	(Hondeklip Bay)	0.00	0.00-0.00
(Hondeklip Bay) (HB)	(Port Nolloth)	21.91	3.97-87.92
(Hondeklip Bay)	(Lambert‟s Bay)	0.00	0.00-1.56
(Lambert′s Bay) (LB)	(Hondeklip Bay)	15.93	8.21-31.14
(Lambert′s Bay)	(Gansbaai)	0.00	0.00-0.00
(Gansbaai) (GB)	(Lambert′s Bay)	31.68	8.69-62.01
(Gansbaai)	(Cape Agulhas)	18.30	0.85-98.83
(Cape Agulhas) (CA)	(Gansbaai)	14.52	9.00-53.58
(Cape Agulhas)	(Herold′s Bay)	0.00	0.00-171.90
(Herold′s Bay) (HB)	(Cape Agulhas)	3.80	2.20-6.38
(Herold′s Bay)	(Knysna Heads)	5.96	3.52-79.04
(Knysna Heads) (KH)	(Herold′s Bay)	28.96	12.94-69.62
(Knysna Heads)	(Port Elizabeth)	27.57	15.85-48.95
(Port Elizabeth) (PE)	(Knysna Heads)	2.15	0.99-38.32
(Port Elizabeth)	(Haga Haga)	44.23	20.53-102.93
(Haga Haga) (HH)	(Port Elizabeth)	0.00	0.00-1.01

4.3.4. Demographic history

4.3.4.1 Haplotype networks

For COI, visual examination of network characteristics, neutrality tests, mismatch distributions and BSPs indicate that recent demographic expansion occurred in all three species. The haplotype networks for all three species exhibited shallow topologies with each of the common haplotypes being surrounded by rare descended alleles, creating star-like phylogenies (Fig. 4.2) indicative of departures from the neutral model due to recent population expansions or selection.

4.3.4.2 Fu's Fs and mismatch distributions

As only weak population genetic structure was observed in *O. sinensis* and *O. tigrina* across the entire distribution range, historical demographic analyses were performed on the pooled data sets for these two species. For *O. variegata*, given the geographic orientation of haplotypes, tests for demographic expansion were carried out on the pooled data set, as well as separately for the Namaqua Bioregion genetic assemblage and the Agulhas Bioregion genetic assemblage for COI.

As expected from shallow haplotype networks, Fu′s Fs values were negative and significant ($p < 0.02$) for all species (Table 4.12) indicating an excess of low frequency mutations, which is expected under the neutral model, for species that have experienced a recent demographic expansion event. The McDonald and Kreitman test was not significant all three species - *O. sinensis* (Neutrality index = 0.302, Fisher test p = 0.10); *O. tigrina* (Neutrality index = 0.667, Fisher test p = 0.39), and *O. variegata* (Neutrality index = 1.281, Fisher test p = 0.64) - indicating that COI sequences for these species were not under selection.

Further evidence of recent demographic expansion was obtained from mismatch distributions, which were smooth and unimodal (non-significant *r* and *SSD* values, Table 4.12), conforming both to pure demographic expansion and range expansion models for all species (Figs 4.5 - 4.7). Based on a COI mutation rate of 2% Myr^{-1}, the estimate of τ for the whole data set for *O. sinensis* corresponded to a timing of expansion c. 140 kya (95% CI = 40 – 240 kya) and for *O.*

tigrina expansion began c. 170 kya (95% CI = 70 – 280 kya). In *O. variegata*, signals of population expansion were detected in both genetic assemblages as well as the whole data set, and in all cases, the observed mismatch distributions conformed both to the pure demographic expansion model and the range expansion model (Fig. 4.7). Estimates of times of expansion for the Agulhas Bioregion genetic assemblage of c. 90 kya (95% CI = 30–130 kya) was consistent with the date inferred for the whole data set, c. 110 kya (95% CI = 30–190 kya), whereas that of the Namaqua Bioregion genetic assemblage, c. 120 kya (95% CI = 10–140 kya), also suggests a pre-LGM expansion, although a post- LGM expansion cannot be outright rejected if 95% CI is considered. The pronounced overlaps among the confidence intervals for estimates of intraspecific times of expansion suggest that a hypothesis that demographic expansions occurred at the same time in all three species cannot be rejected. Interestingly, times of expansion for all three *Oxystele* species considerably predated the LGM (19-26.5 kya, Clark *et al*., 2009), (Fig. 4.8). Using the lower mutation rate of 0.35% Myr^{-1}, demographic expansion would have begun much earlier between c.150 and 1 470 kya (Table 4.14), a period spanning the middle to late Pleistocene. Additionally, θ values for contemporary populations (θ_1) were consistently greater than for the ancestral populations (θ_0) supporting a significant increase in effective population size in all species (Table 4.12).

As at the COI locus, Fu′s F_s values for ITS2 were significantly negative indicating departure from neutrality (Table 4.13). Likewise, mismatch distributions in conjunction with *SSD* and *r* statistics for ITS2 presented unimodal distributions conforming both to pure demographic expansion and range expansion models for all species (Figs 4.5 – 4.7).

Table 4.12 Fu′s F_s values and demographic parameters for COI sequences in *Oxystele sinensis*, *O. tigrina* and *O. variegata*. Number of individuals sequenced (N), Fu′s F_s values (* means significant at $p < 0.02$), Harpending′s raggedness indices (r), sum of squared deviations (SSD) (** means significant at $p < 0.05$), and mismatch distribution parameter τ (95% confidence intervals), are listed.

Locality	N	Fu′s F_s	Pure demographic expansion			Range expansion		
			r	SSD	τ	*r*	SSD	τ
O. sinensis								
Cape Infanta	14	-4.33*	0.04	0.06	4.10(1.37;6.99)	0.04	0.02	3.49(1.18;6.01)
Herold′s Bay	21	-3.75	0.02	0.01	3.80(1.10;6.85)	0.02	0.01	2.38(0.74;5.74)
Knysna Heads	23	-9.12*	0.02	0.00	3.30(1.07;5.53)	0.02	0.00	2.51(0.92;4.87)
Port Elizabeth	13	-2.17	0.05	0.02	4.0(1.35;6.36)	0.05	0.02	3.73(0.96;5.58)
Port Alfred	23	-2.16	0.05	0.02	2.7(0.2;5.3)	0.02	0.00	2.20(0.40;4.45)
Haga Haga	21	-6.28*	0.04	0.10**	1.50(0.52;2.55)	0.04	0.02	1.49(0.44;4.89)
All localities	115	-26.63*	0.02	0.00	3.50(1.00;5.83)	0.02	0.01	2.43(0.83;4.72)
O. tigrina								
Jacob′s Bay	22	-3.88	0.03	0.01	4.50(1.21;8.04)	0.03	0.01	2.73(0.85;6.97)
Wooley′s Pool	21	-6.26*	0.02	0.00	3.70(1.18;6.30)	0.02	0.00	2.57(0.80;5.33)
Betty′s Bay	22	-5.45*	0.01	0.00	4.50(1.49;8.01)	0.01	0.00	2.98(1.11;6.67)
Gansbaai	18	-7.06*	0.02	0.00	2.60(1.07;6.05)	0.02	0.00	2.33(1.10;4.93)
Cape Agulhas	19	-7.52*	0.03	0.00	2.90(1.18;4.19)	0.03	0.00	2.46(1.09;4.31)
Cape Infanta	22	-7.38*	0.02	0.00	3.00(0.92;7.69)	0.02	0.00	2.12(0.83;6.16)
Herold′s Bay	17	-7.63*	0.03	0.00	2.90(1.28;5.34)	0.03	0.00	2.75(1.31;4.79)
Knysna Heads	22	-5.20*	0.02	0.01	4.10(1.34;6.72)	0.02	0.01	3.50(1.17;5.69)
Port Elizabeth	23	-3.36	0.03	0.01	4.10(0.72;7.84)	0.03	0.01	3.35(0.63;5.99)
Port Alfred	22	-2.06	0.06	0.01	4.70(1.28;8.58)	0.06	0.01	3.31(1.06;7.28)
Haga Haga	24	-4.66*	0.18	0.04	3.10(1.18;7.11)	0.18	0.04	2.71(1.07;5.83)
All localities	234	-25.88*	0.01	0.00	4.20(1.61;6.82)	0.01	0.00	2.83(1.32;5.51)

Table 4.12 continued

Locality	N	Fu′s F_s	Pure demographic expansion			Range expansion		
			r	SSD	τ	*r*	SSD	τ
O. variegata								
Port Nolloth	20	-1.86*	0.41	0.00	3.0(0.4; 3.2)	0.41	0.00	0.16(0.00;1.44)
Hondeklip Bay	21	-3.13*	0.19	0.00	3.0(0.0; 4.3)	0.77	0.00	0.68(0.00;3.08)
Lambert′s Bay	21	-1.83	0.26	0.01	3.0(0.0; 4.2)	0.62	0.00	2.91(0.00;5.75)
Gansbaai	9	-3.62*	0.07	0.01	2.2(0.7; 3.9)	0.81	0.01	2.23(0.72;3.88)
Cape Agulhas	15	-3.48*	0.02	0.00	2.8(0.4; 6.0)	0.89	0.00	1.88(0.53;5.17)
Herold′s Bay	22	-5.00*	0.04	0.01	2.1(0.9; 4.3)	0.23	0.01	2.50(0.77;3.69)
Knysna Heads	23	-1.76	0.10	0.02	2.3(0.0; 4.4)	0.36	0.02	2.12(0.47;3.78)
Port Elizabeth	17	-6.31*	0.06	0.00	1.9(0.8; 3.1)	0.55	0.00	1.86(0.66;2.91)
Haga Haga	15	-6.25*	0.21	0.04	1.6(0.6; 2.9)	0.05	0.04	1.61(0.41;2.77)
West coast	62	-7.87*	0.28	0.01	3.0(0.3;3.5)	0.61	0.01	3.080.00;6.55)
South-east coast	101	-27.02*	0.03	0.00	2.1(0.8; 3.2)	0.49	0.00	2.08(0.71;2.91)
All localities	163	-26.94*	0.04	0.01	2.6(0.7; 4.5)	0.57	0.01	2.46(0.64;3.85)

Table 4.13 Fu′s F_s values and demographic parameters for ITS2 sequences in *Oxystele sinensis*, *O. tigrina* and *O. variegata*. Localities, number of individuals sequenced (N), number of haplotypes (N_h), haplotype diversity (h), nucleotide diversity (π), Fu′s Fs value, Harpending′s raggedness indices (r), and sum of squared deviations (SSD), and mismatch distribution parameter τ (95% confidence intervals) (*asterisks* represent significant results * $p < 0.02$).

Locality	N	Fu′s F_s	Pure demographic expansion		Range expansion	
			r	SSD	*r*	SSD
O. sinensis						
Cape Infanta	11	-2.89	0.06	0.00	0.06	0.00
Herold′s Bay	21	-11.67*	0.04	0.00	0.04	0.00
Kysna Heads	19	-5.81*	0.04	0.00	0.04	0.00
Port Elizabeth	14	-7.62*	0.06	0.01	0.06	0.00
Port Alfred	19	-8.99*	0.04	0.00	0.04	0.00
Haga Haga	23	-11.44*	0.06	0.00	0.06	0.00
All localities	107	-26.17*	0.04	0.00	0.04	0.00
O. tigrina						
Jacob′s Bay	18	-2.51	0.05	0.00	0.05	0.00
Wooley′s Pool	13	-0.58	0.08	0.01	0.08	0.01
Betty′s Bay	21	0.15	0.09	0.02	0.09	0.02
Gansbaai	21	-3.34	0.27	0.01	0.05	0.00
Cape Agulhas	24	-3.99	0.26	0.01	0.08	0.01
Cape Infanta	22	-0.58	0.34	0.01	0.07	0.01
Herold′s Bay	15	-7.58*	0.42	0.01	0.08	0.01
Kysna Heads	17	-1.24	0.29	0.01	0.11	0.01
Port Elizabeth	19	-2.07	0.28	0.01	0.11	0.01
Port Alfred	16	-0.85	0.42	0.01	0.09	0.01
Haga Haga	21	-0.11	0.27	0.01	0.11	0.01
All localities	173	-29.49	0.13	0.00	0.05	0.00
O. variegata						
Port Nolloth	18	-7.73*	0.05	0.00	0.05	0.00
Hondeklip Bay	20	-6.59*	0.03	0.00	0.03	0.00
Lambert′s Bay	20	-9.89*	0.05	0.00	0.05	0.00
Gansbaai	7	-2.30	0.05	0.01	0.05	0.00
Cape Agulhas	11	-1.70	0.06	0.01	0.05	0.01
Herold′s Bay	15	-4.30	0.05	0.01	0.05	0.01
Knysna Heads	22	-15.41*	0.03	0.00	0.03	0.00
Port Elizabeth	14	-7.96*	0.06	0.00	0.06	0.00
Haga Haga	12	-3.01	0.04	0.00	0.04	0.00
All localities	139	-28.25*	0.03	0.00	0.03	0.00

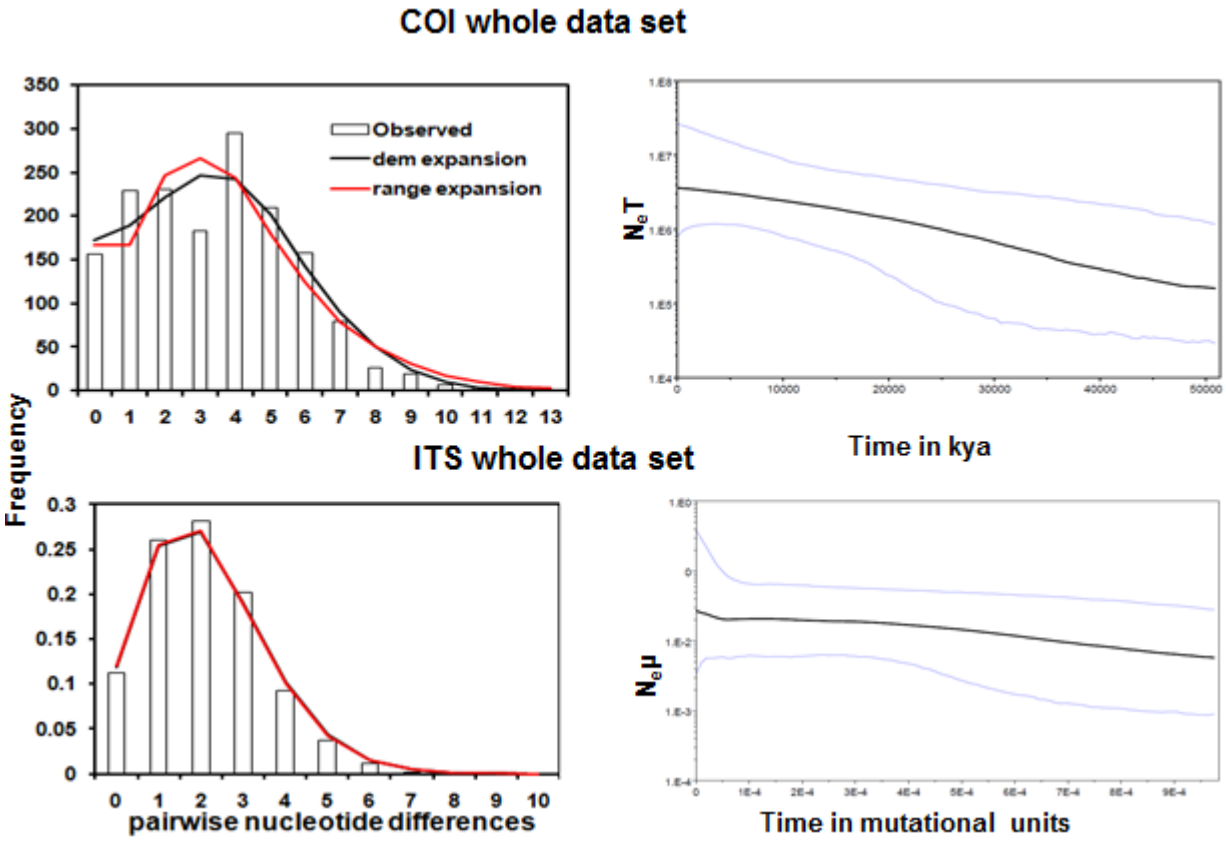

Figure 4.5 Demographic history of *Oxystele sinensis* inferred from COI and ITS2 sequences for whole data set. **(left)** Frequency distribution of pairwise differences among COI haplotypes: histograms show the observed distribution; lines show the expected distribution under a model of pure demographic expansion (solid line) and spatial expansion (dashed line). **(right)** Bayesian skyline plot for: COI (based on a mutation rate of 2.3 x 10^{-8} substitutions $site^{-1}$ yr^{-1}) and ITS2 (no specified mutation rate). Time (x-axis) is in thousands of years ago (kya) for COI and mutational units for ITS2. The central bold line represent the median value of N_eT for COI or $N_e\mu$ for ITS2, where N_e = effective population size, T = generation time, μ = mutation rate. The narrow lines denote the upper and lower confidence limits of the 95% Highest Posterior Density (HPD) interval.

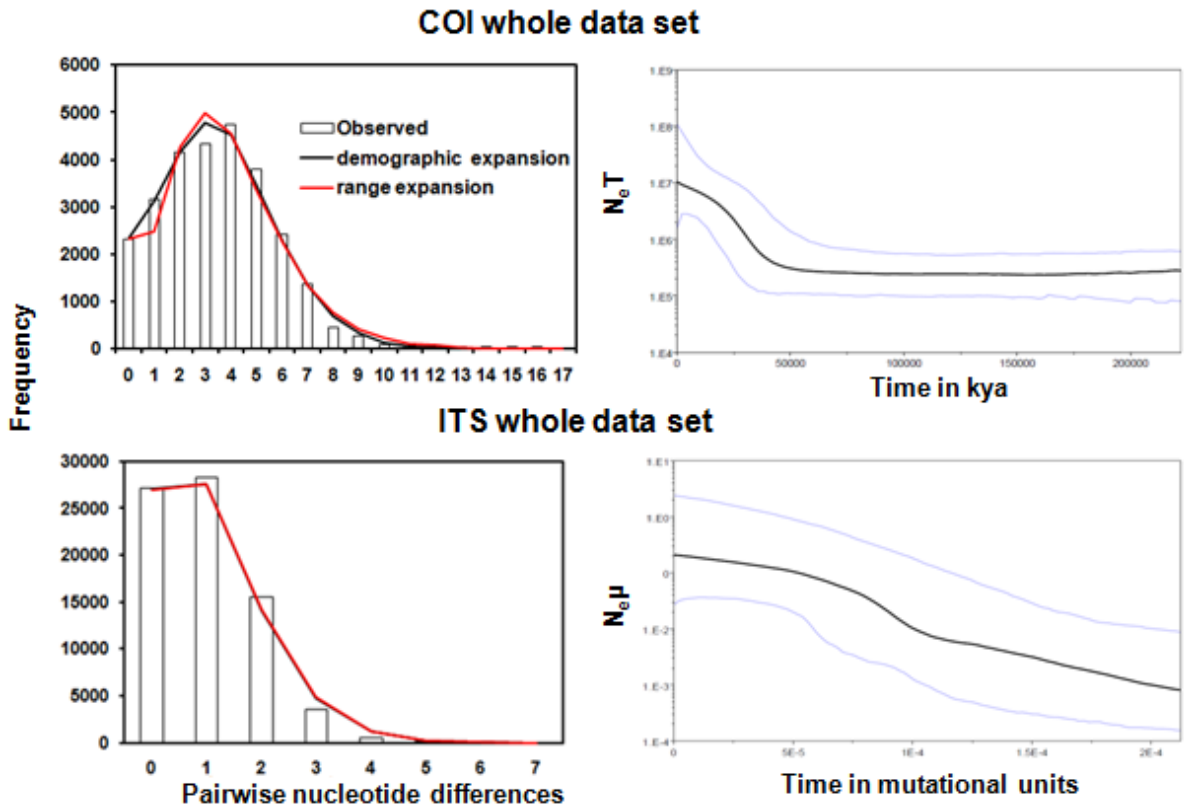

Figure 4.6 Demographic history of *Oxystele tigrina* inferred from COI and ITS2 sequences for whole data set. **(left)** Frequency distribution of pairwise differences among COI haplotypes: histograms show the observed distribution; lines show the expected distribution under a model of pure demographic expansion (solid line) and spatial expansion (dashed line). **(right)** Bayesian skyline plot for: COI (based on a mutation rate of 2.4 x 10^{-8} substitutions $site^{-1}$ yr^{-1}) and ITS2 (no specified mutation rate). Time (x-axis) is in thousands of years ago (kya) for COI and mutational units for ITS2. The central bold line represent the median value of N_eT for COI or $N_e\mu$ for ITS2, where N_e = effective population size, T = generation time, μ = mutation rate. The narrow lines denote the upper and lower confidence limits of the 95% Highest Posterior Density (HPD) interval.

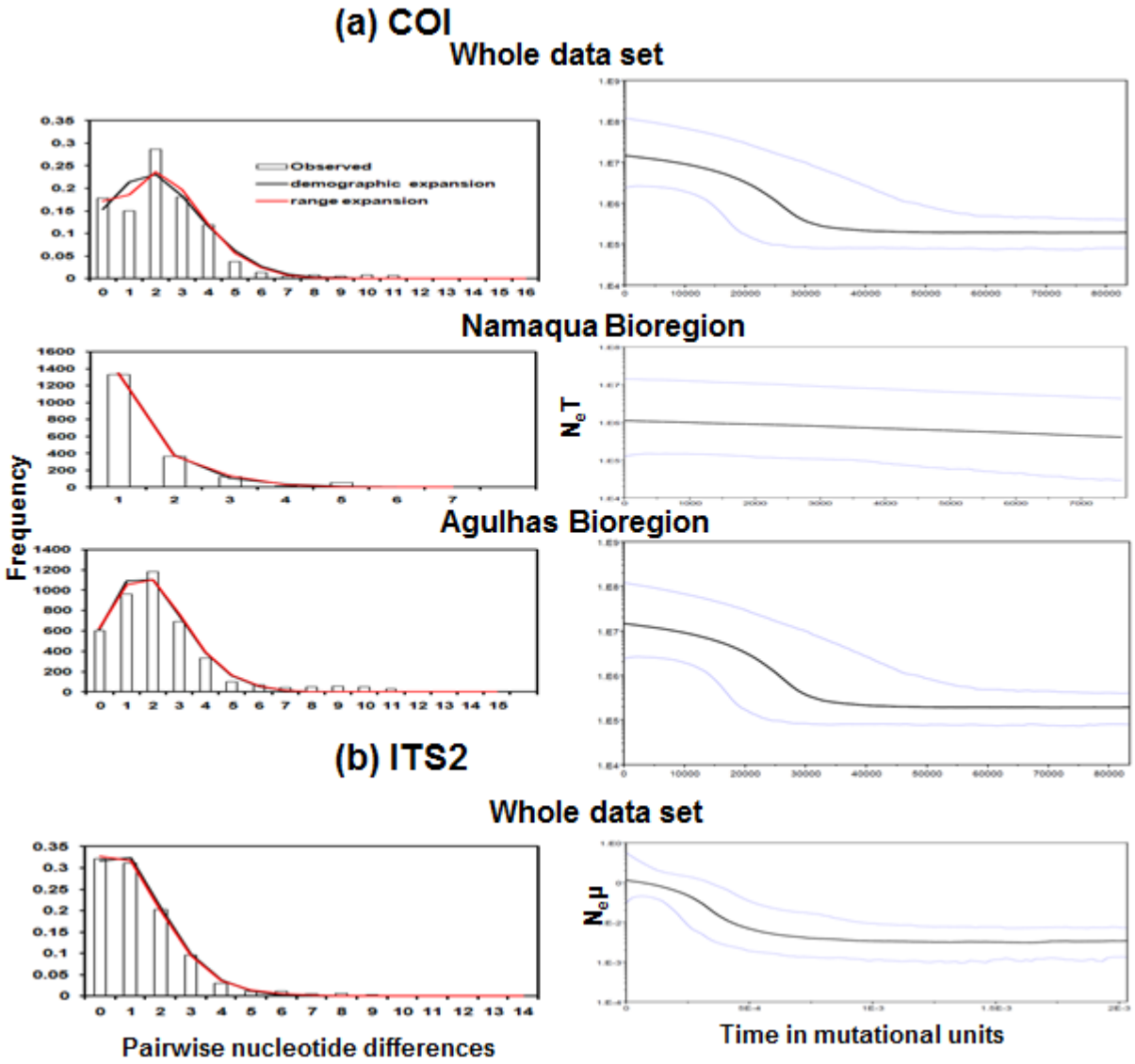

Figure 4.7 Demographic history of *Oxystele variegata* inferred from (a) COI sequences and (b) ITS2 sequences. **(left)** Frequency distribution of pairwise nucleotide differences among (a) COI haplotypes for: the whole data set, Namaqua Bioregion genetic assemblage, Agulhas Bioregion genetic assemblage, and (b) ITS2 haplotypes for the whole data set: histograms show the observed distribution; lines show the expected distribution under a model of pure demographic expansion (solid line) and spatial expansion (dashed line). **(right)** Bayesian skyline plots for (a) COI based on a mutation rate of 2.4 x 10^{-8} substitutions $site^{-1}$ yr^{-1} for: the whole data set, Namaqua Bioregion genetic assemblage, Agulhas Bioregion genetic assemblage: time (x-axis) in thousands of years ago (kya) The central bold line represent the median value of N_eT, where N_e = effective population size, T = generation time, the narrow lines denote the upper and lower confidence limits of the 95% Highest Posterior Density (HPD) interval, and (b) ITS2 haplotypes for the whole data set: time (x-axis) in mutational units , The central bold line represent the median value of $N_e\mu$, where N_e = effective population size, μ =mutation rate or, the narrow lines denote the upper and lower confidence limits of the 95% Highest Posterior Density (HPD) interval.

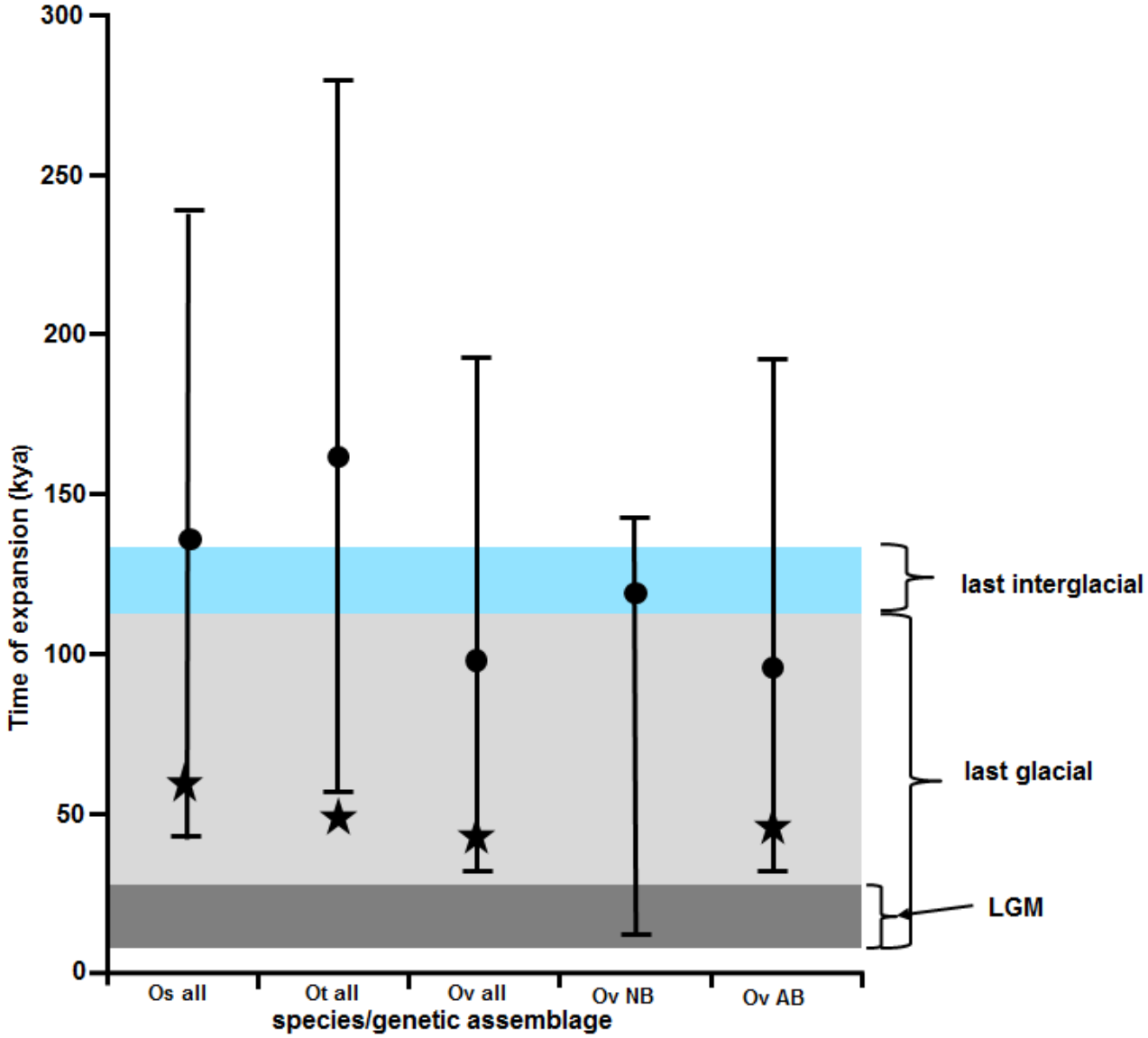

Figure 4.8 Population expansion times (in thousands of years ago, kya) and corresponding confidence intervals inferred from COI based on estimated mutation rates of 2.3 x 10^{-8} substitutions site^{-1} yr^{-1} (Os) and 2.4 x 10^{-8} site-1 yr^{-1} (Ot and Ov). Confidence intervals and solid circles show expansion times estimated by mismatch distributions. Stars show expansion times estimated by Bayesian skyline plots. No evidence of demographic expansion for Ov NB from the BSP. Abbreviations are as follows: Os all, *Oxystele sinensis* pooled data; Ot all, *O. tigrina* pooled data; Ov all, O. *variegata* pooled data; Ov NB, *O. variegata* Namaqua Bioregion genetic assemblage; Ov AB, *O. variegata* Agulhas Bioregion genetic assemblage. Shaded rectangles represent the approximate beginning and end of the following: last interglacial (blue), last glacial (both light gray and grey) and the last glacial maximum (grey).

4.3.4.3 Bayesian demographic reconstructions

BSPs further supported a hypothesis of demographic expansions in all three species (except the Namaqua Bioregion assemblage for *O. variegata*). Based on estimated mutation rates for COI, BSPs for all species were consistent with the results from mismatch analyses in that estimates of times of expansion from BSPs fell within the 95 % confidence interval of estimates from mismatch analyses and times of expansion pre-dated the LGM across the species. A COI BSP for *O. sinensis* indicates a 30-fold demographic expansion beginning c. 60 kya and continuing until c. 35 kya before it started levelling off (Fig 4.5). Similarly, in *O. tigrina* a sudden and huge (40-fold) increase in N_e began a bit later (c. 50 kya, Fig. 4.6) following a prolonged phase of demographic stability (50-200kya) (Fig. 4.5). Growth rate began to decline c. 25 kya.

The most dramatic demographic expansion occurred for the whole population in *O. variegata* in which a 30-fold increase in N_e occurred over a period of 20 000 years beginning c. 40 kya until c. 17 kya when the population began to stabilise (Fig. 4.7). A BSP for the genetic assemblage in the south coast Agulhas Bioregion is consistent with that of the whole population in that it shows a pre-LGM expansion beginning c. 40 kya until c. 25 kya before levelling off (Fig. 4.7), whereas that of the genetic assemblage in the west coast Namaqua Bioregion shows no clear evidence of expansion (Fig. 4.7). The lower substitution rate of 0.35% gives estimates of the timing of expansion between 230 and 340 kya for all three species (Table 4.14), still suggesting that demographic expansions began in the late Pleistocene.

Concordant with COI data, BSPs for the ITS2 locus suggest recent increases in effective population sizes in all three species; however, the demographic expansions were more modest than those shown for the COI locus (Figs 4.5 and 4.6). Interestingly, the nDNA also captures the stabilization in effective population size after expansion that was revealed by COI. Lack of data for mutation rate for ITS2 precluded the estimation of expansion times for the nuclear data.

Table 4.14 Time since expansion began in *Oxystele spp* based on different estimates of COI mutation rates (mutation rate in substitutions site^{-1}Myr^{-1})

Species	Mismatch distribution				Bayesian skyline plots		
	Tau (95% confidence interval)	Time of expansion (in years ago)			Time of expansion (in years ago)		
		0.35% Myr^{-1}	1.0 % Myr^{-1}	2.0% Myr^{-1}	0.35% Myr^{-1}	1.0 % Myr^{-1}	2.0% Myr^{-1}
O. sinensis	3.5 (1.00-5.83)	750,000 (210,000;1,250,000)	260,000 (80,000;440,000)	130,000 (40,000;220,000)	340,000	120,000	60,000
O. tigrina	4.20 (1.61-6.82)	900,000 (350,000;1,470,000)	320,000 (120,000;520000)	160,000 (60,000;260,000)	290,000	100,000	50,000
O. variegata	2.6 (0.70-4.50)	560,000 (150,000;970,000)	200,000 (50,000;340,000)	100,000 (30,000;170,000)	230,000	80,000	40,000

4.4 Discussion

4.4.1 Population structure and gene flow

All the three species *Oxystele sinensis, O. tigrina* and *O. variegata* showed negligible population structure where they occur sympatrically. For this geographic range genetic variation is characterised by low pairwise Φ_{ST} and AMOVA recovered weak or no structuring for all configurations that were tested. This outcome suggests high connectivity among populations, at least across the geographic range that was sampled in this study. High genetic connectivity is consistent with the life history of the species. They are all broadcast spawners and with pelagic larval stages which can facilitate long-distance dispersal. These findings should be regarded as preliminary for *O. sinensis* as a whole since no samples were collected across the Cape Agulhas and Cape Point regions, which have been identified as genetic barriers for several other marine invertebrates (see Teske *et al.*, 2011). A similar result has been found for a rocky shore fish *Caffrogobius caffer* (Neethling *et al*., 2008). If this lack of genetic structure is due to high levels of gene flow, then *O. sinensis* should have relatively higher capacity to disperse than the other *Oxystele* species since it exhibits the lowest degree of population differentiation.

An explanation for lack of population differentiation that is compatible with the demographic history of the species is that this pattern reflects recent range expansion throughout the coastline as individuals rapidly colonised previously uninhabited sites or recolonised previously lost habitat (Lasota *et al*., 2004; Crandall *et al*., 2010; McGovern *et al*., 2010). This explanation is corroborated by evidence from demographic analyses that clearly indicate that these species began expanding in the late Pleistocene between 30 and 340 kya. Alternatively, low differentiation could mean that the species have maintained high equilibrium levels of gene flow across their distribution range for a considerable period of time (Lasota *et al*., 2004; Peters *et al*., 2005; McGovern *et al*., 2010). In light of the relatively high rates of historical gene flow exhibited by all three species (Fig

4.4), the hypothesis of high population connectivity due to considerable gene flow cannot be rejected. Further, high gene flow among populations is compatible with the life history of the species characterised by broadcast spawning and pelagic larval development. Although the hypotheses given above are not mutually exclusive (e.g. Peters *et al*., 2005), the former seems more plausible. If gene flow had been high among localities (as the latter hypothesis proposes) not even weak population differentiation would have recorded. Although the method implemented in MIGRATE-N suggests relatively high levels of gene flow among neighbouring localities, one of its drawbacks is that it cannot differentiate between the effects of an episode of range expansion accompanied by high gene flow and high levels of recurrent gene flow (Brito, 2005).

Oxystele variegata shows a strong genetic disjunction between the west coast Namaqua Bioregion and the south coast Agulhas Bioregion, possibly across the Cape Point region. This is the only genetic barrier that has been confirmed by the coalescent based BAPS analysis. Whereas mitochondrial DNA returned a genetic barrier across Cape Point, nDNA did not. The discrepancy between nDNA and mtDNA could be a result of a selective sweep acting on individuals harbouring certain mtDNA lineages on the west coast. A selective sweep occurring in mtDNA would not affect nDNA diversity resulting in the observed disparity. This explanation is however, unlikely given the negative MK test suggesting no selection. An alternate explanation is that the genetic variability at ITS2 is not high enough to recover a signal of divergence.

This barrier has been recorded in other marine taxa in the region (e.g. crustacean *Exosphaeroma hylecoetes*, Teske *et al*., 2006; fish *Clinus cottoides*, von der Heyden *et al.*, 2008; Muller *et al*., 2012). The timing of the divergence between the Namaqua Bioregion and Agulhas bioregion genetic assemblages (between c. 110 and 230 kya using the estimated mutation rates) suggests a late Pleistocene origin of the genetic disjunction. At the lower mutation rate of 0.35% Myr^{-1}, the two genetic assemblages would have diverged between c. 630 and 1 350 kya, suggesting middle Pleistocene origin of the barrier. The timing of divergence at both mutation rates is much latter than that estimated by Teske *et al.* 2006 (2.5 million years ago) for a crustacean, probably

because the estimates are, in each case, based on a single marker, and therefore, prone to stochastic variance. Intraspecific lineage sorting process can be complicated by lineage-specific demographic factors population growth and substructure, reproductive and dispersal behaviours (Harling-Cognato *et al*., 2005). Furthermore, the differences in divergence time could have resulted from different methods used (conventional method based on divergence in Teske *et al*. (2006) whereas a coalescent-based method was used in this study).

A plausible explanation of the population genetic differentiation in *O. variegata* can be proposed after observing the following: (i) the west coast Namaqua Bioregion assemblage shows much lower haplotypic and nucleotide diversity than the south coast Agulhas Bioregion assemblage, (ii) the haplotypes from the Namaqua Bioregion coalesce much later than those from the Agulhas assemblage, and (iii) historical gene flow is from the latter towards the former assemblage. A combination of low haplotype and low nucleotide diversity is generally indicative of a bottleneck, strong selection pressures or a recent founder event (Grant and Bowen 1998; Matthee *et al*., 2007). Additionally, reduced genetic variation such as that observed in *O. variegata* on the west coast, is common in reinvaded habitats following Pleistocene glacial periods (Hewitt, 2000). Since haplotypes from the genetic assemblage in Namaqua Bioregion coalesce latter than those from the Agulhas Bioregion assemblage, it is logical to assume that the former assemblage originated from the latter assemblage. Thus, the low genetic variation is most likely to be a result of a founder effect when a few larvae dispersed from the Agulhas Bioregion to the Namaqua Bioregion settled there most probably during the late Pleistocene. Further, the colonisation of the Namaqua Bioregion from the Agulhas Bioregion was probably followed by a severe restriction of gene flow across Cape Point region. This scenario is supported by the historical gene flow pattern across this region, which shows high gene flow from the south-east but none in the opposite direction. Overall, the evidence presented above points to a scenario in which climate-driven physiographic changes in the Pleistocene allowed a few individuals to episodically migrate from the south-east coast across the Cape Point region to colonise the west coast. Perhaps, the conditions on

the west coast are not as favourable for *O. variegata* as those on the rest of the coast hence the demographic stability in on the south-east coast.

Although there was no evidence that selection was acting on the COI locus (negative MK test), the role of selection in causing the disjunction between the Namaqua Bioregion and the Agulhas Bioregion cannot be rejected outright. As has been proposed for the co-distributed mussels *Callianassa kraussi* and *Perna perna* (Teske *et al.*, 2011), sea urchin *Parechinus angulosus* (Muller *et al.*, 2012), individuals might have physiologically adapted to their respective bioregion. Therefore, if individuals from the Agulhas Bioregion are successfully transferred across the Cape Point, environmental differences (e.g. in temperature) might prevent their settlement, growth or reproduction resulting in genetic isolation of the Namaqua Bioregion assemblage (Teske *et al.*, 2011; Muller *et al.*, 2012).

There were no clear trends in gene flow patterns obtained for *O. sinensis* and *O. variegata in the Agulhas Bioregion*, although *O. tigrina* shows symmetrical gene flow throughout its distribution range. The bidirectional gene flow pattern shown by *O. tigrina* throughout its distribution range is not surprising given that the coast is under the influence of wind-induced near shore currents. The gene flow patterns in the Agulhas Bioregion (from CA to JB) suggest the influence of the ring eddies of the Agulhas Current that occasionally pinch off and carry propagules to the south-west coast. The localities in False Bay (GB, BB WP) are sheltered from the main currents such that gene flow among them is influenced by locally generated wave action. Thus, the symmetrical gene flow observed among these localities is not surprising. The north-westward gene flow on the Namaqua Bioregion (from LB to PN) in *O. variegata* reflects the influence of near shore wind-driven upwelling on dispersal. Since the Benguela Current flows at a great distance from the coast it cannot disperse larvae of coastal species, and if the larvae become entrained in it they probably cannot be transported back to the coast to settle. Gene flow patterns cannot be entirely explained in terms of the current oceanographic regime. In fact, the markers used in this study are more amenable for depicting historical gene flow rather than contemporary trends. Contemporary

oceanography might be different from the historical conditions that gave rise to the observed gene flow patterns. A clearer picture of contemporary gene flow can be obtained by using markers with higher evolutionary rates, such as microsatellites.

There was no obvious relationship between habitat preference, population structure and gene flow patterns in the study species. For example, *O. tigrina* , which occurs higher up the rocky shore than *O. sinensis* appeared to take advantage of both the Agulhas Current and the counter currents yet *O. sinensis* seems to be mainly influenced by the counter currents on the east coast. Thus, any differences among the species in their genetic structure might be ascribed to other attributes of their life history like differences in larval behaviour (e.g. ability to control vertical position in response to currents) as observed for decapod larvae (Queiroga and Blanton 2005) and as suggested by a simulations of oyster larvae (North *et al*., 2008). It is expected that other co-distributed gastropods with pelagic larval stages will show similar genetic patterns to those exhibited by *Oxystele* species.

4.4.2 Demographic history

The demographic histories of the three trochids studied here are characterised by late Pleistocene demographic expansions pre-dating the LGM (c. 19-26.5 kya, Clark *et al*., 2009). Concordance between the mitochondrial and nuclear markers and agreement among four types of analyses boost confidence in the inferred history of recent and large population expansions (at least 10-fold increases in N_e).

Demographic expansion generates an excess of recent mutations, which leads to an excess of singletons (Tajima, 1989, Slatkin and Hudson, 1991). The pattern observed for the three trochids of a few frequent haplotypes surrounded many low-frequency haplotypes is compatible with a hypothesis of population growth. Both COI and ITS2 returned intraspecific genealogies characterised by a few frequent haplotypes giving rise to many low frequency haplotypes echoing what has been found in other marine invertebrates (Zane *et al*., 2000; Lejeusne and Chevaldonné,

2006, Calderón *et al*., 2008). This pattern is generally regarded as supportive of a hypothesis of demographic expansion associated with historical events (Clark *et al*., 1999; Maggs *et al*., 2008; So *et al*., 2011).

Significant and negative Fu′s F_s values caused by a high proportion of low-frequency haplotypes could be the evolutionary signature of recent population expansion in the absence of selection, otherwise these rare mutations would be eliminated by genetic drift (Zane *et al*., 2006). Further support for the hypothesis of population growth comes from smooth and unimodal mismatch distributions. Finally, all BSPs suggest that population expansion has been an important feature of the demographic history of all three species.

An alternative explanation for the observed signal of demographic expansion is recovery following a selective sweep, where selectively advantageous haplotypes go to fixation (Strasser and Barber, 2009). This is an unlikely explanation in this study for the following reasons. (1) The McDonald and Kreitman test returned a non-significant result indicating that the COI segment was not under selection. (2) A selective sweep is unlikely to have affected the two unlinked mtDNA and non-coding nuclear markers simultaneously; particular given that the signal of demographic expansion occurs during the Pleistocene (e.g. Strasser and Barber, 2009). (3) The concordance of results across multiple species makes it unlikely to be a signal of selection. Thus, while purifying selection cannot be totally excluded, Pleistocene expansion is likely a more parsimonious explanation for the observed patterns, especially given the timing of demographic expansion.

Mismatch distribution analyses and BSPs provide a tentative time frame that helps to fit demographic events into a paleoclimatic context (Zane *et al*., 2006). For these *Oxystele* species (except the western genetic assemblage in *O. variegata*), mismatch distribution analyses suggest pre-LGM demographic expansions beginning between 30 and 260 kya for all species, at the higher estimated mutation rates. At the same mutation rates, BSPs corroborate these pre-LGM expansions for all three species. Such pronounced pre-LGM demographic expansions have been reported for other rocky-shore invertebrates elsewhere (Gómez *et al*., 2007; intertidal snails *Nerita scabricosta*

and *Nerita funiculata,* Hurtado *et al*., 2007; other molluscs *Mytilus trossulus* and an echinoderm *Pisaster ochraceus*, Marko *et al*., 2010). Pre-LGM expansions have been regarded as evidence that climatic changes prior to the LGM were more important to the historical demography of coastal species (Couceiro *et al*., 2007).

A striking similarity among the species studied here is that they all expanded for about 30 000 years before they began to stabilise around the LGM between 17 and 21 kya. This demographic stabilisation could indicate when the species began to experience limiting factors such as low temperatures and unavailability of new favourable habitat to colonise. The period of demographic expansion overlaps with the last glacial period (12-112 kya). It is evident that the sea level was stable and lower than the current one on the South African coast in the period between c. 21 and 50 kya (Tankard, 1976). This period might have caused demographic expansion of the species. However, close to the LGM the drop in temperatures might have neggatively affected the species resulting in no population growth. Perhaps, as the sea level fell further towards the LGM, the topology of the coastline changed resulting in loss of suitable habitat

A notable contrast was observed between the western and the south-eastern genetic assemblages in *O. variegata*. Whereas the south-eastern genetic assemblage experienced a dramatic late Pleistocene demographic expansion, the west coast assemblage exhibits only a modest demographic expansion. In addition, the west coast assemblage shows lower genetic diversity than its south-eastern counterpart. The observed demographic pattern together with the observed low haplotype diversity and low nucleotide diversity suggests that the population on the west coast could have fluctuated considerably during its evolutionary history and has recently undergone only a modest or no population expansion. While several demographic processes could have resulted in the shallow coalescence of mtDNA haplotypes on the west coast, local extinction followed by recolonisation in response to sea level fluctuations in the Pleistocene is a plausible explanations (e.g. the gastropod *Littorina sitkana*, sea stars *Pisaster ochraceus* and *Evasterias troschelli*; Marko *et al*. 2010). Furthermore, this pattern could be a result of either a founder effect after the western

region was seeded from a small group of founders from the south-eastern population or the western region underwent a severe population bottleneck after the split from the south-eastern populations. If the Namaqua Bioregion was recently recolonized from the Agulhas Bioregion as hypothesised above, the assemblage on the west coast is expected to (1) represent a subset of genetic variation (haplotypes) of the south-east assemblage, which is the source population, and (2) show the genetic signature of rapid expansion because the assemblage is unlikely to have reached equilibrium between mutation and demographic change (Wares and Cunningham, 2001). Contrary to these expectations, the west coast assemblage has a high proportion of private haplotypes relative to the south-east assemblage and it does not show clear evidence of expansion. This scenario suggests that the two assemblages have been evolving separately for an evolutionarily long period of time possibly due to genetic barriers between the two coasts. The few shared haplotypes between the bioregions could be ancestral polymorphism.

At the lower mutation rate of 0.35% Myr^{-1}, demographic expansion would have begun in a period stretching from the middle Pleistocene to just before the LGM. While this period may include the actual time of expansion, it includes several glacial-interglacial cycles and makes it difficult to associate the demographic expansions with any particular glacial or interglacial period. Moreover, estimates based on the higher estimated rates echo estimates reported for other taxa in the region. Therefore, conclusions in this study will be based on the latter rate. However, the following salient points can be made about the demographic expansions regardless of the mutation rate used. (1) There was temporal concordance among the three species in the timing of population expansion. Temporal congruence in the onset of demographic expansion strongly implicates a common historical process (Donoghue and Moore, 2003) in shaping the demographic history of these three species. (2) Demographic expansions substantially predate the LGM except the western genetic assemblage of *O. variegata*, which remained demographically stable since colonisation or re-colonisation of the region. (3) Events predating the LGM have been more important in shaping the demographic histories of these rocky-shore species elsewhere.

4.4.3 Conclusions

An outstanding feature of the demographic history of the congeneric species *O. sinensis*, *O. tigrina* and *O. variegata* was their pre-LGM onset of demographic expansion followed by population size stabilisation around the LGM. The results of this study support the hypothesis that the climatic events and their consequent physiographic changes in the late Pleistocene have had a major impact on the phylogeographic structure and demographic history of most taxa on the South African coast. This recent demographic expansion could have resulted in the genetic homogeneity observed in *O. sinensis* and shallow population differentiation recovered in *O. tigrina*. Alternatively, the low differentiation observed could be a result of contemporary gene flow eroding the effects of historical vicariant events. *Oxystele variegata* was an exception in that in addition to shallow population differentiation on the Agulhas Bioregion, it returned a pronounced genetic differentiation dating to the late Pleistocene between the west coast Namaqua Bioregion and the south-east coast Agulhas Bioregion. Genetic disjunction could be attributed to a recent episode of south-east to west migration followed by gene flow restriction between the two regions possibly around the Cape Point. A negative MKT rules out adaptive selection as a possible explanation of the differentiation between the two regions.

CHAPTER 5

PLEISTOCENE RANGE EXPANSION AND HIGH POPULATION CONNECTIVITY IN A DIRECT DEVELOPING PLOUGH SHELL, *BULLIA RHODOSTOMA* ON THE SOUTH AFRICAN COAST

5.1 Introduction

Sandy beaches globally comprise 70% of open ocean coasts and have high socioeconomic and ecosystem value. Furthermore, they are highly vulnerable to climate change because of their position at the land-sea interface. However, there is a paucity of beach studies, perhaps due to a lack of appreciation to recognize them as distinct ecosystems (Dugan *et al*., 2010). Concordant with this global scenario, of the several phylogeographic studies of coastal taxa that have been conducted along the South African coast, only two of these studies to date have focussed on sandy shore species (Grant and da Silva-Tatley, 1997; Laudien *et al*., 2003). To gain a more complete insight into historical processes shaping the biodiversity of a region, data from multiple species with varying life histories and habitat preferences is required (Avise *et al*., 1998). Since sandy shores comprise about 42% of the South African coastline, it is instructive to place greater research effort towards the phylogeography of sandy shore taxa (Teske *et al*., 2011). Thus, data on phylogeography of *Bullia rhodostoma*, a sandy shore inhabitant with direct development, are valuable to provide more informed inferences about the underlying processes shaping biodiversity along the South African coast.

Plough shells of the genus *Bullia* are common on South African sandy beaches where they inhabit the intertidal zone (Kilburn and Rippey, 1982). Their current distribution ranges from False Bay (east of Cape Point) to the northern part of the eastern coast of South Africa (Fig. 5.1).

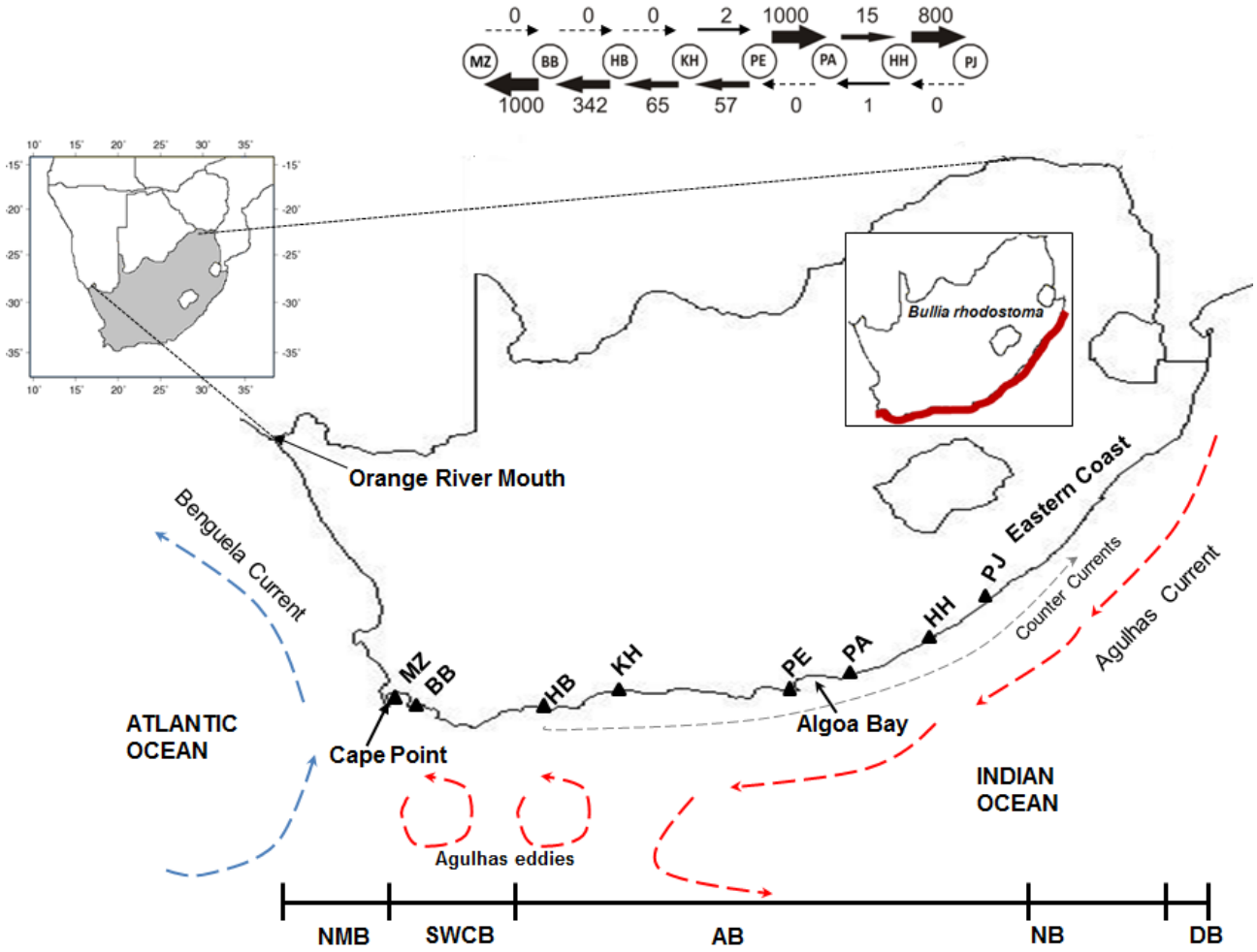

Figure 5.1 Sampling localities, oceanic currents, biogeographic regions, and directionality of gene flow between adjacent localities for *Bullia rhodostoma* on the South African coast. Arrows indicate the direction of gene flow and the thickness of an arrow is proportional to relative migration rate. Numbers above and below the arrows indicate the relative migration rates. The insert shows current distribution of *B. rhodostoma*. Locality abbreviations are as follows: MZ, Muizenburg; BB, Betty′s Bay; HB, Herold′s Bay; KH, Knysna Heads; PE, Port Elizabeth; PA, Port Alfred; HH, Haga Haga; PJ, Port St Johns. Biogeographic regions abbreviations are as follows: NMB, Namaqua Bioregion; SWCB, South-western Cape Bioregion; AB, Agulhas Bioregion; NB, Natal Bioregion, DB, Delagoa Bioregion.

The two-phase life cycle of *Bullia* involves benthic eggs that undergo up to five weeks of lecithotrophic development to hatch directly into miniature snails (Brown, 1971; da Silva and Brown, 1985). Numerous egg capsules, each with at least 150 eggs are deposited 4 to 12 cm in the sand or on the ventral surface of the foot of the females (Brown, 1971; da Silva & Brown, 1985). Owing to the direct developmental mode, and that sandy beaches are interspaced with rocky shores, *Bullia* are expected to exhibit high genetic differentiation. However, an allozyme-based study of the

population genetics of the co-distributed and congeneric *B. digitalis* recovered genetic homogeneity over a geographical range of about 2 400 km and concluded that there was a yet unknown mechanism of dispersal, or that the geographical range of the species had recently expanded to produce the appearance of high levels of gene flow (Grant and da Silva-Tatley, 1997).

This chapter presents work on *B. rhodostoma* as a model species with which to study how Pleistocene climatic oscillations influenced population genetic structure and demographic history of sandy shore species on the South African coast. Furthermore, this chapter presents, for the first time, a DNA sequence-based phylogeographic study of a sandy shore species on the South African coast focussing on addressing the following questions (1) What role may the Pleistocene climatic changes have played to shape the present-day distribution of genetic diversity in *B. rhodostoma*? (2) Is there any concordance between known biogeographical boundaries and the distribution of genetic assemblages in *B. rhodostoma*? (3) Would the phylogeographic pattern shown conform to the life history of the species? As *B. rhodostoma* does not possess a planktonic larval stage, it is predicted that gene flow is likely to be limited to proximate populations leading to a pattern of isolation by distance.

5.2 Materials and Methods

Materials and methods were as described in **Chapter 2** with the following additional information. A total of 140 individuals of *B. rhodostoma* were collected from eight localities as shown on Fig. 1 and Table 5.1. No nuclear DNA was analysed for *B. rhodostoma* despite numerous attempts to find suitable data to address the question. The following markers with primers provided in Jarman *et al*. (2002) were tested, but exhibited no genetic variation among haplotypes: ATPSα, ATPSβ, ANT, SRPS4, TBP, LTRS, and ZMP. In addition, although ITS2 worked for other marine snails studied here, it did not amplify for *B. rhodostoma*.

Although the BIC as implemented in jMODELTEST selected the HKY substitution model (Hasegawa *et al*., 1985) as the most appropriate substitution model for COI, this model is not available in ARLEQUIN. The Tamura-Nei distances were used for calculating molecular diversity, AMOVA and pairwise Φ statistics. The HKY model was used in BEAST for generating a BSP for the whole population. An estimated mutation rate of 2.6×10^{-8} site^{-1} yr^{-1} was used. The McDonald Kreitman test was performed using *Mitrella bincicta* as an outgroup based on sequences obtained from GenBank (accession numbers HM180687 and HM180691).

Table 5.1 Geogrphical location and sample sizes of the eight localities sampled for *Bullia rhodostoma*

Bioregion	Locality (Abbreviation)	Latitude	Longitude	Sample size
Namaqua	Muizenburg (MZ)	S34^0 03	E18^{0}21	15
Agulhas	Betty‟s Bay (BB)	S34^{0}12	E18^{0}33	24
Agulhas	Herold′s Bay (HB)	S34^{0}01	E22^{0}13	9
Agulhas	Knysna Heads (KH)	S34^{0}03	E23^{0}01	19
Agulhas	Port Elizabeth (PE)	S33^{0}34	E25^{0}23	11
Agulhas	Port Alfred (PA)	S33^{0}21	E26^{0}31	20
Agulhas	Haga Haga (HH)	S32^{0}27	E28^{0}08	20
Agulhas	Port St Johns (PJ)	S31^{0}21	E29^{0}19	22
	Total			140

5.3 Results

5.3.1 Genetic variation

A total of 140 COI sequences, each comprising 636 nucleotides after editing, were obtained. Thirty one (22%) sites were polymorphic (28 transitions and 3 transversions), 10 (32%) of which were parsimony informative. Twenty seven haplotypes were recovered, two of which occurred at all localities and 20 (74%) were singletons (Table 5.2). All haplotypes have been deposited with GenBank accession numbers JX303496-JX303522. Both haplotype and nucleotide diversity were high across all sampled populations ranging from 0.71±0.10 to 0.94±0.07 and 0.05±0.04 to 0.11±0.07, respectively. However, nucleotide diversity was considerably higher at HH and PJ on the south-east coast than at the rest of the localities (Table 5.3).

Table 5.2 Haplotype frequencies for the eight localities for *Bullia rhodostoma* sampled along the South African coast. N is the number of individuals sequenced for COI or ITS for each locality.

Locality	N	Haplotypes																										
		1	2	3	4	5	6	7	8	9	10	11	12	13	14	15	16	17	18	19	20	21	22	23	24	25	26	27
Muizenburg	**15**	1	1	1	1	1	1	1	1	3	1																	
Betty′s Bay	**24**			8		2	3			2		1	3	1	1	2	1											
Herold′s Bay	**9**	1		2		2				1						1		1	1									
Knysna Heads	**19**	2		10		3	1									2				1								
Port Elizaberth	**11**	2		4		3				1											1							
Port Alfred	**20**	4		9		4	2															1						
Haga Haga	**20**	8		4	1	1				1			1										1	1	1			
Port St Johns	**22**	8		4		3				3						1										1	1	1

Table 5.3 Neutrality and demographic parameters for COI sequences in *Bullia rhodostoma*. Number of individuals sequenced (N), number of haplotypes (N_h), haplotype diversity (*h*), nucleotide diversity (π), Fu′s F_s values (* means significant at $p < 0.02$), Harpending′s raggedness indices (r), sum of squared deviations (SSD) (** means significant at $p < 0.05$), and mismatch distribution parameter τ (95% confidence intervals**)** are listed. Coalescence values that could not be resolved are designated by infinity signs.

Locality	N	N_h	h±SD	π±SD	Fu′s Fs	Demographic expansion			Range expansion		
						SSD	r	τ	SSD	r	τ
Muzeinberg	15	10	0.91±0.06	0.07±0.04	-5.81*	0.01	0.09	1.94(0.50; 3.22)	0.01	0.09	1.95(0.71;3.04)
Betty′s Bay	24	10	0.86±0.05	0.06±0.04	-3.85*	0.00	0.04	2.12(0.69; 3.39)	0.00	0.04	1.58(0.75;3.44)
Herold′s Bay	9	7	0.94±0.07	0.09±0.06	-2.83	0.02	0.08	1.28(0.00; 5.97)	0.02	0.08	1.28(0.40;5.76)
Knysna Heads	19	6	0.71±0.10	0.05±0.04	-0.92	0.02	0.09	0.35(0.00; 3.71)	0.02	0.09	0.35(0.25;6.05)
Port Elizabeth	11	5	0.82±0.08	0.06±0.05	-0.27	0.06	0.16	5.50(0.00; 60.50)	0.05	0.16	0.48(0.17;55.27)
Port Alfred	20	5	0.74±0.07	0.07±0.05	1.09	0.01	0.04	4.92(0.14; 11.46)	0.01	0.04	2.56(029;13.44)
Haga Haga	23	9	0.81±0.07	0.11±0.07	-1.21	0.02	0.05	5.59(0.74; 9.69)	0.02	0.05	3.89(0.78;8.75)
Port St Johns	22	8	0.83±0.06	0.10±0.06	-0.61	0.05	0.09	5.56(0.27; 12.59)	0.05	0.09	3.50(0.34;13.36)
Pooled samples	140	27	0.84±0.02	0.08±0.05	-13.94*	0.01	0.03	4.42(0.38; 8.81)	0.01	0.03	0.48(0.22;12.11

5.3.2 Population structure and gene flow

The global Φ_{ST} across all samples was low ($\Phi_{ST} = 0.07$; $p < 0.05$, Table 5.4), and pairwise Φ_{ST} values were low and not significant except for those between the localities at the end of the range, the east coast (HH and PJ) and BB on the south-west coast (Table 5.5). AMOVA returned significant structure when populations were split into three groups roughly corresponding to bioregions: South-western Cape (MZ, BB), Agulhas Bioregion (HB, KH, PE, PA) and the Natal Bioregion (HH, PJ) ($\Phi_{CT} = 0.14$; $p < 0.05$, Table 5.4). This suggests that the hypothesis of reduction in gene flow around Cape Agulhas and Algoa Bay for this species cannot be rejected. There was a significant correlation between linearised genetic distance and geographic distance (Mantel′s test $r = 0.62$, $p < 0.05$) suggesting that populations were genetically isolated by distance.

Coalescent analyses of gene flow indicates asymmetrical gene flow patterns and typically high numbers of female migrants per generation between localities (Fig. 5.1; Table 5.6). There is a high number of female migrants ($N_em = 57 – 1000$) from east to west on the central and south-west coasts (from PE to MZ), but virtually none in the opposite direction ($N_em = 0$-2). Similarly, gene flow on the eastern coast is strongly directional, with a large number of migrants moving north-eastward (from PE to PJ) ($N_em = 15$ -1000) against the flow of the Agulhas Current, contrasting with very little to no gene flow in the opposite direction (Fig. 5.1; Table 5.6). Compared to general patterns of gene flow along the eastern coast, there was markedly reduced gene flow between PA and HH, and between KH and PE indicating a notable gene flow restriction around the Algoa Bay region. The PE region is likely a source region since it provides a larger number of migrants to the other regions, but receives little in return (Fig. 5.1; Table 5.6).

Table 5.4 Hierarchical analysis of molecular variance for the mitochondrial COI in *Bullia rhodostoma.* (a) global without grouping localities; (b) among putative groups defined by known genetic barriers: south-west (MZ, BB) vs south (HB, KH, PE,PA) vs south-east (HH, PJ).

Source of Variation	df	Percentage variation	Φ statistics	P
(a) Global (without grouping localities)				
Among populations	7	6.98	0.07	0.01
Within populations	132	93.02		
(b) Testing for bioregion groups: South-western vs Agulhas vs Natal				
Among groups	2	13.69	0.14	0.00
Among populations within groups	5	0.00	0.00	0.97
Within populations	132	86.31	0.14	0.01

MZ, Muizenberg; BB, Betty′s Bay; HB, Herold′s Bay; KH, Knysna Heads; PE, Port Elizabeth; PA, Port Alfred; HH, Haga Haga; PJ, Port St Johns

Table 5.5 Pairwise Φ_{ST} values of mitochondrial COI among the eight *Bullia rhodostoma* sampling sites included in the present study. Φ_{ST} Values in bold represent those that were significant after B-Y false discovery rate correction ($p < 0.013$).

	MZ	BB	HB	KH	PE	PA	HH	PJ
MZ	0							
BB	0	0						
HB	0	0.007	0					
KH	0	0.027	0	0				
PE	0	0.059	0	0	0			
PA	0.011	0.074	0	0	0	0		
HH	0.131	**0.222**	0.083	0.096	0.024	0.033	0	
PJ	0.177	**0.275**	0.117	0.139	0.050	0.082	0	0

MZ, Muizenberg; BB, Betty′s Bay; HB, Herold′s Bay; KH, Knysna Heads; PE, Port Elizabeth; PA, Port Alfred; HH, Haga; PJ, Port St Johns

Table 5.6 Directionality of gene flow for *Bullia rhodostoma* between each locality pair for the stepping stone migration model along the South African coast based on COI sequences. Numbers indicate relative migration rates of females ($N_{ef}m$) and in brackets are the 95% confidence intervals.

From population	To population	$N_{ef}m$	95% Confidence Interval
Muzeinberg (MZ)	Betty′s Bay	0.0	0.0-0.0
Betty′s Bay (BB)	Muzeinberg	1000.0	19.2-1500.0
Betty′s Bay	Herold′s Bay	0.0	0.0-0.0
Herold′s Bay (HB)	Betty′s Bay	341.6	39.0-4700.0
Herold′s Bay	Knysna Heads	0.0	0.0-0.0
Knysna Heads (KH)	Herold′s Bay	64.6	21.7-2200.0
Knysna Heads	Port Elizabeth	2.1	0.9-7.0
Port Elizabeth (PE)	Knysna Heads	56.9	24.3-2700.0
Port Elizabeth	Port Alfred	1000.0	79.6-2100.0
Port Alfred (PA)	Port Elizabeth	0.0	0.0-0.0
Port Alfred	Haga Haga	14.7	5.9-2700.0
Haga Haga (HH)	Port Alfred	0.7	0.0-0.0
Haga Haga	Port St Johns	800.0	11.8-2600.0
Port St Johns (PJ)	Haga Haga	0.0	0.0-0.0

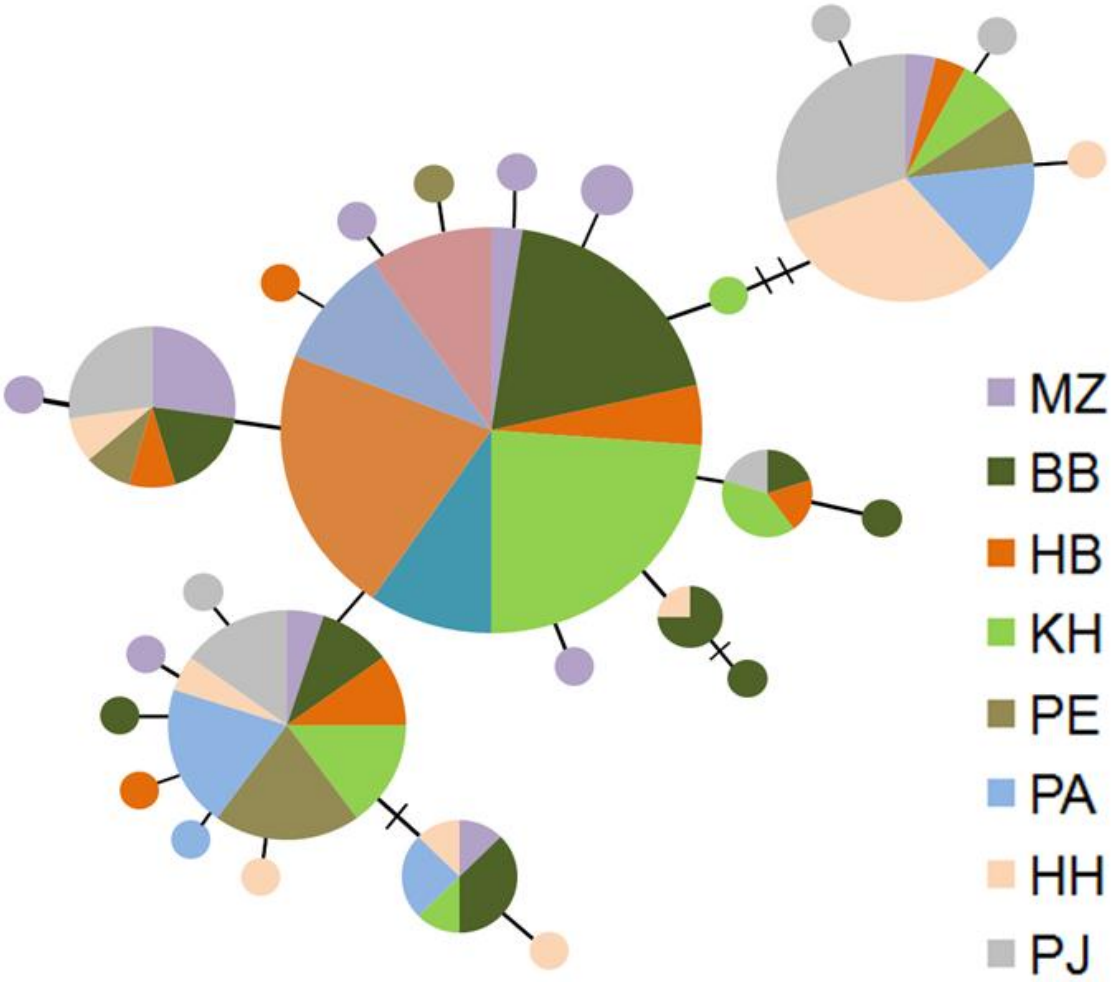

Figure 5.2 Statistical parsimony network of 36 COI haplotypes of *Bullia rhodostoma* based on 140 sequences. A circle represents a haplotype and its size is proportional to the frequency of the haplotype. The smallest solid circle represents a frequency of one. Each connection between haplotypes represents a single mutational step between the haplotypes. Cross hatching indicates inferred intermediate haplotypes (mutational steps) not observed in the data.

A parsimony haplotype network showed no clear geographic association among the haplotypes (Fig. 5.2) supporting a hypothesis of no or limited genetic structure. Similarly, BAPS did not recover any spatial population structuring, as all the populations were part of the same cluster.

5.3.3 Demographic history

5.3.3.1 Fu's F_s and mismatch distributions

In light of the shallow population structure suggested by AMOVA, demographic analyses were performed only for the pooled data set. The McDonald and Kreitman test showed that the data conformed to selective neutrality (Neutrality index = 3.197, Fisher test $p > 0.05$), thus the deviation from neutrality detected by Fu′s F_s test could rather be ascribed to population expansion rather than selection.

The Fu′s F_s value for the whole data set was negative and significant ($p < 0.02$) as expected for populations that have experiences recent demographic changes (Table 5.3) and the mismatch distribution did not show a significant deviation from the null distribution of population expansion. However, if Fu′s F_s values for the individual localities are considered, only those for MZ and BB were significant and negative indicating departure from demographic stability whereas those for the rest were negative but not significant, indicating demographic stability or the result is due to the effect of small sample sizes. The expected mismatch distribution under a range expansion model yielded a better fit to the observed data than a model of pure demographic expansion for the whole data set (Fig. 5.3). At the higher estimated mutation rate, the mismatch distribution suggests that *B. rhodostoma* began expansion between 15 and 350 kya. The lower mutation rate of 0.35% gave an estimate of onset of expansion between c. 85 to 2 200 kya, a period spanning the early to late Pleistocene. Additional support for a demographic expansion comes from a shallow and almost star-like haplotype network recovered (Fig. 5.2).

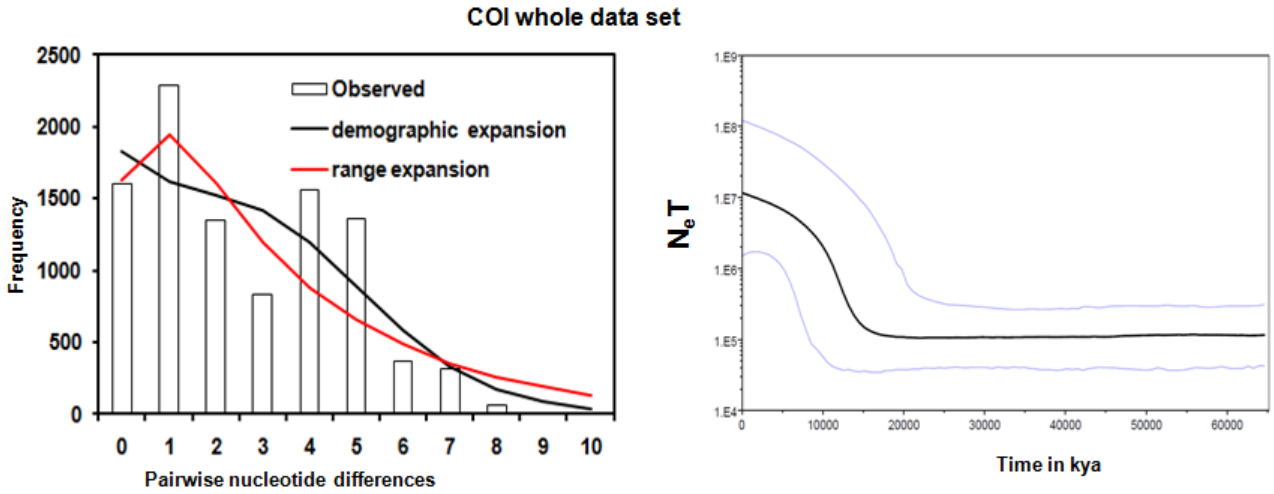

Figure 5.3 Demographic history of *Bullia rhodostoma* inferred from COI gene sequences for the pooled data set. (left) Frequency distribution of pairwise nucleotide differences among COI haplotypes: histograms show the observed distribution; lines show the expected distribution under a model of pure demographic expansion (solid line) and spatial expansion (dashed line). (right) Bayesian skyline plots based on a mutation rate of 2.6 x 10^{-8} substitutions $site^{-1}$ yr^{-1}: time (x-axis) in thousands of years ago (kya), population size (y-axis) is represented by N_eT where N_e = female effective population size, T = generation time. The central bold line represent the median value of effective female population size, the narrow lines denote the upper and lower confidence limits of 95% Highest Posterior Density (HPD) interval

5.3.3.2 Bayesian reconstruction of demographic history

The BSP for the pooled data set, generated under the HKY model of nucleotide substitution and a strict molecular clock, shows a pronounced post-LGM demographic expansion (100-fold) in effective population size dating c. 15 kya (estimated rate of 2.55% Myr^{-1}) and noticeable population stability after 10 kya (Fig. 5.3). The lower mutation rate of 0.35% Myr^{-1}gave an estimate of c.115 kya for the whole data set for the onset of expansion (Table 5.7).

Table 5.7 Time of expansion estimated by mismatch distribution analyses and Bayesian skyline plots for *Bullia rhodostoma* based on different estimates of COI mutation rates (mutation rates are given as percentage divergence per site per million years)

Group	Mismatch distribution				Bayesian skyline plots		
	Tau (confidence interval)	Time of expansion (in years ago)			Time of expansion (in years ago)		
		0.35% Myr^{-1}	1.0 % Myr^{-1}	2.0% Myr^{-1}	0.35% Myr^{-1}	1.0 % Myr^{-1}	2.0% Myr^{-1}
Pooled samples	4.42 (0.38; 8.81)	990,000 (85,000;2,000,000)	350,000 (30,000; 690,000)	175,000 (15,000-350,000)	115,000	30,000	15,000

5.4 Discussion

5.4.1 Population genetic structure and gene flow

The salient features of the population genetic structure in *B. rhodostoma* were: (i) a combination of high haplotype and high nucleotide diversities, (ii) weak population differentiation, (iii) a significant pattern of isolation by distance, and (iv) highly asymmetrical gene flow.

The high number of singletons in *B. rhodostoma* coupled with high genetic diversity per locality might indicate the species has large effective population sizes, which resist genetic drift. Populations with large effective sizes maintain high levels of genetic diversity because of a combination of low genetic drift and high rate of accumulation of mutations (Ibáñez *et al*. 2011). Additionally, accumulation of singletons is not surprising in *B. rhodostoma* since it has limited dispersal ability associated with directd-developing. The range expansion that followed amelioration of climatic conditions involved dispersal of large numbers of migrants that prevented founder effects, which normally cause low genetic diversity in populations established recently through recolonisation (Bernatchez and Wilson, 1998; Maggs *et al*., 2008;). The possible mechanisms of dispersal are discussed below.

A hypothesis of lack of differentiation or weak population differentiation in *B. rhodostoma* is supported by: (i) coalescent analyses of spatial genetic structure (BAPS) recovering no structure, (ii) the haplotype network (recovering no geographic association of haplotypes), (iii) low and non-significant pairwise Φ_{ST} values, (iv) a weak global Φ_{ST} (Table 5.5), and (v) shared haplotypes even between distant localities (e.g. MZ and PJ share three haplotypes, Table 5.2, but are over 1,000 km apart). These results echo those reported for a co-distributed congener *B. digitalis* (Grant and da Silva-Tatley, 1997), which has been attributed to an evolutionarily recent range expansion (Grant and da Silva-Tatley, 1997). Thus, the shared haplotypes among distant regions might represent ancestral polymorphism (Keeney *et al*., 2009), which is retained because of large effective

population sizes as explained above. Moreover, the low differentiation such as that observed in *B. rhodostoma* has been reported for many other species that have been subjected to recent population expansions (Lecomte *et al*., 2004; So *et al*., 2011).

This genetic pattern also occurs in species with high effective population sizes that have undergone recent range expansion followed by restrictions on gene flow (Zardi *et al*., 2007). This would suggest that climatic changes after the LGM caused circulatory changes and physiographic changes that created favourable conditions for *B. rhodostoma* to expand its range from refugial regions (explained below). For example, more sandy beaches could have been exposed and oceanographic currents facilitated movement of adult individuals. Perhaps as sea level rose again after the LGM, more sandy beaches became available for *B. rhodostoma* until a certain level above which no increase in sandy beaches occurred. This increase in available sandy beaches probably was accompanied by circulatory patterns favourable to migration and settlement on them. It is evident that on the South African coast weathering resulted in substantial deposition of littoral sands in the Holocene and some of the sands were lithified into beachrocks (Ramsay, 1991). Since *B. rhodostoma* is a direct-developer, the migration to occupy newly available sandy beaches was probably through movement of adults. The high frequency of private haplotypes might be an indication that the post-LGM range expansion was followed by a period of restricted gene flow.

Another possible explanation for the limited genetic differentiation could be that *B. rhodostoma* is highly dispersive (e.g. Lasota *et al*., 2004) and persisted through the glacial period without population fragmentation. If *B. rhodostoma* is highly dispersive, its dispersion cannot be through larvae since it is a direct-developer and lacks a planktonic larval phase. Nevertheless, evidence of long-distance dispersal exists in other direct developing marine gastropods that otherwise display genetic differentiation over small geographic scales and has been attributed to active movements of adults and/or juveniles through shipping (Miura *et al*., 2005), migratory birds (Wilke and Davis, 2000), floating (Anderson, 1971; Adachi and Wada, 1999), drifting (Martel and Chia, 1991) or rafting (Helmuth *et al*., 1994; Grant and da Silva-Tatley, 1997; Donald *et al*., 2005).

One further plausible mechanism of dispersal is that since adults are able to surf by extending the foot to capture the energy of waves (Odendaal *et al.*, 1992), they can be dispersed among sandy beaches if they are caught in currents. This mechanism is supported by the direction of gene flow (north-eastwards from PE region to HH and south-westwards on the south-west) which appears to follow oceanic currents. The gene flow patterns suggest that *B. rhodostoma* uses the near shore wind-induced counter currents on the north-east coast for dispersal whereas it utilises the Agulhas Current on the south-west coast. Another possible mechanism of dispersal in *B. rhodostoma* is subtidal crawling of adults or juveniles or both between sand beaches which then would explain the isolation by distance observed for this species. To date there is no documented evidence of these mechanisms in *B. rhodostoma* and explaining long distance gene flow of the species, if real, remains a challenge. Additionally, if connectivity in *B. rhodostoma* is through dispersal then singletons would not have accumulated with such high levels of gene flow. Possibly, the high frequency of singletons could be an artefact caused by incomplete sampling.

The recovery of a significant pattern of isolation by distance for *B. rhodostoma* contrasts sharply with that of a co-distributed sister species, *Bullia digitalis* (Grant and da Silva-Tatley, 1997) for which there was no correlation between geographic distance and genetic differentiation. A significant pattern of IBD suggests that gene flow is higher between adjacent localities than distant ones, and follows a stepping stone model. This is expected for a direct developing species as it is assumed to have a limited capacity for long-distance dispersal. Should purely recent range expansion account for the low differentiation observed, the challenge to discover the mechanism of dispersal still remains to be determined.

The gene flow pattern shown must be taken as preliminary results given the unreliability of genealogies from single gene data sets. Nonetheless, long-term gene flow patterns (Fig. 5.1) in *B. rhodostoma* suggest that the PE region is a source donating migrants to the east and west, but receiving very little in return. Whereas haplotypes that arise in the PE region would end up in other localities due to gene flow, there would be no reciprocal exchange of haplotypes between the PE

region and other regions. Thus, the PE region would have lower genetic diversity and a lower number of private haplotypes than other localities giving rise to the pattern apparent in the data.

If relatively high genetic diversity could be an indication of refugia, then *B. rhodostoma* is most likely to have survived the Pleistocene climatic changes in refugia lying on the south-west and south east on either side of the central PE region. Whereas the east coast (the region encompassing HH and PJ) accumulated mutations *in situ* during the refugial period, it would receive more mutations from the PE region through gene flow but would not donate migrants to the PE region in return. Thus, the high genetic diversity in the Natal Bioregion could be explained as a result of the confluence of genetic assemblages from the central region and those that originated *in situ*.

The pattern of gene flow, being predominantly westwards on the south coast and north-eastwards from PE to PJ, suggests that the Agulhas Current does not have a significant direct influence on dispersion of species on the coast. It is difficult to explain how the Agulhas Current could facilitate westward gene flow on the south coast when its flow is offshore along the edge of the Agulhas Bank beginning from PE. On the contrary the Agulhas Current flows closer to the coast between PJ and PE. The gene flow pattern in *B. rhodostoma*, as that of the other species studied here, reiterates the importance of near shore wind-induced currents in influencing gene flow on the Agulhas Bank. Use of the near shore wind-driven counter currents on the east coast has been recorded in other marine species (e.g. sardines, Shillington, 1995; *Clinus cottoides*, von der Heyden *et al*., 2008). It is notable that *B. rhodostoma* is not influenced by the Agulhas Current on the south-east coast when the current is closer to shore than on the east coast.

Whilst apparent gene flow restrictions across the Algoa Bay region and the Cape Agulhas region suggested by AMOVA results cannot be dismissed outright because of the existence of upwelling zones in these regions, the apparent restrictions could be evidence of differences among localities at the ends of the distribution range (MZ and BB on the west end being different from HH and PJ on the east end as indicated by the Φ_{ST} values). Given that BAPS did not recover structure and the star-like nature of the haplotype network, it is more likely that any suggestion of structure

from the AMOVA is an artefact caused by differences between the edge localities. The genetic difference among the peripheral localities is expected considering the stepping stone migration model experienced in this species, which results in the most distant localities being the most genetically differentiated.

5.4.2 Demographic history

Estimates of timing of expansion from the mismatch distribution (15-350 kya) and BSP (15 kya) suggest that the predominant demographic pattern in *B. rhodostoma* is a late Pleistocene range expansion in the proximity of the LGM (19-26.5 kya) with a possibility of a post-LGM expansion. Evidence of demographic expansion came from a significantly negative Fu′s F_s value, a unimodal mismatch distribution conforming to both pure demographic and range expansion models, and a BSP showing increases in effective population size. The Fu′s F_s values suggest that range expansion was more important on the west as only the western most localities (MZ and BB) showed evidence of expansion whereas the remainder of the localities had negative but nonsignificant values suggestive of demographic stability, slow expansion or contraction (Nuñez *et al*., 2011).

These apparent signals of demographic expansion could also signal recovery from a selective sweep where selectively advantageous haplotypes go to fixation. However, in this case, a selective sweep is unlikely to be the cause because (i) the McDonald and Kreitman test showed no significant deviation from selective neutrality, (ii) the extant populations exhibit high genetic diversity yet a selective sweep is expected to have eroded genetic diversity, (iii) the concordance between the results of this study and those reported for other species on the southern Africa coast (e.g. *T. sarmaticus*, *O. sinensis*, *O. variegata*, this study), points to demographic change and not selection as the most likely explanation of the observed pattern.

At the higher mutation rate of 2.6% Myr^{-1}, mismatch distribution analyses estimate the time of expansion to be between 15 and 350 kya. The BSP, which takes genealogy into account and

gives more precise estimates (Kokita and Nohara, 2011), suggest post-LGM demographic expansions beginning c. 15 kya. As suggested for *T. sarmaticus* (Chapter 3, this study), the demographic history of *B. rhodostoma* could have been influenced by temperature changes. Low temperatures could have restricted the species to the south-east coast where temperatures could have been higher due to latitude and the influence of the warm Agulhas Current. After the LGM the rising temperatures could have seen *B. rhodostoma* expanding its range as it recolonized previously lost areas. Fu‟s Fs values of the of individual localities shows that only two localities (MZ and BB) near the western end of the current distribution range of the species are negative indicating that these localities have been recently recolonized. If this is the case then *B. rhodostoma* is still expanding its range westwards from its assumed refugium on the south-east coast.

Using the lower slower mutation rate of 0.35% Myr^{-1}, demographic expansions would have started within a period spanning the early to late Pleistocene (between c. 85 and 2 200 kya) based on mismatch distributions. At the same mutation rate, BSPs would suggest late Pleistocene onset of demographic expansion between c. 110 and 115 kya. Interestingly, whether the higher or lower mutational rate is used, demographic expansion would still begin in the late Pleistocene and thus would not alter the main conclusions about the role played by the Pleistocene climatic changes.

5.4.3 Conclusions

The population genetic structure of *B. rhodostoma* is characterised by shallow differentiation and IBD. Isolation by distance suggests a stepping stone model of migration among localities, which was expected given that *B. rhodostoma* is a direct-developer with a limited potential for dispersal. The stepping stone pattern of migration might have led to high connectivity among neighbouring localities leading to the observed lack of population differentiation.

Demographic reconstruction suggests a post-LGM range expansion, which is concordant with the shallow genetic differentiation recorded. A proposed hypothesis for the observed phylogeographic structure is that during low temperatures associated with the last glacial (Late Pleistocene), *B. rhodostoma* could have been restricted to the south-west coast, on the central Agulhas Bioregion around Port Elizabeth and probably also on the east coast. When climatic conditions changed and temperatures began to rise after the LGM *B. rhodostoma* began a rapid range expansion from the refugial region.

CHAPTER 6

GENERAL DISCUSSION AND IMPLICATIONS FOR CONSERVATION

6.1 Genetic signatures of Pleistocene climatic changes

6.1.1 A note on strengths and need for caution when interpreting results

The main strengths of the approach in this study were: (1) the use of both a mitochondrial gene and a nuclear locus (except for *B. rhodostoma*), and (2) use of a combination of traditional frequency and Bayesian coalescent analyses to simultaneously study multiple co-distributed species; which gave a more complete and robust picture of phylogeographic and demographic patterns of each taxon. Moreover, the congruence between COI and the ITS2 data sets indicates that the inferred historical events had impacts that extend across both the organellar and nuclear genomes (Wilson and Veraguth, 2010) of the species studied. This specifically provides strong evidence that the demographic patterns observed herein are not artefacts (e.g. due to the stochastic nature of the coalescent, Marko *et al*., 2010) but true signatures of most likely the Pleistocene climatic oscillations. Additionally, this study highlights the advantages of using both traditional and Bayesian coalescent analyses especially when studying demographic history. For instance, the estimation and visualization of the population dynamics of periods of stability and expansion, as well as the magnitude of expansion would have been much more limited without BSPs. The concordance between the analyses boosted our confidence in our estimation of the timing of population expansion, a ubiquitous signal across the species studied.

However, although an effort was made within practical limits to include all the possible mutation rates for COI found in literature, the conclusions are entirely dependent on the mutation rates used and the fact that species specific rates were not available, is certainly one of the drawbacks of the study. The decision to base the main conclusions of this study on the relatively

faster estimated mutation rates above 2% Myr^{-1}, as in Marko *et al*. (2010), is conservative with respect to detecting evidence supporting post-LGM demographic expansions. In addition, although nDNA confirmed the demographic expansions, it would have been more informative and desirable if a mutation rate for the ITS2 region could have been obtained.

6.1.2 Traditional vs Bayesian and Coalescent-based methods

Two main types of analyses were used to address the objectives of this study: the traditional frequentist methods including pairwise Φ_{ST} values, AMOVA (for population genetic structure), mismatch distribution (MMD) analyses, Fu′s F_s (for demographic history), haplotype networks which can provide information on population structure and demographic history; and the Bayesian coalescent-based methods comprising BAPS, coalescent analyses of divergence time (for structure), BSPs (for demographic history) and coalescent-based analyses of gene flow. A notable difference between these two approaches was that whereas AMOVA inferred weak structure for COI in all taxa except *O. sinensis*, BAPS recovered structure only for COI in *O. variegata* between the Namaqua Bioregion (west coast) and the rest of localities. This suggests that BAPS was more conservative with respect to recovering structure than Φ statistics. BAPS might be conservative owing to the (1) severe penalty it places on postulating additional populations (Waples and Gaggiotti, 2006) or (2) effect of recent migrations which could have obscured differences among populations (J. Corander pers comm. to Waples and Gaggiotti, 2006). Although low Φ_{ST} values are not always caused by high gene flow between localities, it is interesting that generally low levels of pairwise Φ_{ST} were recorded and relatively high coalescent-based gene flow rates were associated with them in all species. Confirming the ideas of McGorvern *et al*. (2010), the estimation of divergence time for *O. variegata* using BEAST clarified some aspects of the population biology that would not be as clear from AMOVA-based analyses alone.

There was remarkable agreement between traditional and Bayesian analyses in demographic reconstruction in that they both recovered late Pleistocene demographic expansions in all species. Estimates of demographic expansion from BSPs lie within the 95% CI of the MMD estimates, indicating agreement between the two approaches. This agreement between traditional and coalescent-based analyses increases the level of confidence in the reconstructed demographic history. The conclusions on demographic history of species leaned more on BSPs than MMD analyses because BSPs, like other Bayesian analyses, consider genealogical information in the sequence data and therefore provide more precise estimates than the MMD analyses which do not consider the underlying genealogy (Crandall *et al*., 2012). Apart from showing when demographic expansions occurred, BSPs provided additional valuable information such as the duration and magnitude of demographic changes, which would not be obtained from MMD analysis. These findings corroborate McGorvern *et al*. (2010) in showing the importance of coalescent-based analyses in placing phylogeographic reconstructions into a comprehensive temporal and historical context.

6.1.3 The take home message from this study

Notwithstanding the possible limitations stated above, this study adds valuable insight into the accumulating knowledge of the impact of the Pleistocene climatic changes on the South African coast, not only by confirming some previous results but also by providing more detailed characterisation of demographic expansions and divergences among regional genetic assemblages through the use of Bayesian reconstruction of demographic history. For instance, BSPs indicate that *T. sarmaticus* and *O. tigrina* began expansions after long periods of demographic stability (Figs 3.4 and 4.9, respectively), providing valuable information in terms of dating demographic expansions that traditional mismatch analysis would not be able to reveal. But caution must be exercised in interpreting apparent periods of demographic stability from BSPs since it is now evident that only

the most recent episodes of rapid population changes can be detected even if the populations experienced several periods of growth and decline (Grant *et al*., 2012; Karl *et al*., 2012). Also, a seemingly stable population history preceding a recent population expansion might be an artefact of coalescence analysis (Karl *et al*., 2012). The latter explanation is unlikely in this study considering that the periods of demographic stability were detected in two independent markers and in several co-distributed species (Crandall *et al*., 2012).

An especially important outcome of this study was that all species experienced late Pleistocene demographic expansions confirming the importance of the late Pleistocene as an epoch of population expansion for many marine organisms from different geographic regions (Benzie *et al*., 2002; Uthicke and Benzie, 2003; Couceiro *et al*., 2007; Marko *et al*., 2010). Additionally, most species studied here (all *Oxystele* species) exhibited pre-LGM expansions, indicating that late Pleistocene events pre-dating the LGM have been more important in shaping the demographic histories of coastal species on the South African coast. This finding echoes previous studies elsewhere that suggest that most marine taxa have followed a pre-LGM expansion model (Duran *et al*., 2004; Chevolot *et al*., 2006; Hoarau *et al*., 2007; Marko *et al*., 2010). *Turbo sarmaticus* and the sandy shore species *B. rhodostoma*, on the contrary, experienced demographic expansion post-dating the LGM.

Also notable was the discovery of spatially variable demographic history within *O. variegata* in which the Namaqua Bioregion lineage (west coast) appears to have remained demographically stable in the recent past in contrast to the south-east region which expanded prior to the LGM. These spatial variations could be corresponding to spatially variable physiographic effects of Pleistocene climatic changes.

The present study also indicated that co-distributed species responded differently to the same historical processes. This is exemplified by the disparities in demographic history between the sandy shore species *B. rhodostoma*, and the rocky shore species. The former began expanding after the LGM whereas the rocky shore species exhibited peri-LGM expansion (*T. sarmaticus*) or pre-

LGM expansions (*O. sinensis*, *O. tigrina* and *O. variegata*). Also notable was the difference in population genetic structure between *O. variegata* which exhibited a clear disjunction between the west coast lineage and the south-east lineage, whereas the other four species displayed shallow genetic structuring. These different responses are not surprising, since it has been documented that co-distributed species can respond differently owing to even subtle differences in habitat preference, dispersal ability, life history and ecological tolerance (e.g. Maggs *et al*., 2008; Marko *et al*., 2010). For example, it is evident that body temperature in rocky shore species does not depend on atmospheric temperature alone but is influenced by a complex interaction between organism and environment, modified by factors such as local weather, shoreline position, wave exposure, and timing of aerial exposure (Helmuth *et al*., 2002; Gilman *et al*., 2006; Princebourde *et al*., 2008). The observed differences between the rocky shore species and the sandy shore species could be attributed to different habitat specificity and differences in mode of reproduction. Caution should also be applied in interpreting the different expansion times among species since coalescent and mutation randomness can produce a variety of mtDNA genealogies for taxa with the same population history (Karl *et al*., 2012).

Temporally concordant demographic patterns among the rocky shore species *T. sarmaticus*, *O. sinensis*, *O. variegata*, and *O. tigrina* are important in two ways. First, the concordant results among these co-distributed species provide evidence that the observations were not due to chance but a true reflection of the impact of climatic change on rocky shore gastropods by ruling out the stochasticity of the coalescent as the explanations for these results. Secondly, they suggest that similar evolutionary processes have shaped their evolutionary histories. It is generally agreed that in models of environmentally driven evolution, concordant patterns across taxa indicate that similar environmental forces have shaped species evolutionary histories (Lorenzen *et al*., 2010).

A prominent feature of the population genetic structure of these intertidal snails was relatively high gene flow with negligible population differentiation. *Oxystele variegata* was exceptional in that it recovered a genetic barrier around Cape Point, which was the only barrier deep

enough to be recovered with coalescent analyses, resulting in the west coast and south-east coast genetic assemblages. However, each assemblage was still characterised by shallow population differentiation. Whilst the shallow population differentiation or genetic homogeneity in the four rocky shore species was expected, given that their life histories include a pelagic larval stage which can facilitate long distance dispersal, the genetic homogeneity observed for the sandy shore *B. rhodostoma* is surprising since it is a direct developer expected to have limited potential for dispersal. The low population differentiation is consistent with the evidence for recent range expansions recorded and the data available do not deny the possibility of high gene flow also contributing to this pattern. Alternatively, low differentiation might be evidence of contemporary gene flow eroding the imprint of historical vicariant events. Also interesting about the population structure of these species is that the direct developing *B. rhodostoma* exhibited isolation by distance whereas the other species with pelagic larvae did not. This suggests that in the former, gene flow was generally limited to adjacent localities, which is concordant with the expected limited ability for dispersal in direct developers.

6.2 Conservation and management implications

Identification of conservation units below the species level is a crucial task in avoiding loss of genetic diversity (Abellán *et al.*, 2007). Conservation of these intraspecific components helps to maintain adaptive diversity and evolutionary potential of the species (Burns *et al*., 2007). Thus, phylogeographic analyses of intraspecific sequence variation provide valuable information on how genetic variation is partitioned within species and can therefore aid in the implementation of effective conservation strategies (Burns *et al.*, 2007). Two main issues emerge as important in achieving effective management of coastal species, namely, establishing connectivity of populations and characterising the distribution of genetic diversity. Ridgway *et al*. (2008) and Bird *et al*. (2007)

emphasize the importance of establishing patterns of connectivity of populations and identifying areas likely to act as larval sources.

In this study, the region stretching from Cape Infanta to Knysna Heads on the south coast appears to be important as a source of recruits for areas to the east and to the west for species such as *T. sarmaticus*, *O. sinensis* and *B. rhodostoma*. For instance, the Cape Infanta region is a source region, at least on a historical time scale, in *T. sarmaticus* while the Port Elizabeth region is a source in *O. sinensis*. The „source" status of this region is thought to be caused by high primary productivity which in turn could result in high reproductive rate of coastal organism (Jackson *et al*. 2012). It is therefore recommended that management plans should prioritise the central region (from Cape Infanta to Knysna Heads) for conservation as they will be important in seeding other regions should they experience local extinction. Protection of these regions through separate Marine Protected Areas has been recommended in previous studies for similar reasons, as well as for their high genetic diversity (von der Heyden *et al*., 2008; von der Heyden, 2009).

Also related to the issue of connectivity is determining whether identified genetic groups constitute management units or evolutionarily significant units. A management unit may be defined as a population that exchanges migrants with other populations but so few that it will remain as a demographically independent unit in the present time (Avise, 2000). Such populations are typically exemplified by shallow phylogeographic separation. Another widely used framework to distinguish units for conservation purposes has been that of evolutionarily significant units (ESUs) originally proposed by Ryder (1986) but further developed by different authors, e.g. Morizt (1994) defines ESUs as populations (or genetic assemblages) that are monophyletic for mtDNA haplotypes and show significant divergence in allele frequencies at a nDNA loci. Furthermore, the concept has been extended to include geographical regions within which several species display phylogenetically distinct populations, thus making them candidates for conservation priority (Avise, 2000).

Although, evidence is accumulating that most species occurring on the south-east and east coast (region stretching from Cape Point to Port St Johns) display phylogenetically distinct genetic

assemblages corresponding to bioregions (e.g. *Upogebia africana*, Teske *et al.*, 2006; *Clinus cottoides*, von der Heyden *et al*., 2008; Bester-van der Merwe *et al*., 2010), there was no strong evidence for the existence of such genetic assemblages in this region for four out the five species studied here. Thus, owing to their low or lack of genetic structuring neither management units nor ESUs were identified for *T. sarmaticus*, *O. sinensis*, *O. tigrina* and *B. rhodostoma*. There is, however, clear evidence of two genetic assemblages in *O. variegata* corresponding to the west coast and the south-east coast. These lineages do not qualify for ESU status since they were based on mtDNA data alone without clear support from nDNA. Therefore, the minimum precautionary measure would be to regard the genetic assemblages in *O. variegata* as separate management units.

REFERENCES

Abellán, P., Gómez-Zurita, J., Millán, A., Sánchez-Fernández, D., Velasco, J., Galián, J. and Ribera, I. (2007) Conservation genetics in hypersaline inland waters: mitochondrial diversity and phylogeography of an endangered Iberian beetle (Coleoptera: Hydraenidae). *Conservation Genetics* **8:** 79-88.

Adachi, N. and Wada, K. (1999) Distribution in relation to life history in the direct-developing gastropod *Batillaria cumingi* (Batillariidae) on two shores of contrasting substrata. *Journal of Molluscan Studies* **65:** 275-287.

Anderson, A. (1971) Intertidal activity, breeding and the floating habit of *Hydrobia ulvae* in the Ythan estuary. *Journal of Marine Biology Association (UK)* **51:** 423-437.

Avise, J.C. (1998) The history and purview of phylogeography: a personal reflection. *Molecular Ecology* **7:** 371-379.

Avise, J.C. (2000) *Phylogeography: the history and formation of species*. Havard University Press, Cambridge, MA.

Avise, J.C. (2009) Phylogeography: retrospect and prospect. *Journal of Biogeography* **36:** 3-15.

Avise, J.C., Ball, R.M. and Arnold, J. (1998) Speciation durations and Pleistocene effects on vertebrate phylogeography. *Proceedings of the Royal Society of London. Series B, Biological Sciences* **265:** 1707-1712.

Avise, J.C., Ball, R.M. Arnold, J., Bermingham, E., Lamb, T., Neigel, J.E., Reeb, C.A. and Saunders, N.C. (1987) Intraspecific phylogeography: the mitochondrial DNA bridge between population genetics and systematics. *Annual Review of Ecology and Systematics* **18:** 489-522.

Babbucci, M., Buccoli, S., Cau, A., Cannas, R., Goñi, R., Díaz, D., Marcato, S., Zane, L. and Patarnello, T. (2010) Population structure, demographic history, and selective processes: contrasting evidences from mitochondrial and nuclear markers in the European spiny lobster *Palinurus elephas* (Fabricius 1787). *Molecular Phylogenetics and Evolution* **56:** 1040-1050.

Banks, S.C., Piggot, M.P., Williamson, J.E., Bove, U., Holbrook, N.J. and Beheregaray, L.B. (2007) Oceanic variability and coastal topography shape genetic structure in a long-dispersing sea urchin. *Ecology* **88:** 3055-3064.

Bard, E. and Rickaby, R.E.M. (2009) Migration of the subtropical front as a modulator of glacial climate. *Nature* **460:** 380-384.

Bass, D., Richards, T.A., Matthai, L., Marsh, V. and Cavalier-Smith, T. (2007) DNA evidence for global dispersal and probable endemicity of Protozoa. *BMC Evolutionary Biology* **7:**162

Beaumont, M.A. and Ranala, B. (2004) The Bayesian revolution in genetics. *Nature Reviews Genetics* **5:** 251-261.

Beckley, L.E., Hulley, P.A. and Skelton, P.H. (2002) Synoptic overview of marine ichthyology in South Africa. *Marine Freshwater Research* **53:** 99-105.

Beerli, P. and Felsenstein, J. (1999) Maximum likelihood estimation of migration rates and effective population numbers in two populations using a coalescent approach. *Genetics* **152:** 763-773.

Benjamini, Y. and Yekutieli, D. (2001) The control of the false discovery rate in multiple testing under dependency. *Annals of Statistics* **29:** 1165-1188.

Benzie, J.A.H., Ballment, E., Forbes, A.T., Demetriades, N.T., Sugama, K. and Haryanti, M.S. (2002) Mitochondrial DNA variation in Indo-Pacific populations of the giant tiger prawn, *Penaeus monodon*. *Molecular Ecology* **11:** 2553-2569.

Bernatchez, L. and Wilson, C.C. (1998) Comparative phylogeography of Nearctic and Palearctic fishes. *Molecular Ecology* **7:** 431-452.

Bester-van der Merwe, A.E., Roodt-Wilding, R., Volckaert, F.A.M. and D′Amato, M.E. (2011) Historical isolation and hydrodynamically constrained gene flow in declining populations of the South-African abalone, *Haliotis midae*. *Conservation Genetics* **12:** 543–555.

Bigg, G.R. Cummingham, C.W., Ottersen, G., Pogson, G.H., Wadley, M.R., and Williamson, P. (2008) Ice-age survival of Atlantic cod: agreement between palaeoecology models and genetics. *Proceedings of the Royal Society of London. Series B* **275:** 163-173.

Bilton, D.T., Freeland, J.R. and Okamura, B. (2001) Dispersal in freshwater invertebrates. *Molecular Biology and Evolution* **32:** 159-181.

Bird, C.E., Holland, B.S., Bowen, B.W. and Toonen, R.J. (2007) Contrasting phylogeography in three endemic Hawaii limpets (*Cellana spp.*) with similar life histories. Molecular Ecology**16:** 3173-3186.

Branch, G.M., Hauck, M., Siqwana-Ndulo, N., Dye, A.H. (2002) Defining fishers in the South African context: Subsistence, artisanal and small-scale commercial sectors. *South African Journal of Marine Science* **24:** 475-487.

Branch, G.M., Odendaal, F. and Robinson, T.B. (2010) Competition and facilitation between the alien mussel *Mytilus galloprovincialis* and indigenous species: Moderation by wave action. *Journal of Experimental Marine Biology and Ecology* **383:** 65-78.

Brito, P.H. (2005) The influence of Pleistocene glacial refugia on tawny owl genetic diversity and phylogeography in western Europe. *Molecular Ecology* **14:** 3077-3094.

Brito, P.H. and Edwards, S.V. (2009) Multilocus phylogeography and phylogenetics using sequence based markers. *Genetica* **135:** 439-455.

Brown, A.C. (1971) The ecology of the sandy beaches of the Cape Peninsula, South Africa. Part 2. The mode of life of *Bullia* (Gastropoda: Proscobranchiata). *Transactions of the Royal Society of South Africa* **39:** 281-321.

Burns, E.L., Eldridge, M.D.B., Cryan, D.M. and Houlden, B.A. (2007) Low phylogeographic structure in a wide spread endangered Australian frog *Litoria aurea* (Anura: Hylidae). *Conservation Genetics* **8:** 17-32.

Calderón, I., Giribet, G. and Turon, X. (2008) Two makers and one history: phylogeography of the edible common sea urchin Paracentrtus lividus in the Lusitanian region. *Marine Biology* **154:** 137-151.

Campo, D., Molares, J., Garca, L., Fernandez-Rueda, P., Garcia-Gonzalez, C. and Garcia-Vazquez, E. (2010) Phylogeograpy of the European stalked barnacle (Pollicipes pollicipes): identification of glacial refugia. *Marine Biology* **157:** 147-156.

Canino, M.F., Spies, I.B., Cunningham, K.M., Hauser, L., and Grant, S. (2010) Multiple ice-age refugia in Pacific cod, *Gadus macrocephalus*. *Molecular ecology* **19:** 4339-4351.

Cassone, B.J. and Boulding, E.G. (2006) Genetic structure and phylogeography of the lined shore crab, *Pachygrapsus crassipes*, along the north-eastern and western Pacific coasts. *Marine Biology* **149:** 213-226.

Chevolot, M., Hoarau, G., Rijnsdorp, A.D., Stam, W.T. and Olsen, J.L. (2006) Phylogeography and population structure of thornback rays (*Raja clavata L.*, Rajidae). *Molecular Ecology* **15:** 3693-3705.

Clark, P.U., Dyke, A.S., Shakun, J.D., Carlson, A.E., Clark, J., Wohlfarth, B., Mitorvica, J.X., Hostetler, S.W. and McCabe, A.M. (2009) The Last Glacial Maximum. *Science* **325:** 710-714.

Clement, M., Posada, D. & Crandall, K. A. (2000) TCS: a computer program to estimate gene genealogies. *Molecular Ecology* **9:** 1657-1660.

Connolly, S.R., Menge, B.A. and Roughgarden J. (2001) A latitudinal gradient in recruitment of intertidal invertebrates in the Northeast Pacific ocean. *Ecology* **82:** 1799-1813.

Corander, J. and Tang, J. (2007). Bayesian analysis of population structure based on linked molecular information. *Mathematical Biosciences* **205:** 19-31.

Corander, J., Marttinen, P., Sirén, J. and Tang J. (2008) Bayesian modelling in BAPS software for learning genetic structures of populations. *BMC Bioinformatics* **9:** 539.

Couceiro, L., Barreiro, R., Ruiz, J.M., and Sotka, E.E. (2007) Genetic isolation by distance among populations of the netted dog whelk *Nassarius reticulates* (L.) along the European Atlantic coastline. *Journal of Heredity* **98:** 603-610.

Crandall, E.D., Frey, M.A., Grosberg, R.K. and Barber, P.H. (2008) Contrasting demographic history and phylogeographical patterns in two Indo-Pacific gastropods. *Molecular Ecology* **17:** 611-626.

Crandall, E.D., Sbrocco, E.J., DeBoer, T.S., Barber, P.H. and Carpenter, K.E. (2012) Expansion dating, calibrating molecular clocks in marine species from expansions onto the Sunda Shelf following the Last Glacial Maximum. *Molecular Biology and Evolution* **29**: 707-719.

Crandall, E.D., Taffel, J.R. and Barber, P.H. (2010) High gene flow due to pelagic larval dispersal among South Pacific archipelagos in two amphidromous gastropods (Neritomorpha: Neritidae). *Heredity* **104:** 563-572.

Crandall, K.A., Bininda-Emonds, O.R.P., Mace, G.M., and Wayne, R.K. (2000) Considering evolutionary processes in conservation biology. *Trends in Ecology and Evolution* **15:** 290-295.

da Silva, F.M. and Brown, A.C. (1985) Egg capsules and veligers of the whelk *Bullia digitalis* (Gastropoda; Nassaridae). *Veliger* **28:** 200-203.

Derycke, S., Remerie T., Backljau T., Vierstraete A.., Vanfleteren J, Vincx, M. and Moens, T. (2008) Phylogeography of the *Rhabditis* (*Plliooditis*) *marina* species complex: evidence for long-distance dispersal, and for range expansions and restricted gene flow in the northeast Atlantic. *Molecular Ecology* **17:** 3306–3322.

Dingle, R.V. and Rogers, J. (1972) Effects of sea-level changes on the Pleistocene palaeoecology of the Agulhas Bank. *Palaeoecology of Africa* **6:** 55-58.

Domínguez-Domínguez, O., Vázquez-Domínguez, E. (2009) Phylogeography: Applications in taxonomy and conservation. *Animal Biodiversity and Conservation* **32:** 59-70.

Donald, K.M., Kennedy, M. and Spencer, H.G. (2005) Cladogenesis as the result of long-distance rafting events in South Pacific topshells (Gastropoda, Trochidae). *Evolution* **59:** 1701-1711.

Donoghue, M.J. and Moore, B.R. (2003) Toward an integrative historical biogeography. *Integrative and Comparative Biology* **43:** 261-270.

Drummond, A.J. and Rambaut, A. (2007) BEAST: Bayesian evolutionary analysis by sampling trees. *BMC Evolutionary Biology* **7:** 214

Drummond, A.J., Rambaut, A., Shapiro, B. and Pybus, O.G. (2005). *Molecular Biology and Evolution* **22:** 1185-1192.

Dugan, J.E., Defeo, O., Jaramillo, E., Jones, A.R., Lastra, M., Nel, R., Peterson, C.H., Scapini, F., Schlacher, T. and Schoeman, D. S. (2010) Give beach ecosystems their day in the sun. *Science* **329:** 1146

Duran, S., Palacin, C., Becerro, M.A., Turon, X. and Giribet, G. (2004) Genetic diversity and population structure of commercially harvested sea urchin *Paracentrotus lividus* (Echinodermata, Echinoidea). M*olecular Ecology* **13:** 3317-3328.

Elderkin, C.L., Christian, A.D., Metcafe-Smith, J.L. and Berg, D.J. (2008) Population genetics and phylogeography of freshwater mussels in North America, *Elliptio dilatata* and *Actinonaias ligamentina* (Bivalvia: Unionidae). *Molecular Ecology* **17:** 2149-2163.

Emmanuel, B.P., Bustamante, R.H., Branch, G.M., Eekhout, S. and Odendaal, F.J. (1992) A zoogeographic and functional approach to the selection of marine reserves on the west coast of South Africa. *South African Journal of Marine Science* **12:** 341-354.

Evans, B.S., Sweijd, N.A., Bowie, R.C.K., Cook, P.A. and Elliot, N.G. (2004) Population genetic structure of the perlemoen *Haliotis midae* in South Africa: evidence of range expansion and founder events. *Marine Ecology Progress Series* **270:** 163-172.

Excoffier, L. and Lischer, H.L.E. (2010) Arlequin suite ver 3.5: A new series of programs to perform population genetics analyses under Linux and Windows. *Molecular Ecology Resources* **10:** 564-567.

Excoffier, L. (2004) Patterns of DNA sequence diversity and genetic structure after a range expansion: lessons from the infinitive-island model. *Molecular Ecology* **13:** 853-864.

Excoffier, L., Laval, G. and Schneider, S. (2006) Arlequin 3.11: an integrated software package for population genetics data analysis. http://cmpg.unibe.ch/software/arlequin3

Fisher, E.C., Bar-Mattews, M., Jerardino, A. and Marean, C.W. (2010) Middle and Late Pleistocene paleaoscape modelling along the southern coast of South Africa. *Quaternary Science Review* **29:** 1382-1398.

Folmer, O., Black, M., Hoeh, W., Lutz, R. and Vrijenhoek, R. (1994) DNA primers for amplification of mitochondrial cytochrome c oxidase subunit I from diverse metazoan invertebrates. *Molecular Marine Biology and Biotechnology* **3:** 294-299.

Foster, G.G. and Hodgson, A.N. (2000) Intertidal population structure of the edible mollusc *Turbo sarmaticus* (Vetigastropoda) at an unexploited and exploited sites along the coast of the Eastern Cape Province, South Africa. *African Zoology* **35:** 173-183.

Fu, Y. X. (1997) Statistical tests of neutrality of mutations against population growth, hitchhiking and background selection. *Genetics* **147:** 915-925.

Garrick, R., Sunnucks, P. and Dyer, R. (2010) Nuclear gene phylogeography using PHASE: dealing with unresolved genotypes, lost alleles and systematic bias in parameter estimation. *BMC Evolution Biology* **10:** 118.

Gaylord, B. and Gaines, S.D. (2000) Temperature or transport? Range limits in marine species mediated solely by flow. *American Naturalist* **155:** 769-789.

Gaziev, A.I. and Shaikhaev, G.O. (2010) Nuclear mitochondrial pseudogenes. *Molecular Biology* **44:** 358–368.

Gibbard, P., and van Kolfschoten, T. (2004) The Pleistocene and Holocene epochs. In: Gradstein, F.M., Ogg, J.G. and Smith, A.G. (eds) *A geologic time scale*. Cambridge University Press. Cambridge.

Gilman, S.E. Wethey, D.S. and Helmuth, B. (2006) Variation in the sensitivity of organismal body temperature to climate change over local and geographic scales. *Proceedings of the National Academy of Sciences* **103:** 9560-9565.

Gómez, A., Hughes, R.N. Wright, P.J., Carvolho, G.R. and Lunt, D.H. (2007) Mitochondrial DNA phylogeography and mating compatibility reveal marked genetic structuring and speciation in the NE Atlantic bryozoans *Celleporella hyalina*. *Molecular Ecology* **16:** 2173-2188.

Gopal, K., Tolley, K.A., Groeneveld. and Matthee, C.A. (2006) Mitochondrial DNA variation in spiny lobster Palinurus delagoae suggests genetically structured populations in the southwester Indian Ocean. *Marine Ecology Progress Series* **319:** 191-198.

Graham, C.H., Moritz, C. and Williamsa, S.E. (2006) Habitat history improves prediction of biodiversity in rainforest fauna. *Proceedings of the National Academy of Sciences of the United States of America* **103:** 632-636.

Grant, W.S. and Bowen, B.W. (1998) Shallow population histories in deep evolutionary lineage of marine fishes: insights for sardines and anchovies and lesson for conservation. *Journal of Heredity* **89:** 415-426.

Grant, W.S. and da Silva-Tatley, F.M. (1997) Lack of genetically-subdivided population structure in *Bullia digitalis*, a southern African marine gastropod with lecithotrophic development. *Marine Biology* **129:** 123-137.

Grant, W.S., Liu, M., Gao, T., and Yanagimoto, T. (2012) Limits of Bayesian skyline plot analysis of mtDNA sequences to infer historical demographies in Pacific herring (and other species). *Molecular Phylogenetics and Evolution* **65:** 203-212.

Griffiths, C.L. and Branch, G.M. (1997) The exploitation of coastal invertebrates and seaweeds in South Africa: historical trends, ecological impacts and implications for management. *Transactions of the Royal Society of South Africa* **52:** 121-148.

Griffiths, C.L., Robinson, T.A., Lange, L. and Mead, A. (2010) Marine biodiversity in South Africa: an evaluation of current states of knowledge. *Plos One* **5:** 1371.

Grindley, J.R. (1969) The Quaternary marine palaeoecology in South Africa. *South African Archaeological Bulletin* **24:** 151-157.

Gutiérrez-García, T. A. and Vázquez-Domínguez, E. (2011) Designing Studies while surviving the process. *Bioscience* **61:** 857-868.

Hall, T.A. (1999) BioEdit: a user-friendly biological sequence alignment editor and analysis program for windows 95/98NT. *Nucleic Acids Symposium Series* **41:** 95-98.

Hare, M.P. (2001) Prospects for nuclear gene phylogeography. *Trends in Ecology and Evolution* **16:** 700-706.

Harlin-Cognato, A., Bickham, J.W., Loughlin, T.R. and Honeycutt, R.L. (2006) Glacial refugia and the phylogeography of Steller′s sea lion (Eumatopias jubatus) in the North Pacific. *Journal of Evolutionary Biology* **19:** 955-969.

Harpending, H.C., Batzer, M.A., Guvern, M., Jorde, L.B., Rogers, A.R. and Sherry, S.T. (1998) Genetic traces of ancient demography. *Proceedings of National Academy of Science (USA)* **95:** 1961-1967.

Harrigan, R.J., Mazza, M.E. and Sorenson, M.D. (2008) Computation vs. cloning: evaluation of two methods for haplotype determination. *Molecular Ecology Resources* **8:** 1239–1248.

Hasegawa, M., Kishino, H. and Yano, T.-A. (1985) Dating of the human-ape splitting by a molecular clock of mitochondrial DNA. *Journal of Molecular Evolution* **22:** 160-174.

Hellberg, M.E., Balch, D.P. and Roy, K. (2001) Climate-driven range expansion and morphological evolution in a marine gastropod. *Science* **292:** 1707-1710.

Heller, J. and Dempster, Y. (1991) Detection of two coexisting species of *Oxystele* (Gastropoda: Trochidae) by morphological and electrophoretic analyses. *Journal of Zoology* **223:** 395-418.

Helmuth, B., Veit, R.R. and Holberton, R. (1994) Long-distance dispersal of a subantarctic brooding bivalve (*Gaimardia trapesina*) by kelp-rafting. *Marine Biology* **120:** 421-426.

Helmuth, B.S.T., Harley, C.D.G., Halpin, P., O'Donnell, M., Hofmann, G.E., and Blanchette, C. (2002) Climate change and latitudinal patterns of intertidal thermal stress. *Science* **298:** 1015-1017.

Hewitt, G.M. (2000) the genetic legacy of the Quaternary ice ages. *Nature* **405:** 907-913.

Hewitt, G.M. (2001) Speciation, hybrid zones and phylogeography- or seeing genes in space and time. *Molecular Ecology* **10:** 537-549.

Hewitt, G.M. (2004) Genetic consequences of climatic oscillations in the Quaternary. *Philosophical Transactions of the Royal Society Britain* **359:** 183-195,

Hewitt, G.M. (2011) Quaternary phylogeography: the roots of hybrid zones. *Genetica* **139:** 617-638.

Hey, J. (2006) Recent advances in assessing gene flow between diverging populations and species. *Current Opinion in Genetics and Development* **16:** 592-596.

Hey, J. and Nielsen, R. (2004) Multilocus methods for estimating population sizes, migration rates and divergence time, with applications to the divergence of *Drosophila pseudoobscura* and *D. perimilis*. *Genetics* **167:** 747-760.

Hoarau, G., Coyer, J.A., Velsink, J.H., Stam, W.T. and Olsen, J.L. (2007) Glacial refugia and recolonization pathways in the brown seaweed *Fucus serrtus*. *Molecular Ecology* **16:** 3606-3616.

Hudson, R.R. and Truelli, M. (2003) Stochasticity overrules "the three-times rule": genetic drift, genetic draft, and DNA. *Evolution* **57:** 182-190.

Hurtado, L.A., Frey, M., Gaube, P. and Pfeiler, E. (2007) Geographical subdivision, demographic history and gene flow in two sympatric species of intertidal snails, *Nerita scabricosta* and *Nerita funiculata*, from the tropical eastern Pacific. Marine biology **151:** 1863-1873.

Ibáñez, C.M., Cubillos, L.A., Tafur, R., Argüelles, J., Yamashiro, C. and Poulin, E. (2011) Genetic diversity and demographic history of *Dosidicus gigas* (Cephalopoda: Ommastrephidae0 in the Humboldt Current System. *Marine Ecology Progress Series* **431:** 163-171.

Jackson, J.M., Rainville, L., Roberts, M.J., Mcquaid, C.D. and Lutjeharms, R.E. (2012) Mesoscale bio-physical interactions between the Agulhas Current and the Agulhas Bank, South Africa. *Continental shelf Research* **49:** 10-24.

Jarman, S. N., R. D. Ward, and N. G. Elliott. (2002) Oligonucleotide primers for PCR amplification of coelomate introns. *Marine Biotechnology* **4:** 347-355.

Jolly, M.T., Viard, F., Gentil, F., Thiebault, E., Jollivet, D. (2006) Comparative phylogeography of two coastal polychaete tubeworms in the Northeast Atlantic supports shared history and vicariant events. *Molecular Ecology* **15:** 1841-1855.

Karl, S.A., Toonen, R.J., Grant, W.S. and Bowen, B.W. (2012) Common misconceptions in molecular ecology: echoes of the modern synthesis. Molecular Ecology 21: 4171-4189.

Keeney, D.B., King, T.M., Rowe, L.D. and Poulin, R. (2009) Contrasting mtDNA diversity and population structure in a direct-developing marine gastropod and its trematode parasites. *Molecular Ecology* **18:** 4591–4603.

Kenchington, E.L., Harding, G.C., Jones, M.W. and Prodöhl, P.A. (2009) Pleistocene glaciations events shape genetic structure across the range of the American lobster, *Homarus americanus*. *Molecular Ecology* **18:** 1654-1667.

Kilburn, R. and Rippey, E. (1982) *Sea shells of southern Africa*. Macmillan South Africa (Pty) Ltd. Johannesburg.

Kimura, M. (1980) A simple method for estimating evolutionary rates of base substitutions through comparative studies of nucleotide sequences. *Journal of Molecular Evolution* **16:** 111-120.

Kokita, T. and Nohara, K. (2011) Phylogeography and historical demography of the anadromous fish *Leucopsarion petersii* in relation to geological history and oceanography around the Japanese Archipelago. *Molecular Ecology* **20:** 143-164.

Lasota, R., Hummel, H. and Wolowicz, M. (2004) Genetic diversity of European populations of the invasive soft-shell *Mya arenaria* (Bivalvia). *Journal of Marine Biology Association UK* **84:** 1051-1056.

Laudien, J., Flint, N.S., van der Bank, F.H. and Brey, T. (2003) Genetic morphological variation in four populations of the surf clam *Donax serra* (Röding) from southern Africa sandy beaches. *Biochemical Systematics and Ecology* **31:** 751-772.

Lecomte, F., Grant, W.S., Dodson, J.J., Rodriguez-Sanchez, R. and Bowen, B.W. (2004) Living with uncertainty: genetic imprints of climate shifts in east Pacific anchovy (*Engraulis mordax*) and sardine (*Sardinops sagax*). *Molecular Ecology* **13:** 2169-2182.

Lee, H. J. and Boulding, E.G. (2007) Mitochondrial DNA variation in space and time in the northeastern Pacific gastropod, *Littorina keenae*. *Molecular Ecology* **16:** 3084-3103.

Lejeusne, C. and Chevaldonné, P. (2006) Brooding crustaceans in a highly fragmented habitat: the genetic structure of Mediterranean marine cave-dwelling mysid populations. *Molecular Ecology* **15:** 4123-4140.

Librado, P. and Rozas, J. (2009) DnaSP v5: a software for comprehensive analysis of DNA polymorphism data. *Bioinformatics* **25:** 1451-1452.

Lorenzen, E.D., Masembe, C., Arctander, P. and Siegismund, H.R. (2010) A long-standing Pleistocene refugium in southern Africa and a mosaic of refugia in East Africa: insights from mtDNA and the common eland antelope. *Journal of Biogeography* **37:** 571-581.

Lourie, S.A., Green, D.M. and Vincent, C.J. (2005) Dispersal, habitat, differences, and comparative phylogeography of Southeast Asian seahorses (Syngnathidae: *Hippocampus*). *Molecular Ecology* **14:** 1073-1094.

Lutjeharms, J.R.E (2006) *The Agulhas Current*. Springer. Berlin.

Lutjeharms, J.R.E. and Ansorge, I.J. (2001) The Agulhas Return Current. *Journal of Marine Systems* **30:** 115-138.

Lutjeharms, J.R.E. and Ballegooyen, R.C. (1988) Anomalous upstream retroflection in the Agulhas Current. *Science*, **240:** 1770-1772.

Lutjeharms, J.R.E., Cooper, J., and Roberts, M. (2000) Upwelling at the inshore edge of the Agulhas Current. *Continental Shelf Research* **20:** 737-761.

Lutjeharms, J.R.E., de Ruiter, W.P.M. and Peterson, R.G. (1992) Interbasin exchange and the Agulhas retroflection: the development of some oceanographic concepts. *Deep-Sea Research* **39:** 1791-1807.

Maggs, C.A. Castilho, R., Foltz, D., Henzler, C., Jolly, M.T., Kelly, J., Olsen, J., Perez, K.E., Stam, W., Vainola, R., Viard, F. and Wares, J. (2008) Evaluating signatures of glacial refugia for north Atlantic benthic marine taxa. *Ecology* **89:** S108-S122.

Marko, P.B. (2002) Fossil calibration of molecular clocks and the divergence times of geminate species pairs separated by the Isthmus of Panama. *Molecular Biology and Evolution* **19:** 2005-2021.

Marko, P.B. (2004) „What's larvae go to do with it?" Disparate patterns of post-glacial population structure in two benthic marine gastropods with identical dispersal potential. *Molecular Ecology* **13:** 597-611.

Marko, P.B., Hoffman, J.M., Emme, S.A., McGovern, T.M., Keever, C.C. and Cox, L.N. (2010) The „Expansion-Contraction" model of Pleistocene biogeography: rocky shores suffer a sea change? *Molecular Ecology* **19:** 146-169.

Martel, A. and Chia, F.S. (1991) Drifting and dispersal of small bivalves and gastropods with direct development. *Journal of experimental Marine Biology and Ecology* **150:** 131-147.

Matthee, C.A., Cockroft, A.C., Gopal, K. and von der Heyden, S. (2007) Mitochondrial DNA variation of the west-coast rock lobster, *Jusus lalandii*: marked genetic diversity differences among sampling sites. *Marine and Freshwater Research* **58:** 1130-1135.

McDonald, J. and Kreitman, M. (1991) Adaptive protein evolution at the *ADh* locus in Drosophila. *Nature* **351:** 652-654.

McGaughran, A., Torricelli, G., Carapelli, A., Frati, F., Stevens, M.I., Convey, P. and Hogg, I.D. (2010) Contrasting phylogeographical patterns for springtails reflect different evolutionary

histories between the Antarctic Peninsula and continental Antarctica. *Journal of Biogeography* **37:** 103-119.

McGovern, T.M., Keever, C.C., Saski, C.A., Hart, M.W. and Marko, P.B. (2010) Divergence genetics analysis reveals historical population genetic process leading to contrasting phylogeographic patterns in co-distributed species. *Molecular Ecology* **19:** 5043-5060.

McQuaid, C.D. (1983). Population dynamics and growth of the gastropod *Oxystele variegata* (Anton) on an exposed shore. *South African Journal of Zoology* **18:** 56–61.

Miller, K.G., Kominz, M.A., Browning, J.V., Wright, J.D., Mountain, G.S., Katz, M.E., Sugarman, P.J., Cramer, B.S., Christie-Blick, N. and Pekar, S.F. (2005) The Phanerozoic record of global sea-level change. *Science* **310:** 1293-1298.

Mills, L.S. and Allendorf, F.W. (1996) The one-migrant-per-generation rule in conservation and management. *Conservation Biology* **10:** 1509-1518.

Miura, O., Kuris, A.M., Torchin, M.E. Hechinger, R.F., Dunham, E.J. and Chiba, S. (2005) Molecular-genetic analyses reveal cryptic species of trematodes in the intertidal gastropod, *Batillaria cumingi* (Crosse). *International Journal for Parasitology* **35:** 793-801.

Moritz, C., Dowling, T.E. and Brown, W.M. (1987) Evolution of animal mitochondrial DNA: relevance for population biology and systematics. *Annual Review of Ecology and Systematics* **18:** 269-292.

Moritz, C.S. (1994) Defining 'Evolutionary Significant Units' for conservation. *Trends in Ecology and Evolution* **9:** 373-375.

Narum, S.R. (2006) Beyond Bonferroni: Less conservative analyses for conservation genetics. *Conservation Genetics* **7:** 783-787.

Neethling, M., Matthee, C.A., Bowie, R.C.K. and von der Heyden, S. (2008) Evidence for panmixia despite barriers to gene flow in the southern African endemic, *Caffrogobius caffer* (Teleostei: Gobidae). *BMC Evolutionary Biology* **8:** 325.

Nei M (1987) Molecular evolutionary genetics. Colombia University Press. New York.

Nicolas, V., Bryja, J., Akpatou, B., Konecny, A., Lecompte, E., Colyn, M., Lalis, A., Couloux, A., Denys, C. and Granjon, L. (2008) Comparative phylogeography of two sibling species of forest-dwelling rodents (*Praomys rostratus* and *P. tullbergi*) in West Africa: different reactions to past forest fragmentation. *Molecular Ecology* **17:** 5118-5134.

Nicolas, V., Missoup, A.D., Denys, C., Kerbis-Peterhans, J., Katuala, P., Couloux, A. and Colyn, M. (2011) the roles of rivers and Pleistocene refugia in shaping genetic diversity in *Praomys misonnei* in tropical Africa. *Journal of Biogeography* **38:** 191-207.

North, E.W., Schlag, Z., Hood, R.R., Li, M., Zhong, L., Gross, T. and Kennedy, V.S. (2008) Vertical swimming behaviour influences the dispersal of simulated oyster larvae in a coupled particle-tracking and hydrodynamic model of Chesapeake Bay. *Marine Ecology Progress Series* **359**: 99-115.

Nuñez, J.J., Wood, N.K., Rabanal, F.E., Fontanella, F.M. and Sites, J.W. (2011) Amphibian phylogeography in the Antipodes: refugia and postglacial colonization explain mitochondrial haplotype distribution in the Patagonian frog *Eupsophs calcaratus* (Cycloramphidae). *Molecular Phylogenetics and Evolution* **58:** 343-352.

O′Neill, S. B., Buckley, T.R., Jewell, T.R. and Ritchie, P.A. (2009) Phylogeographic history of the New Zealand stick insect *Niveaphasma annulata* (Phasmatodea) estimated from mitochondrial and nuclear loci. *Molecular Phylogenetics and Evolution* **53:** 523-536.

Odendaal, F.J., Turchin, P., Hoy, G., Wickens, P., Wells, J. and Schroeder, G. (1992) *Bullia digitalis* actively pursues moving prey by swash-riding. *Journal of Zoology* **228:** 101-113.

Palero, F., Abello, P., Macpherson, E., Gristina, M. and Pascaul, M. (2008) Phylogeography of the European spiny lobster (*Palinurus elephas*): Influence of current oceanographical features and historical processes. *Molecular Phylogenetics and Evolution* **48:** 708-717.

Pamilo, P. and Nei, M. (1988) Relations between gene trees and species trees. *Molecular Biology and Evolution* **5:** 568-583.

Pérez-Losada, M., Nolte, M.J., Crandall, K.A. and Shaw, P.W. (2007) Testing hypotheses of population structuring in the northeast Atlantic Ocean and Mediterranean Sea using the common cuttlefish *Sepia officinalis*. *Molecular Ecology* **16:** 2667-2679.

Perrin, C., Wing, S.R. and Roy, M.S. (2004) Effects of hydrographic barriers on population genetic structure of the sea star *Coscinasterias muricata* (Echinodermata, Asteroidea) in the New Zealand fiords. *Molecular Ecology* **13:** 2183-2195.

Peters, J.L., Gretes, W. and Omland, E. (2005) Late Pleistocene divergence between eastern and western populations of wood ducks (*Aix sponsa*) inferred by the ′isolation with migration′ coalescent method. *Molecular Ecology* **14:** 3407-3418.

Pineda, J. (1999) Circulation and larval distribution in internal tidal bore warm fronts. *Limnology and Oceanography* **44:** 1400-1414**.**

Pineda, J., Riebensahm, D., and Medeiros-Bergen, D. (2002) *Semibalanus balanoides* in winter and spring: Larval concentration, settlement, and substrate occupancy. *Marine Biology* **140:** 789-800**.**

Porreta, D., Canestrelli, D., Bellini, R., Celli, G. and Urbanelli, S. (2007) Improving insect pest management through population genetic data: a case of the mosquito *Ochlerotatus caspius* (Pallas). *Journal of Applied Ecology* **44:** 682-691.

Porreta, D., Canestrelli, D., Urbanelli, S. Bellini, R., Schaffner, F., Petric, D. and Nascetti, G. (2011) Southern crossroads of the Western Palaearctic during the Late Pleistocene and their imprints on current patterns of genetic diversity: insights from the mosquito *Aedes caspius*. *Journal of Biogeography* **38:** 20-30.

Posada, D. (2008) jMODELTEST: Phylogenetic Model Averaging. *Molecular Biology and Evolution* **25:** 1253-1256.

Posada, D. and Crandall, K.A. (2001) Intraspecific genealogies: trees grafting into networks. *Trends in Ecology and Evolution* **16:** 37-45.

Princebourde, S., Sanford, E. and Helmuth, B.S.T. (2008) Body temperature during low tide alters the feeding performance of a top intertidal predator. *Limnology and Oceanography* **53:** 1562-1573.

Proudfoot, L., Kaehler, S., McGarry, D.K., Uppink, P.A., Aereboe, M. and Morris, K.M. (2006) Exploitation status of infralittoral abalone (*Haliotis midae*) and alikreukel (*Turbo sarmaticus*) in the southern section of the Eastern Cape coast, South Africa. *South African Journal of Science* **102:** 162-168.

Queiroga, H. and Blanton, L.M. (2005) Interactions between behaviour and physical forcing in the control of horizontal transport of decapods larvae. In: Southward, A., Tyler, P., Young, C. and Fuiman, L (eds) *Advances in Marine Biology, volume 7*. Elsevier Science Ltd. San Diego.

Rambaut, A. and Drummond, A.J. (2007) Tracer v1.5, Available from http://beast.bio.ed.ac.uk/Tracer

Ramos-Onsins, S.E. and Rozas, J. (2002) Statistical properties of new neutrality tests against population growth. *Molecular Biology and Evolution* **19:** 2092-2100.

Ramsay, P.J. (1991) Sedimentology, coral reef zonation, and the late Pleistocene coastline models of the Sodwana Bay continental shelf, northern Zululand. PhD thesis. University of Natal. South Africa.

Ray, N., Currat, M., and Excoffier, L. (2003) Intra-deme molecular diversity in spatially expanding populations. *Molecular Biology and Evolution* **20:** 76-86.

Revell, L.J., Harmon, L.J. and Collar, D.C. (2008) Phylogenetic Signal, Evolutionary Process, and Rate. *Systematic Biology*, **57**: 591-601.

Ridgway, T., Riginos, C., Davis, J. and Hoegh-Guldberg, O. (2008) Genetic connectivity patterns of *Pocillopora verrucosa* in southern African marine protected areas. *Marine Ecology Progress Series* **354:** 161-168.

Roberts, M., van der Lingen, C.D., Whittle, C. and van der Berg, M. (2010) Shelf curents, lee-trapped and transient eddies on the inshore boundary of the Agulhas Current, South Africa:

their relevance to the KwaZulu-Natal sardine run. *African Journal of Marine Science* **32:** 423-447.

Rocha, L.A., Robertson, D.R., Roman, J. and Bowen, B.W. (2005) Ecological speciation in tropical reef fishes. *Proceedings of the Royal Society of Britain* **272:** 573-579.

Rogers, A. (1995) Genetic evidence for a Pleistocene population explosion. *Evolution* **49:** 608-615.

Rogers, A.R. and Harpending, H. (1992) Population growth makes waves in the distribution of pairwise genetic differences. *Molecular Biology and Evolution* **9:** 552-569.

Ryder, O.A. (1986) Species conservation and systematic: the dilemma of subspecies. *Trends in Ecology and Evolution* **1:** 9-10.

Sánchez, F. and Gil, J. (2000) Hydrographic mesoscale structures and Poleward Current as a determinant of hake (*Merluccius merluccius*) recruitment in southern Bay of Biscay. *ICES Journal of Marine Science* **57:** 152-170.

Schmitt, T. (2007) Molecular biogeography of Europe: Pleistocene cycles and postglacial trends. *Frontiers in Zoology* **4:** 11

Shannon, L.V. (1989) The physical environment. In: Payne, A.I.L. and Crawford, R.J.M. (eds) *Oceans of life off southern Africa*. Vlaeberg. Cape Town. pp12-27

Shannon, L.V., Hutchings, L., Bailey, G.W. and Shelton, P.A. (1984) Spatial and temporal distribution of chlorophyll in southern African waters as deduced from ship and satellite measurements and their implications for pelagic fisheries. *South African journal of marine Science* **2**: 109-130.

Shillington, F.A. (1995) Oceanography of the southern African region. In: Smith, M.M. and Heemstra, P.C. (eds) Smiths‟ sea fishes, 2nd edition. Sruik Publishers. Cape Town.

Skibinski, D.O.F. (2000) DNA tests of neutral theory: applications in marine genetics. *Hydrobiologia* **420:** 137-152.

Slatkin, M. and Hudson, R.R. (1991) Pairwise comparisons of mitochondrial DNA sequences in stable and exponentially growing populations. *Genetics* **129:** 555-562.

So, J.J., Uthicke, S., Hamel, J-F. and Mercier, A. (2011) Genetic population structure in a commercial marine invertebrate with long-lived lecithotrophic larvae: *Cucumaria frondosa* (Echinodermata: Holothuroidea). *Marine Biology* **158:** 859–870.

Stephens, M. and Donnelly, P. (2003) A comparison of Bayesian methods for haplotype reconstruction from population genotype data. *American Journal of Human Genetics* **73:** 1162-1169.

Stephens, M., Smith, N., Donelly, P. (2001) A new statistical method for haplotype reconstruction from population data. *American Journal of Human Genetics* **68:** 978-989.

Strasser, C.A. and Barber, P.H. (2009) Limited genetic variation and structure in softshell clams (*Mya arenaria*) across their native and introduced range. *Conservation Genetics* **10:** 803-814.

Tajima, F. (1989) Statistical testing for the neutral mutation hypothesis by DNA polymorphism. *Genetics* **123:** 585-595.

Tamura, K. and Nei, M. (1993) Estimation of the number of nucleotide substitution in the control region of mitochondrial DNA in humans and chimpanzees. *Molecular Biology and Evolution* **10:** 512-526.

Tankard, A.J. (1976) Cenozoic sea-level changes: a discussion. *Annals of the South African Museum* **71:** 1-17.

Teske, P.R. Cherry, M.I. and Matthee, C.A. (2004) The evolutionary history of seahorses (Syngthidae: Hippocampus): Molecular data suggest a West Pacific origin and two invasions of the Atlantic Ocean. *Molecular Phylogenetics and Evolution* **30:** 273-286.

Teske, P.R., Forget, F.R.G., Cowley, P.D., von der Heyden, S. and Beheregaray, L.B. (2010) Connectivity between marine reserves and exploited areas in the philopatric reef fish *Chrysoblephus laticeps* (Teleostei: Sparidae). *Marine Biology* **157:** 2029-2042.

Teske, P.R., Froneman, P.W., Barker, N.P. and McQuaid, C.D. (2007b) Phylogeographic structure of the caridean shrimp *Palaemon peringueyi* in South Africa: further evidence for intraspecific

genetic units associated with marine biogeographic provinces. *African Journal of Marine Science* **29:** 253-258.

Teske, P.R., McQuaid, C.D., Froneman, C.D. and Barker, N.P. (2006) Impact of marine biogeographic patterns of three South African estuarine crustaceans. *Marine Ecology Progress Series* **314:** 283-293.

Teske, P.R., Papadopoulos, I., Zardi, G.I., McQuaid, C.D., Edkins, M.T., Griffiths, C.L. and Barker, N.P. (2007a) Implications of life history for genetic structure and migration rates of southern African coastal invertebrates: planktonic, abbreviated and direct development. *Marine Biology* **152:** 697-711.

Teske, P.R., von der Heyden, S., McQuaid, C.D. and Barker N.P. (2011) A review of marine phylogeography in southern Africa. *South African Journal of Science* **107:** 514.

Teske, P.R., Winker, H., McQuaid, C.D. and Barker, N.P. (2009) A tropical/subtropical biogeographic disjunction in south-eastern Africa separates two Evolutionarily Significant Units of an estuarine prawn. *Marine Biology* **156:** 1265-1275.

Thompson, J.D., Higgins, D.G. and Gibson, T.J. (1994) CLUSTAL W: improving the sensitivity of progressive multiple sequence alignment through sequence weighting, position-specific gap penalties and weight matrix choice. *Nucleic Acids Research* **22***:* 4673-4680.

Toews, D.P.L. and Brelsford, A. (2012) The biogeography of mitochondrial and nuclear discordance in animals. *Molecular Ecology* **21:** 3907-3930.

Tolley, K.A., Groeneveld, J.C. Gopal, K. and Matthee, C.A. (2005) Mitochondrial DNA panmixia in spiny lobster *Palinurus gilchristi* suggests a population expansion. *Marine Ecology Progress Series* **297:** 225-231.

Turpie, J.K., Beckley, L.E. and Katua, S.M. (2000) Biogeography and the selection of priority areas for conservation of South African coastal fishes. *Biological Conservatio*n **92:** 59-72.

Uthicke, S. and Benzie, J.A.H. (2003) Gene flow and population history in high dispersal marine invertebrates: mitochondrial DNA analysis of *Holothuria nobilis* (Echnodermata: Holothuronidea) populations from the Indo-Pacific. *Molecular Ecology* **12:** 2635-2648.

von der Heyden, S. (2009) Why do we need to integrate population genetics into South African marine protected area planning? *African Journal of Marine Science* **31:** 263-269.

von der Heyden, S., Groeneveld, J.C. and Matthee, C.A. (2007) Long current to nowhere?-Genetic connectivity of Jasus tristani in the southern Atlantic. *African Journal of Marine Science* **29:** 491-497.

von der Heyden, S., Lipinski, M.R., and Matthee, C.A. (2010) Remarkably low mtDNA control region diversity in an abundant demersal fish. *Molecular Phylogenetics and Evolution* **55:** 1183-1188.

von der Heyden, S., Prochazka, K. and Bowie, R.C.K. (2008) Significant population structure and asymmetric gene flow patterns amidst expanding populations of *Clinus cottoides* (Perciformes, Clinidae): application of molecular data to marine conservation planning in South Africa. *Molecular Ecology* **17:** 4812-4826.

Voris, H.K. (2000) Maps of Pleistocene sea levels in Southeast Asia: shorelines, river systems and time durations. *Journal of Biogeography* **27:** 1153-1167.

Waples, R.S. and Gaggiotti, O. (2006) What is a population? An empirical evaluation of some genetic methods for identifying the number of gene pools and their degree of connectivity. *Molecular Ecology* **15:** 1419-1439.

Wares, J.P. and Cunningham, C.W. (2001) Phylogeography and historical ecology of the north Atlantic intertidal. *Evolution* **55:** 2455–2469

Waters, J.M., King, T.M., O′Loughlin, P.M., and Spenser, H.G. (2005) Phylogeographical disjunction in abundant high dispersal littoral gastropods. *Molecular Ecology* **14:** 2789-2802.

Wedepohl, P.M., Lurjeharms, J.R.E. and Meeuwis, J.M. (2000) Surface drift in the south-east Atlantic Ocean. *South African Journal of Marine Science* **22:** 71-79.

Wilke, T. and Davis, G.M. (2000) Infraspecific mitochondrial sequence diversity in *Hydrobia ulvae* and *Hydrobia ventrosa* (Hydrobiidae: Rissooidea: Gastropoda): Do their different life histories affect biogeographic patterns and gene flow? *Biological Journal of the Linnean Society* **70:** 89-105.

Wilson, A.B. and Veraguth, I.E. (2010) the impact of Pleistocene glaciations across the range of a widespread European coastal species. *Molecular Ecology* **19:** 4535-4553.

Wirgin, I., Waldman, J., Stabile, J. Lubinski, B. and King, T. (2002) Comparison of mitochondrial DNA control region sequence and microsatellite DNA analyses in estimating population structure and gene flow in Atlantic sturgeon *Acipenser oxyrinchus*. *Journal of Applied Ichthyology* **18:** 313-319.

Zane, L., Marcato, S., Bargelloni, L., Bortolloto, E., Papetti, C., Simonato, M., Varotto, V., and Patarnello, T. (2006) Demographic history and population structure of the Antarctic silverfish *Pleuragramma antarcticum*. *Molecular Ecology* **15:** 4499-4511.

Zane, L., Ostellari, L., Maccatrozzo, L., Bargelloni, L., Cuzin-Roudy, J. Buchholz, F. and Patarnello, T. (2000) Genetic differentiation in a pelagic crustacean (*Meganyctiphanes norvegica*: Euphasiacea) from the North East Atlantic and the Mediterranean Sea. *Marine Biology* **136:** 191-199.

Zardi, G.I., McQuaid, C.D., Teske, P.R., and Barker, N.P. (2007) Unexpected genetic structure in indigenous (*Perna perna*) and invasive (*Mytilus galloproncialis*) mussel populations in South Africa. *Marine Ecology Progress Series* **337:** 135-144.

Zhang, D-X. and Hewitt, G.M. (2003) Nuclear DNA analyses in genetic studies of populations: practice, problems and prospects. *Molecular Ecology* **12:** 563-584.

Zink, R.M. and Barrowclough, G. (2008) Mitochondrial DNA under siege in avian phylogeography. *Molecular Ecology* **17:** 2107-2121.